The Role of Site-1 Protease in Cartilage Development

Ho, Yuen Yee
Joint Diseases Laboratory, Shriners Hospital for Children
Faculty of Medicine
Department of Surgery, Division of Surgical Research
McGill University, Montréal, Québec

August 13, 2006

A thesis submitted to the faculty of Graduate Studies and Research in partial fulfillment of the requirements for the degree of Master of Science.

Your file Votre référence
ISBN: 978-0-494-32719-7
Our file Notre référence
ISBN: 978-0-494-32719-7

TABLE OF CONTENTS

Abstract

During development cartilage originates as condensations of primordial mesenchymal cells which go through a strict program whereby these cells differentiate into chondrocytes, undergo hypertrophy, and are subsequently replaced by osteoblasts. A zebrafish mutant termed *gonzo* has been isolated which displays a phenotype similar to human chondrodysplasias. Recently it was shown that this phenotype is due to a mutation in the zebrafish equivalent of a mammalian serine protease termed SKI-1 or Site-1 protease (S-1P). This enzyme is a member of the prohormone convertase family of subtilisin-like proteases which are known to play a critical role in controlling the processing of sterol regulatory element binding proteins and in the Unfolded Protein Response (UPR). The goal of this research project is to explore the expression and the function of S-1P in chondrocyte differentiation *in vitro*.

In this study, the chondrogenic mouse cell line ATDC5 which recapitulates the steps of cartilage development when cultured in the presence of insulin was used. Result showed that 10 μg/mL of insulin is the optimum concentration to be used to induce chondrogenesis in ATDC5 cells. This was shown by Alcian Blue staining and glycosaminoglycan quantification, where cells induced by 10 μg/mL of insulin produced highest amount of glycosaminoglycan. Using RT-PCR, it was shown that S-1P is constitutively expressed in ATDC5 cells both induced and non-induced with insulin. S-1P was also shown to be expressed in ATDC5 cells induced by ascorbic acid and a combination of ascorbic acid and insulin. Using Real Time-PCR, the expression levels of S-1P in the presence of insulin, ascorbic acid and the combination of both differentiation inducers was determined. The expression levels of type I collagen (early-phase chondrocyte differentiation expressing gene), type II collagen and aggrecan (mature chondrocyte matrix genes) and type X collagen (hypertrophic chondrocyte matrix gene) were also analyzed.

The effect of the inhibition of S-1P on the expression levels of cartilage related components was studied by inhibiting S-1P using an R134E prosegment mutant (pro-SKI-1), which has been shown a potent cellular inhibitor of S-1P. The DNA of the pro-SKI-1 variant was subcloned into pIRES-EGFP (provided by Dr. Nabil Seidah) and transfected into ATDC 5 cells. Stably transfected cells were selected and the expression of S-1P and other cartilage components were quantitatively evaluated by studying the transfected cells using Real Time-PCR. Functional inhibition of S-1P was confirmed using an artificial substrate reporter construct adapted for specific cleavage by this protease.

Overall the results showed that inhibition of S-1P activity had drastic effects in chondrogenesis – the expression of cartilage components (Aggrecan, Collagen I, Collagen II and Collagen X) were significantly lowered. Inhibition of S-1P seemed to prevent the chondrogenesis process in ATDC 5 cells.

Résumé

Lors du développement, le cartilage se forme suite à la condensation de cellules mésenchymateuses primitives qui poursuivent un programme strict lors duquel ces cellules se différencient en chondrocytes, subissent l'hypertrophie et sont subséquemment remplacées par des ostéoblastes.

Un mutant du danio zébré, nommé *gonzo,* démontrant un phénotype similaire à celui rencontré lors de chondrodysplasies humaines a été isolé. Ce phénotype provient d'une mutation chez le danio zébré équivalente à une protéase de sérine mammifère nommée SKI-1 ou protéase de Site-1 (S-1P). Cette enzyme est un membre de la famille des convertases de prohormones des protéases subtilisin-like, reconnues comme jouant un rôle critique dans le contrôle du traitement des protéines liant l'élément régulateur des stérols ainsi que dans la réponse de stress du réticulum endoplasmique. Le but de ce projet de recherche est d'explorer l'expression et la fonction de la S-1P dans la différenciation des chondrocytes *in vitro.*

Dans cette étude nous avons utilisé la lignée de cellules chondrogéniques de souris ATDC 5, qui récapitule les étapes du développement du cartilage en présence d'insuline. Les résultats ont démontré que la concentration optimale d'insuline à utiliser pour induire la chondrogénèse des cellules ATDC 5 est de 10μg/ml. Ceci a été démontré par coloration au bleu alcian ainsi que par la quantification des glycosaminoglycanes. Par la méthode d'amplification en chaîne par polymérase-transcriptase inverse (RT-PCR), il a été démontré que la S-1P est exprimée de façon constitutive par les cellules ATDC 5 induites ou non par l'insuline. Il a également été démontré que la S-1P est exprimée par les cellules ATDC 5 induites par l'acide ascorbique ainsi que par une combinaison d'acide ascorbique et d'insuline. Par PCR en temps réel, les niveaux d'expression de la S-1P en présence d'insuline, d'acide ascorbique et d'une combinaison des deux agents inducteurs de différenciation ont été déterminés. Les niveaux d'expression du collagène de type I (gène de l'expression de la phase immédiate de différenciation des chondrocytes), du collagène de type II et de l'aggrécane (gènes de matrice chondrocytaire mature) et du collagène de type X (gène de matrice chondrocytaire hypertrophique) ont également été analysés.

L'effet de l'inhibition de la S-1P sur les niveaux d'expression des composantes du cartilage a été étudié par l'inhibition de la S-1P en utilisant le prosegment mutant R134E également nommé pro-SKI-1, qui a été démontré comme étant le meilleur inhibiteur cellulaire de la S-1P. L'acide désoxyribonucléique (ADN) du pro-SKI-1 a été subcloné dans pIRES-EGFP (gracieusement fourni par le Dr Nabil Seidah) et transfecté dans des cellules ATDC 5. Les cellules transfectées de façon stable ont été sélectionnées et l'expression de la S-1P et des autres composantes du cartilage a été évaluée de façon quantitative par l'étude des cellules transfectées par PCR en temps réel. L'inhibition fonctionnelle de la S-1P a été confirmée par l'utilisation d'un substrat artificiel pour les clivages spécifiques par cette protéase.

Ces résultats démontrent que l'inhibition de l'activité de la S-1P a des effets drastiques sur la chondrogénèse - l'expression des composantes du cartilage (aggrécane, collagène de type I, II et X) est significativement diminuée. L'inhibition de la S-1P semble avoir empêché le processus de chondrogénèse des cellules ATDC 5.

Acknowledgements

I would like to thank my supervisor, Dr. John S. Mort for offering me the opportunity to gain experience and knowledge in his laboratory. Many thanks for his help, understanding and patience throughout my degree.

I would also like to thank Dr. Nabil Seidah (Clinical Research Institute of Montreal) and his PhD. student Philomena Pulikotil for their help and guidance.

I would like to thank all the members of the Joint Diseases Laboratories and Genetics Unit for their help with experimental techniques and equipment. And many thanks to Guylaine Bedard of the Illustration Unit for helping in part of the illustration work of this thesis.

Last but not least, I would also like to express my appreciation to my parents, my brother, my aunt Grace Lau, my best friends Marianne Schimpl, Daniel Sinclair, and my roommates Margaux Ouimet and Kayo Tamura. Thank you for believing in my abilities. Also thank you for supporting and encouraging me throughout the course of my study.

List of Abbreviations

A	Adenine
ATF6	Activating transcription factor 6
ALPase	Alkaline phosphatase
Asp	Aspartic acid
BMP	Bone morphogenic protein
C	Cytosine
CDP	Chondrodysplasia punctata
CHILD	Congenital hemidysplasia with ichthyosiform erythroderma and limb defects
CMP	Cartilage matrix protein
Col2a1	Collagen II a 1
CREB	CyclicAMP response element binding
CRP	C-reactive protein
CRP	Complement regulatory protein
CSPG	Chondroitin sulfate proteoglycan
DMEM	Dulbecco's modified Eagle's medium
ECM	Extracellular Matrix
EDS	Ehlers-Danlos syndrome
EGF	Epidermal growth factor
EGFP	Enhanced fluorescent green protein
ER	Endoplasmic reticulum
ERSE	ER stress response element
F	Phenylalanine
FACIT	Fibril Associated Collagens with Interupted Triple helices
FGF	Fibroblast growth factors
G	Guanine
GAG	Glycosaminoglycan
GFCR	Growth factor cytokine receptor
Gly	Glycine
Glu	Glutamic acid
Goz	Gonzo
HA	Hyaluronan
HABR	Hyaluronic acid binding region
HMG	High mobility group
HSPG	Heparan sulfate proteoglycan
IGF-I	Insulin-like growth factor I
Ihh	Indian hedgehog
INSIG	Insulin-induced gene
K	Lysine
L	Leucine
LDL	Low density protein
LP	Link protein
MCDS	Schimd type of metaphyseal chondrodysplasia

MGB	Minor groove binder
OASIS	Old astrocytes specifically induced substance
OI	Osteogenesis imperfecta
PTHrP	Parathyroid hormone related peptide
Pro-PDGF-A	Pro-platelet derived growth factor-A
R	Arginine
RCDP	Rhizomelic chondrodysplasia punctata
RSL	Reactive site loop
RT-PCR	Reverse transcription polymerase chain reaction
Real-time PCR	Real-time reverse transcription polymerase chain reaction
S	Serine
S-1P	Site-1 protease
SAP	Serum amyloid P-component
SCAP	SREBP-cleavage activating protein
SKI-I	Subtilisin kexin isoenzyme-1
SOX	SRY-related HMG box
SREBP	Sterol regulatory element binding protein
SRY	Sex-determining region Y gene
T	Thymine
TGF-ß	Transforming growth factor- ß
Thr	Threonine
UPR	Unfolded protein response
Val	Valine

List of Figures **Page**

List of Tables

CHAPTER 1

Review of Literature

1.1 Cartilage

Cartilage is a specialized type of connective tissue consisting mainly of extracellular matrix. Unlike other connective tissues, cartilage does not contain blood vessels or nerves. Cartilage is not abundant in the adult humans, but it is very important during development because of its firmness and its ability to grow rapidly. Cartilage is also formed very early during the repair of bone fractures (1).

There are 4 major types of cartilage:

1) Hyaline cartilage
2) Elastic cartilage
3) Fibrous cartilage
4) Articular cartilage

1.1.1 Hyaline cartilage

Hyaline cartilage is the most common variety of cartilage. It develops, like other types of connective tissue, from mesenchymal cells. In human, from about the fifth foetal week precursor cells become rounded and form densely packed cellular masses, centres of chondrification (1). The cartilage-forming cells, chondroblasts, begin to secrete the components of the extracellular matrix of cartilage, which consists of, ground substance (hyaluronan, chondroitin sulfates and keratan sulfate) and tropocollagen, which polymerises extracellularly into fine collagen fibres. Tropocollagen type II is the dominant form in collagen fibres of almost all types of cartilage (1).

As the amount of matrix increases the chondroblasts become separated from each other and are, from this time on, located isolated in small cavities within the matrix, the lacunae. Concurrently the cells differentiate into mature cartilage cells, the chondrocytes.

1.1.2 Elastic cartilage

Elastic cartilage occurs in the epiglottic cartilage, the corniculate and cuneiform cartilage of the larynx, the cartilage of the external ear and the auditory tube. Elastic cartilage contains a dense network of delicately branched elastic fibres (1).

1.1.3 Fibrous cartilage

Fibrous cartilage is a form of connective tissue transitional between dense connective tissue and hyaline cartilage (1). Chondrocytes may lie singly or in pairs, but most often they form short rows between dense bundles of collagen fibres. In contrast to other cartilage types, collagen type I is dominant in fibrous cartilage. Fibrous cartilage is typically found in relation to joints (forming intra-articular lips, disks and menisci) and is the main component of the intervertebral disks. It merges imperceptibly into the neighbouring tissues, typically tendons or articular hyaline cartilage.

1.1.4 Articular cartilage

Articular cartilage is a specialized form of hyaline cartilage. It transforms the articulating ends of the bones into lubricated, wear-proof, slightly compressible surfaces, which exhibit very little friction. Articular cartilage is not surrounded by perichondrium. Its external portion is less cellular and more densely fibrous. The main components of the extracellular matrix of articular cartilage are type II collagens with lesser amounts of type IX and type XI, hyaluronan (HA) and aggrecan (Figure 1). 15% of the wet weight of cartilage is composed of collagen (3), which functions to provide tensile strength to the tissue and resist movement of interstitial fluid and proteoglycans from the cartilage, especially while it sustains compressional loading. Aggrecan is retained in the matrix through its interaction with HA, which is stabilized by a small glycoprotein termed link protein. The tissue's strength depends of the cross-linking of the collagen. Approximately 75% of articular cartilage matrix is water. The remainder composed of proteoglycan (2) aggregates with chondroitin sulfate and keratin sulfate as the chief glycosaminoglycans. Much of hyaline cartilage of the body ultimately progresses to bone during development.

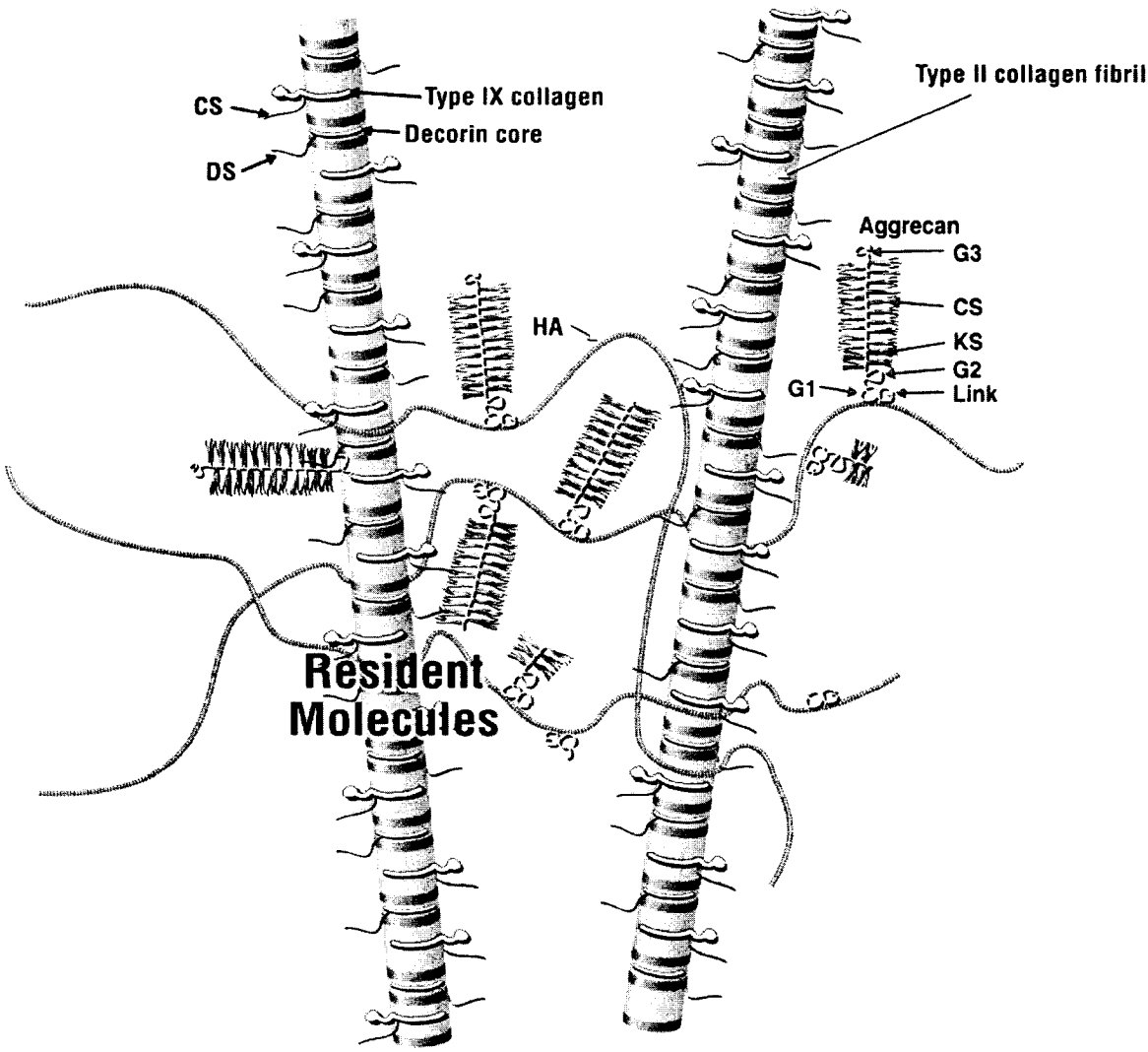

Figure 1: Organization of the cartilage matrix. This figure is drawn approximately to scale. Aggrecan is retained in the form of aggregates by binding to HA. HA interacts with collagen type II directly or through collagen type IX which is covalently bound to collagen type II. The small leucine rich repeat proteoglycans: decorin, biglycan, fibromodulin and lumican bind to collagen through their protein core in a periodic manner.

When calcification occurs, chondrocytes die and the matrix disintegrates. Articular cartilage is unique in that its more superficial zones do not calcify, except in pathologic states such as pseudogout (1).

The main source of nourishment for articular cartilage is the synovial fluid, which fills the joint cavity. Additional small amounts of nutrients are derived from blood vessels that course through the calcified cartilage close to the bone (1). Living chondrocytes have been found in small pieces of cartilage floating in the joint cavity after damage to the articular cartilage.

There are 4 zones of articular cartilage (Figure 2):

1) superficial layer (tangential zone)

This zone makes up 10% of the cartilage and consists of 2 sub-zones:

I) fibrilar sheet / lamina splendens is the more superficial layer. It is a clear film consisting of a sheet of small fibrils with little polysaccharide and no cells.

II) cellular layer with flattened chondrocytes. The flat chondrocytes and collagen fibers are arranged tangentially to the articular surface.

The superficial layer (tangential zone) is the thinnest layer, with the highest content of collagen and the lowest concentration of proteoglycans. Collagen (type IX) is arranged at right angles to adjacent bundles and parallel to the articular surface subsequently this layer has greatest ability to resist shear stresses and serves as a gliding surface for joint. The layer may also function to limit passage of large molecules between synovial fluid and cartilage. The superficial zone is the first to show changes of osteoarthritis.

2) Transitional layer

This zone allows the transition between the shearing forces of surface layer and the compressive forces in the cartilage layers. It is highly enriched in proteoglycans and chondrocytes appeared to be spherical in this zone.

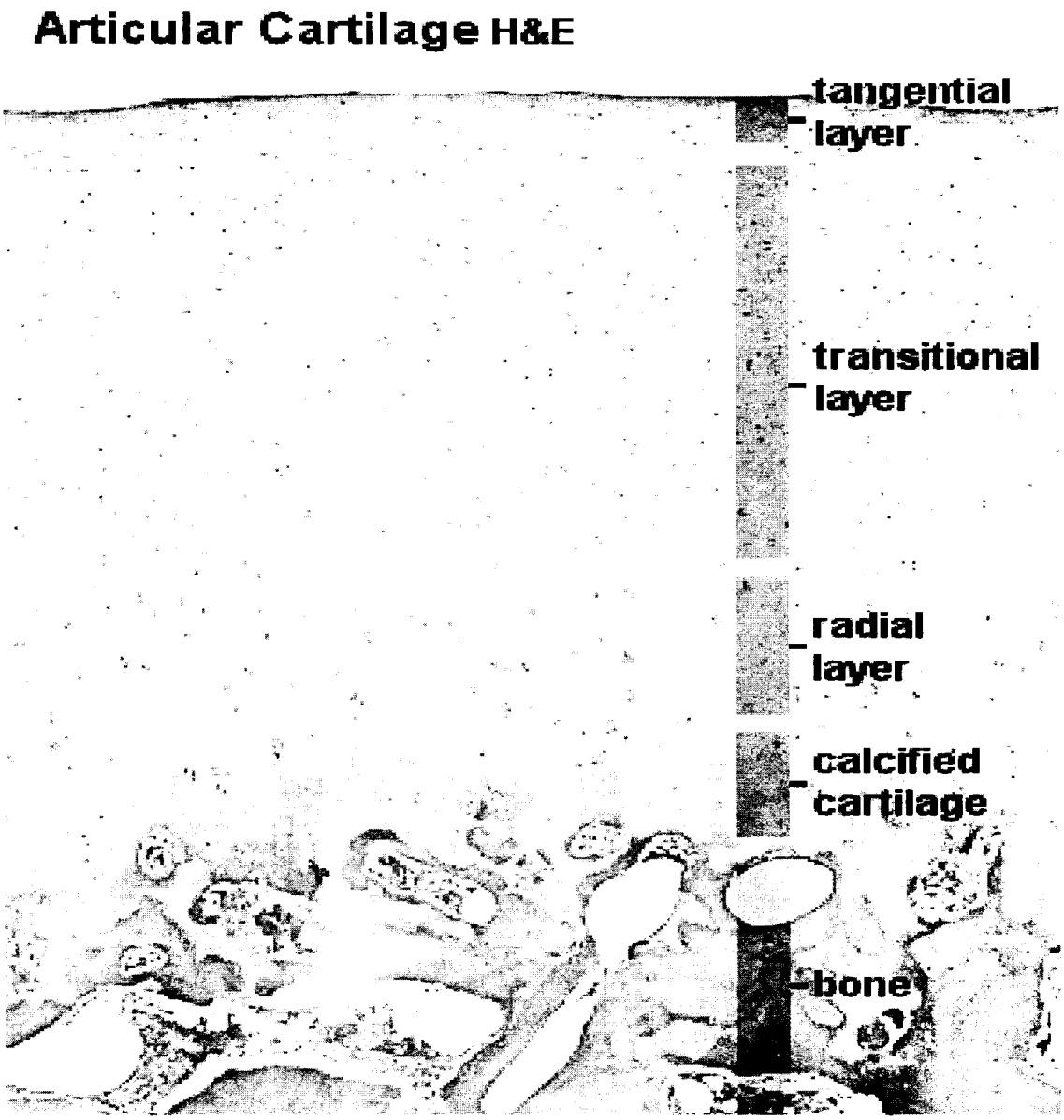

Figure 2: The 4 zones of articular cartilage (Hematoxylin and Eosin staining (H&E). The layers of articular cartilage are easiest to identify in large joints. The collagen fibres are not visible in the slide. The darker hue of the cartilage close to the bone is caused by the calcification of the cartilage. (Adapted from http://www.lab.anhb.uwa.edu.au/mb140/CorePages/Cartilage/Cartil.htm)

1) Deep radial layer

This is the largest part of the articular cartilage. It distributes loads and resists compression. Collagen fibers and chondrocytes are perpendicular to the subchondral plate in this zone.

2) Calcified cartilage layer

This zone contains the tidemark layer; a basophilic line which stradles the boundry between calcified and uncalcified cartilage. The layer separates hyaline cartilage from subchondral bone. Type X collagen is present mainly in the calcified cartilage layer and in hypertrophic zone of the growth plate.

1.2 Cartilage Development

Cartilage functions as a flexible skeletal element, providing a cushion for articular joints, acting as a template for endochondral bone formation, and allowing longitudinal growth in young animals. The differentiation and growth of cartilaginous tissues are processes vital to proper skeletal development and function. Diseases that result when these processes break down cause developmental deformities in children and cartilage degeneration in adults. The production of a functional cartilage extracellular matrix is controlled at a number of levels within and outside of the resident cells.

Cartilage is produced as an intermediate in bone formation. In vertebrates, more than 95% of the skeletal elements are formed by replacement of a cartilage template with bone. This complex process, called endochondral ossification (Figure 3), involves several differentiation steps with concomitant changes in cell morphology and gene expression. As a first step, a cartilage template is formed by the condensation of committed mesenchymal stem cells and their differentiation into chondrocytes by switching their gene expression from mesenchymal markers (e. g., type I collagen) to cartilage-specific products. In the emerging cartilaginous template of future bones, the chondrocytes

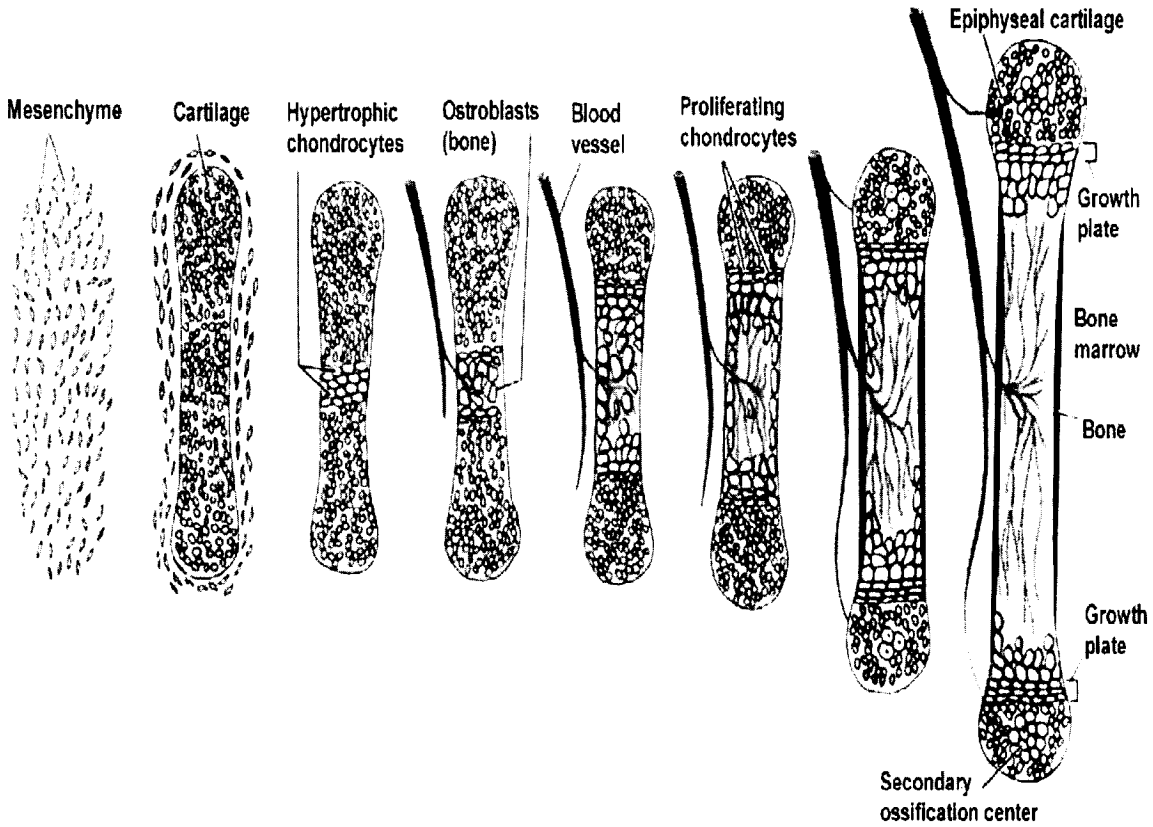

Figure 3: Endochondral ossification. Endochondral bone formation is initiated by the formation of cartilaginous bone rudiments in embryos. Thus the overall pattern of the skeletal elements is determined during the early-phase chondrogenic differentiation mediated by the mesenchymal condensation of undifferentiated cells and the subsequent proliferation of chondrocytes. In the center of the bone rudiments, cells then undergo late-phase differentiation into hypertrophic chondrocytes. The chondrocytes eventually mineralized followed by invasion of blood vessels and bone deposition.

(Image adapted from Developmental Biology, Ed. S.F. Gilbert, Sinauer Assoc. Inc., 1997)

progress through a program of proliferation, maturation and hypertrophy. Based on studies in tissue culture, three distinct chondrocyte differentiation stages can be distinguished, each characterized by the synthesis of a specific repertoire of extracellular matrix components (4).

Stage I, proliferating, chondrocytes synthesize and secrete collagens I, II, IX and XI, aggrecan and link protein (LP). The proliferative stage can be further divided into two substages. The early one (stage Ia) is associated with a high, transient expression of collagen VI genes (5), the late one (stage Ib) with the activation of the matrilin-1 (cartilage matrix protein, CMP) gene and the up-regulation of other cartilage-specific genes. Thereafter, proliferation ceases, and stage II, hypertrophic, chondrocytes appear that produce increasing amounts of collagen X and alkaline phosphatase, followed by matrix calcification (4). Finally, when hypertrophic cartilage is invaded by blood vessels and is replaced by trabecular bone, the hypertrophic chondrocytes either die or may differentiate further to osteoblast-like (stage III) cells (5). In postnatal development, endochondral ossification takes place during bone elongation in growth plates as well as in bone fracture repair by the transient formation of a cartilaginous callus. Permanent cartilage persists throughout life at certain parts of the skeleton (e.g., articular cartilage) where the terminal differentiation of chondrocytes is blocked.

The entire process of endochondral bone formation is under a strict spatio-temporal control. The sheer number of proteins that play a role in cartilage differentiation can be overwhelming. These proteins can be broken down into three major groups: growth factors, signaling molecules, and effector proteins. The first class, the growth factors, is composed of secreted proteins that initiate a cascade of events upon binding to receptors on cellular surfaces. Signaling molecules are the intracellular proteins that convert binding of the growth factor into a cellular response. These proteins are often growth factor-specific, and include membrane-bound receptors as well as intranuclear transcription factors. Lastly, the effector proteins are the downstream result of growth factor signaling. Examples include extracellular matrix proteins. An increasing number of growth factors, including IGFs, FGFs, TGF-beta's, and HGF, have been found to

associate with the extracellular matrix proteins or with heparan sulfate. Rapid and localized changes in the activity of these factors can be induced by release from matrix storage and/or by activation of latent forms. These growth factors, in turn, control cell proliferation, differentiation, and synthesis and remodeling of the extracellular matrix. Interestingly, bone morphogenic proteins (BMP) expression can be a downstream result of growth factor signaling, although they in turn have effector molecules of their own. It is sometimes difficult to distinguish a growth factor's direct effect from that of its downstream effector molecules.

Other than BMPs, activities stimulating cartilage maturation also include insulin, Insulin-like growth factor I (IGF-I) or thyroid hormone. However, late chondrocyte differentiation is mainly subject to negative control by soluble mediators derived from the cartilage itself or from surrounding tissues. These factors differentially act at several checkpoints and include transforming growth factor β (TGF-β) and parathyroid hormone-related peptide (PTHrP). In addition, proteolytic enzymes can activate or inactivate signalling mediators or mediate shedding of their receptors from the surface of the chondrocytes. Recent in vivo studies shed light on the signaling mechanisms controlling the initial events of limb development and revealed the involvement of members of the fibroblast growth factors (FGF), Wnt proteins, the Hedgehog proteins and TGF-ß families, the SRY-related HMG BOX (Sox) proteins: Sox9, Sox5, Sox6 (6,7).

According to a currently accepted model, two secreted peptides, Indian hedgehog (Ihh) and PTHrP regulate the rate and extent of endochondral bone growth in a coordinated way (8, 9). On the basis of studies of mice carrying various combinations of an *Ihh* null mutation, a *PTHrP* (parathyroid hormone-related peptide) null mutation, and a constitutively active receptor for PTHrP controlled by the *Col2a1* (Collagen II a 1) promoter/enhancer, it has been shown that an activated PTHrP receptor can rescue the abnormal maturation of chondrocytes in *Ihh*-deficient mice (10). Ihh, secreted by cells in the prehypertrophic zone, stimulates PTHrP expression in periarticular perichondrial cells (11). PTHrP appears to prevent chondrocyte hypertrophy in the growth plate and maintains a pool of cells above the hypertrophic zone in a proliferative condition (10).

The effects of PTHrP are mediated by the PTHrP receptor, a G protein–coupled receptor expressed in the proliferating and prehypertrophic cells. Thus Ihh and periarticular perichondrial PTHrP are thought to be components of a feedback loop that regulates the relative proportions of proliferating and hypertrophic chondrocytes in growth plates.

Consistent with the above control system, null mutations of *PTHrP* (12) or its receptor in mice cause a decrease in the number of proliferating growth plate chondrocytes and an increase in the hypertrophic zone, whereas overexpression of *PTHrP* has the opposite effects. In both cases, i.e. increased or decreased proliferation of chondrocytes, dwarfism is the consequence. This is demonstrated by the important role of chondrocyte hypertrophy in longitudinal bone growth. A decrease in the pool of proliferating chondrocytes leads to a decreased rate in the production of hypertrophic chondrocytes. Although the hypertrophic zone is relatively large, reduced bone growth resulted. On the other hand, a relative increase in the pool of proliferating chondrocytes leads to a decreased rate of hypertrophy, again resulting in reduced bone growth. The importance of PTHrP is also well illustrated by gene mutations in humans. Activating mutations in the *PTHrP* receptor gene cause Jansen metaphyseal chondrodysplasia with extreme abnormalities in metaphyses of long bones (13). Loss-of-function mutations in the receptor are found in Blomstrand chondrodysplasia, characterized by advanced skeletal maturation (14).

Ihh null mice have a more severe dwarfism than mice lacking *PTHrP*. This suggests that Ihh affects growth plate function in ways that are both dependent and independent of PTHrP and its receptor (10). One independent effect appears to be a direct stimulatory action on chondrocyte proliferation, the other is on osteoblast differentiation in cells of the innermost layer of the diaphyseal perichondrium. In fact, it appears that Ihh is a major positive regulator of chondrocyte proliferation. How Ihh is regulated and restricted to prehypertrophic chondrocytes is not clear, but several factors, both positive and negative, may play a role. Signaling through retinoic acid receptors may also play a role because a retinoic acid induced gene, *Stra6*, is expressed in a belt-like region around the growth plates at the level of Ihh-producing prehypertrophic chondrocytes (18). Finally, a

hedgehog-interacting protein in cartilage may attenuate Ihh signaling in growth plates by directly binding to Ihh (19).

The precise role of FGFR3 and its ligands in growth plate cellular kinetics is of particular importance as demonstrated by the range of human bone disorders that are caused by mutations in this receptor tyrosine kinase (20). Activating mutations in *FGFR3* cause achondroplasia, the most common dwarfism in humans, as well as other related phenotypes, such as hypochondroplasia, thanatophoric dysplasia, and Crouzon syndrome with acanthosis nigricans (21, 22, 23, 24). The growth-retarding effects of these mutations, as well as a number of experimental studies in mice and cell culture, show that signaling through FGFR3 inhibits chondrocyte proliferation and Ihh expression (15). Conversely, targeted deletion of *Fgfr3* in mice leads to skeletal overgrowth (25).

In addition to the above findings, however, regulation of chondrocyte differentiation is known to involve other endocrine, paracrine and autocrine signals as well as cell-matrix interactions (reviewed in Cancedda et al., 1995). Yet, the complexity of the entire multi-step process as well as its regulatory principles are poorly understood at the molecular level. It is not clear, for example, why terminal differentiation of chondrocytes is blocked in permanent cartilage, whereas it can proceed during the formation of other skeletal elements. There remain more regulatory circuits to be characterized. As far as the global transcriptional profiles are concerned, only a few investigations have aimed at monitoring changes in the expression levels in a temporal fashion. Further studies are thus needed to obtain a complete and definitive picture of the evolution of the transcriptome during cartilage development.

1.3 Marker Genes in Cartilage Development

During embryonic development of long bones through endochondral bone formation, chondroprogenitor cells exhibit the transitions of phenotype from type I collagen expressing cells to type II collagen and aggrecan-expressing chondrocytes through cellular condensation (early-phase differentiation) and then to type X collagen-expressing mineralizing chondrocytes (late-phase differentiation).

1.3.1 Proteoglycans

Proteoglycans constitute a family of complex macromolecules characterized by the presence of one or more glycosaminoglycan (GAG) chains covalently linked to a polypeptide backbone. Although originally named and categorized on the basis of the GAG substituent, they are increasingly being viewed as products of gene families that encode the different core proteins. Proteoglycans are found predominantly in the extracellular matrix (ECM) or associated with the cell surface of most eukaryotic cells where they bind to other matrix- and cell-associated components and growth factors (26). The interactive ability of proteoglycans derives from the chemical and structural diversity of either (or both) the polysaccharide or core protein components.

There has been significant progress in the molecular characterization of several proteoglycans as well as in the identification of novel family members, localizations, and biological functions. The importance of proteoglycans as constituents of the ECM and cell surface milieu is illustrated by the drastic change in their expression during development of several tissue systems and in certain disease processes, most notably heritable disorders of the skeleton known as chondrodysplasias.

The proteoglycans are composed of GAG chains consisting of repeated disaccharides, which usually contain a sulfated hexosamine and uronic acid, covalently linked to a central protein core. Type, size, and composition of GAG chains, primary sequence and domain arrangement of the protein core, or degree of substitution and distribution of the GAG chains along the protein core may all vary, leading to proteoglycan structures that are complex and diverse. Hybrid molecules with additional structural diversity may arise by substitution with N- and O-linked glycoprotein-type oligosaccharides or by having more than one type of GAG chain attached to the same core protein. Although there are features common to the GAGs, six distinct classes are recognized based on differences in monosaccharide composition, sulfation, and epimerization of the uronic acid. Four GAG classes—chondroitin sulfate, dermatan sulfate, heparin, and heparan sulfate—are linked to serines of the protein core via a common tetrasaccharide (xylose-galactose-galactose-

glucuronic acid). In addition to the above, keratan sulfate, a proteoglycan from the family of leucine-rich core proteins are often found to aggregate with chondroitin sulfates

The predominant GAG in cartilage is chondroitin sulfate and the major chondroitin sulfate proteoglycan is aggrecan. Aggrecan, together with versican, neurocan ad brevican form the family of large aggregating proteoglycans. Versican has a wide tissue distribution and can be found in articular cartilage, however neurocan and brevican are largely restricted to nervous tissues. All of the proteoglycans mentioned interact with hyaluronan (HA) and the interaction is stabilized by a small glycoprotein termed link protein.

1.3.1.1 Proteoglycans expression during cartilage development

During skeletal development different proteoglycans are expressed in a highly defined pattern that is regulated spatially and temporally. Versican is expressed in the undifferentiated mesenchymal cells of the early limb bud and during the onset of prechondrogenic condensation, then disappears with the differentiation to cartilage (29, 30). This process is inversely correlated with a dramatic upregulation of the cartilage-specific chondroitin sulfate proteoglycan (CSPG), aggrecan, during the establishment and maturation of the chondrocytic phenotype (31).

The process of cartilage formation, chondrogenesis, begins with the outgrowth of limb buds early in embryogenesis. Differentiation of limb bud commences with condensation of mesenchymal cells to form a cartilage primordium, which initiates the secretion of cartilage-specific ECM components. After a period of rapid cell proliferation, the chondrocytes in the center of these cartilaginous elements exit the cell cycle and differentiate to hypertrophic chondrocytes. These chondrocytes undergo apoptosis as their matrix is degraded by the invading vascular tissue, which introduces osteoblasts to initiate bone matrix formation. Chondrocytes also organize their pericellular matrix, composed of type II collagen and aggrecan, in tight association with their cell surface. Aggrecan molecules interact with filaments of hyaluronan to form proteoglycan aggregates, an interaction that is further stabilized by a small glycoprotein. Hyaluronan also interacts

with a cell surface receptor, CD44, which has been suggested to facilitate the assembly and retention of the aggrecan-rich matrix at the surface of chondrocytes (33).

Aggrecan represents the bulk of the proteoglycans expressed during endochondral differentiation. Bone has a low content of fibromodulin, a small keratan sulfate proteoglycan from the family of leucine-rich core proteins. Heparan sulfate proteoglycans (HSPG) are also present in the developing limb at early stages before differentiation of chondrocytes from mesenchyme. The large basement membrane HSPG, perlecan, and syndecan are widely distributed in early limb mesenchyme at many sites in addition to basement membranes (33, 34); later they are reduced in the regions destined for chondrogenesis and become localized in myogenic regions. Perlecan is also localized to developing cartilage, with a low level of expression in precartilaginous condensations and accumulation in cartilage primordia preceded by that of collagen type II (35). The specific roles of HSPGs and assembled binding partners in cartilage development and growth are still largely unknown.

1.3.1.2 Aggrecan

Aggrecan is the shortened name of the large aggregating chondroitin sulphate proteoglycan. Aggrecan, which is one of the most widely studied proteoglycans, is abundant; it represents up to 10% of the dry weight of cartilage (articular cartilage is up to 75% water).

There can be some confusion about the use of the term aggrecan, and to what it refers to. Many individual monomers of aggrecan bind to hyaluronan to form an aggregate, it is the monomer which is termed aggrecan (Figure 4). These aggregates are comprised of up to 100 monomers attached to a single chain of hyaluronan (HA).

An aggrecan monomer consists of a protein backbone of 210-250 kDa to which is attached both chondroitin sulphate and keratan sulfate chains. The chains are attached to the central portion of the core protein, chondroitin sulphate chains (100 - 150 per monomer), being located in the C terminal 90%, while the keratan sulphate (30 - 60 per monomer) is preferentially located towards the N terminus (2).

Individual aggrecan monomers interact with hyaluronan to form an aggregate of very high molecular weight. This interaction involves a globular domain at the N-terminus,

termed G1 or the hyaluronic acid binding region (HABR). The interaction is stabilised by a short protein called link protein which interacts with both the HA and G1.

There is considerable sequence homology between link protein and G1, and with G2, a further globular domain close to G1 on the aggrecan core protein, termed G2. Although it

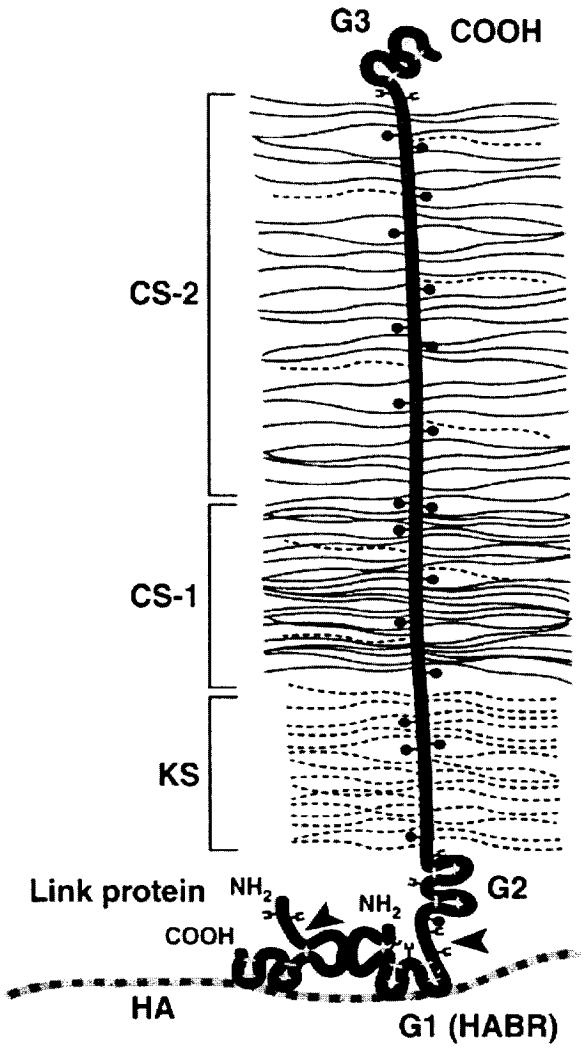

Core protein
Chondroitin sulfate (CS) chain (n = 100); CS-1 & CS-2 domains
Keratan sulfate (KS) chain (n = 30)
HA, hyaluronan / hyaluronic acid
N-linked oligosaccharides
O-linked oligosaccharide (n = 42)
Primary sites of cleavage

Figure 4: The aggrecan aggregate. Aggrecan binds to HA through its G1 domain (Globular domain 1). Link protein stabilizes this interaction. Link protein has structure that is similar to the G1 domain of aggrecan.

is not involved in the binding with either link protein or hyaluronic acid, it shares considerable sequence homology with G1. A function for G2 has not been identified.

A third globular domain, G3, is located at the C-terminus, and has three structural domains: an Epidermal Growth Factor (EGF) repeat, a lectin-like sequence, and a region homologous to the complement regulatory protein (CRP) motif. The lectin-like domain appears to be present in all forms of the molecule, while the EGF and CRP like domains are only present in an alternatively spliced variant (2).

G3 is found to be required for passage of the newly synthesized proteoglycans out of the cell. The lectin-like sequence of G3 can bind to fructose and galactose.

The primary role of aggrecan appears to be a physical one, as it brings about an osmotic swelling and maintains the high levels of hydration in the cartilage extracellular matrix (2). In this way aggrecan plays a crucial role in the normal function of articular cartilage, which is found at the ends of long bones.

The extracellular matrix of articular cartilage is comprised of fibril forming collagens, aggrecan and many other important molecules. The fibrillar collagens form a network which has a very high tensile strength, and which entraps the aggrecan molecules. The presence on aggrecan of a very large numbers of chondroitin sulphate chains generates an osmotic swelling pressure. It is this which accounts for the wet weight of articular cartilage being 75% water.

During resting, such as sitting down and reading, the osmotic swelling is at a maximum, and is contained only by the collagen network. However, during loading, such when one stands up or walks, the weight of the body is supported by the cartilagenous ends of the

long bones. In this state ones's weight compresses the cartilage, the water is literally redistributed. This continues until the osmotic swelling generates a force equal to the compressive force generated by one's weight which it supports. When the load is removed, one sits down again, the compressive force is removed, and the cartilage swells to it's full extent. This osmotic swelling is brought about by the glycosaminoglycan chains attached to the aggrecan core.

1.3.2 Collagens

Collagens, the most abundant proteins in the human body, constitute a multigene family of extracellular matrix proteins. In addition to providing mechanical strength for various organs and tissues, they have a number of other important biological functions. Currently 27 collagen types with at least 42 distinct polypeptide chains have been identified, and their genes are dispersed among at least 15 chromosomes. In addition, more than 20 proteins with collagen-like domains have been identified (37).

All collagen molecules are built up of three polypeptide chains, called α-chains, containing the repeating triplet sequence Gly-X-Y, where X and Y represent amino acids other than glycine. These α-chains then wind together to form a triple helix. The presence of glycine in every third position is essential because it is small enough to fit into the restricted space in the center of the triple helix. Proline is commonly found in the X position and 4-hydroxyproline in the Y position of the Gly-X-Y triplets. These two amino acids are essential for the collagen molecule, in that they provide stability for the triple helix (38).

Collagens provide the structural framework of bone and cartilage and are responsible for shape and biomechanical properties such as resistance to pressure, torsion or tension. Collagens can be grouped into several different families based on their diverse structural features and supramolecular organisations. These families consist of the fibril-forming collagens, Fibril Associated Collagens with Interupted Triple helices (FACIT) collagens, network-forming collagens, basement membrane collagens, transmembrane collagens, microfibrillar collagens and multiplexins (37). Not all of them are found in bone and cartilage, where fibril-forming collagens predominate.

Collagen heterofibrils consisting of types I and type V constitute the fibrillar backbones in bone while collagen type II and collagen type XI provide a similar function in cartilage. In cartilage, the collagen fibrils are often decorated with the FACIT collagen type IX. In the territorial region, close to the cell, collagen type VI forms a network of beaded filaments. In hypertrophic cartilage of the growth plate, a network-forming collagen, type X, plays a key role in this calcifying matrix (37).

The fibrillar organisation of collagen II varies in different compartments. Regulating factors in the formation of the collagen network includes a number of matrix proteins e.g. fibromodulin, lumican, decorin, biglycan, chondroadherin and others (36, 37). The keratan sulphate-rich domain of aggrecan appears to have a role in the pericellular-territorial region (2). It should be emphasized that the surface of the collagen fibre in the tissue is modified by a number of proteins bound at specific sites. These include most of those mentioned above that influence fibril formation.

Since collagens contribute 90% of the dry mass of the major organic component in bone and 60% of the dry mass of the major organic component in cartilage, it may be envisaged that defects in structure, biosynthesis, assembly, turnover and interactions with other matrix proteins may cause some of the serious connective tissue disorders such as most cases of osteogenesis imperfecta as well as in certain cases of osteoporosis, osteoarthritis and chondrodysplasias (38).

1.3.2.1 Collagens expression during cartilage development

Chondrocytes produce several cartilage-specific collagens including the most abundant, type II collagen, as well as other minor collagens, types IX, X and XI. Type I collagen is present at the onset of chondrogenesis, but then becomes undetectable at later stage. Type X collagen is specific for hypertrophic cartilage and is developmentally regulated.

Expression of collagens is regulated by transcription factor of the Sox proteins family. *Sox9* is a member of a large family of transcription factors that contain an *SRY*-related (sex-determining region Y gene) HMG (high-mobility-group) DNA binding region (39). About 20 *Sox* genes have been identified, and they all share at least 50% identity within the 79-amino acid residue-long HMG domain (40). Despite the high homology within the HMG domain, little similarity is found among *Sox* genes outside the DNA-binding motif. Two other members of the family, *L-Sox5* and *Sox6*, are also involved in *Col2a1*

expression. They appear to form a large complex with *Sox9* and other nuclear proteins in chondrocytes, and *L-Sox5* and *Sox6* transcripts are coexpressed with *Sox9* at all chondrogenic sites (41). It is, therefore, believed that the three *Sox* genes cooperatively activate the *Col2a1* gene.

Sox9 is required for expression of cartilage-specific extracellular matrix components such as collagen II, collagens IX and XI, and the large proteoglycan aggrecan (39). The binding of Sox9 to the *Col2a1* first intron enhancer directly activates *Col2a1* expression in cell culture and in transgenic mice (36, 38). No chondrocyte-specific markers are expressed in *Sox9* null cells in mouse chimeras (39). Although the cells participate in mesenchymal condensations, *Sox9* null cells remain in the perichondrium and do not differentiate into chondrocytes in such chimeras.

Endochondral ossification is the process by which the skeletal cartilage anlagen are replaced by bone (42). The anlagen elongate and expand in width by proliferation of chondrocytes, as well as by deposition of cartilage matrix. Shortly after their formation, chondrocytes in the central region of the cartilage undergo further maturation to hypertrophic chondrocytes, which exit the cell cycle and synthesize an extracellular matrix that is different in composition from that of proliferating cartilage. Collagen X, extensively used as a marker for chondrocyte hypertrophy, is a unique component of this matrix.

1.3.2.2 Type I Collagen

When the term collagen is used, it usually means type I collagen, the most common of the collagens in vertebrates. It comprises up to 90% of the skeletons of the mammals and is also widespread all over the body: in addition to bones, it is found in skin, tendons, ligaments, cornea, intervertebral disks, dentine, arteries and granulation tissues as the main locations. Even cartilage, which mainly contains type II collagen, has been mentioned to contain some type I collagen.

Type I collagen molecules give the tissues their mechanical strength and provide the major biomechanical scaffold for cell attachment and anchorage of macromolecules. Many macromolecules such as integrins, fibronectin, fibromodulin and decorin attach to

type I collagen. Type I collagen also interacts with many cells, such as fibroblasts, and with platelets during blood clotting. In bones and dentin type I collagen is mineralized with hydroxyapatite crystals. The process is mediated by non-collagenous proteins after decorin molecules have been removed from the newly-synthesized collagen molecules (37). If the type I collagen gene is mutated, it leads to several forms of osteogenesis imperfecta (OI), characterized by brittle bones, Ehlers-Danlos syndrome (EDS), characterized by hypermobility of joints and abnormalities of skin, or Marfan syndrome, characterized by abnormalities in arteries (43).

Extracellular matrix components of cartilage and bone have critical roles in skeletal development. This is illustrated by the large number of skeletal dysplasias secondary to mutations in matrix molecules. Heterozygous mutations in *COL1A1* and *COL1A2*, the genes coding for the α1(I) and α2(I) chains of collagen type I, respectively, cause OI (44). Mutations that affect the C-terminal propeptide of procollagen type I chains prevent the incorporation of the mutant chain into trimeric molecules and result in the mildest phenotypes. Patients with more severe phenotypes generally have point mutations in the triple-helical domain of either the α1(I) or α2(I) chains that change the codon for glycine to that of a bulkier amino acid residue (37).

1.3.2.3 Type II Collagen

Type II collagen, a homotrimer encoded by *COL2A1*, is the major structural collagen component of cartilage, vitrous of the eye, the nucleus pulposus of intervertebral discs, and the tectorial membrane of the ear. Type II collagen is found in all cartilages and is essentially used to define the phenotype of the tissue. The precursor form of type IIA pro-collagen is synthesized by chondroprogenitor cells. This form of type II pro-collagen binds to bone morphogenetic proteins and acts as a regulator of cartilage induction in the extracellular matrix.

Mutations in type II collagen cause a spectrum of diseases known as type II collagenopathies (46). Their severity ranges from lethality (achondrogenesis type II, hypochondrogenesis) to severe dwarfism (spondyloepiphyseal dysplasia congenita, Kniest dysplasia), as well as normal stature with early-onset osteoarthritis (Stickler

syndrome and others) (47). Patients with *COL2A1* mutations may have retinal detachment and hearing loss in addition to cartilage involvement. Mutations that cause a moderately severe phenotype generally result from reduced secretion of type II collagen into cartilage.

1.3.2.4 Type X Collagen

Type X collagen, a member of the short chain collagen family, is a homotrimeric molecule expressed by hypertrophic chondrocytes during endochondral ossification. Transgenic mice, expressing a large in-frame deletion in the central triple-helical domain of collagen X, develop spondylometaepiphyseal chondrodysplasia after birth (48). In humans, mutations in *COL10A1* have been shown to cause the autosomal dominant disorder Schmid metaphyseal chondrodysplasia, which is characterized by bowing of the legs, growth retardation of the lower extremities, and coxa vara (49). All the mutations found are clustered in the C-terminal nontriple-helical NC1 domain of the molecule, and mutant chains neither participate in the formation of trimeric molecules nor are secreted by the chondrocytes (50).

1.4 Chondrodysplasias

The chondrodysplasias are a group of rare disorders of cartilage that cause the skeleton to develop abnormally. In chondrodysplasias, the growth plate, which contains cartilage, does not make new bone cells (1). Thus, growth of bone is impaired.

Each type of chondrodysplasia produces different symptoms. Chondrodysplasias usually cause short stature (dwarfism). Some cause more shortening of the limbs than the trunk (short-limbed dwarfism); others cause more shortening of the trunk than the limbs. Some children and adults have short limbs, bowlegs, a bulky forehead, an unusually shaped nose (saddle nose), and an arched back. Sometimes, joints do not develop the capacities for their full range of motion.

A doctor usually makes the diagnosis based on the symptoms, physical examination, and x-rays of the bones. Sometimes the abnormal genes responsible for chondrodysplasias can be detected, usually by genetic analysis which is most helpful for predicting the disease before birth. Diagnosis of severe types before birth is also possible using other methods; in some cases, the fetus can be directly viewed with a flexible scope (fetoscopy), or an ultrasound is performed. Surgery may be needed to replace joints that have severely restricted movement with artificial ones.

There are a few types of chondrodysplasias identified in human.

1) Hereditary deforming chondrodysplasia: former name for multiple cartilaginous exostoses (1).

This is an autosomal dominant disorder characterized by exostoses near the extremities of diaphyses of long bones, which may be cartilaginous or osteocartilaginous growths; it is generally benign, although sarcomatous changes have occurred (1).

2) Metaphyseal chondrodysplasia, also termed cleidocranial dysplasia/dysostosis

This is a rare autosomal dominant condition in which there is defective ossification of fetal cartilages, the cranial bones, with large fontanels and delayed closing of the sutures; complete or partial absence of the clavicles, so that the shoulders may be brought together, or nearly together, in front; wide pubic symphysis; short middle phalanges of the fifth fingers; and dental and vertebral anomalies. The Schmid type of metaphyseal chondrodyplasia (MCDS) is characterized by short stature, widened growth plates, and bowing of the long bones. It results from autosomal dominant mutations of *COL10A1*, the gene which encodes α1(X) chains of type X collagen (51).

3) Chondrodysplasia punctata (CDP)

This is a heterogeneous group of bone dysplasias, the common characteristic of which is stippling of the epiphyses in infancy. The group includes a severe autosomal recessive form (rhizomeric dwarfism), an autosomal dominant form (Conradi-Hünermann syndrome), and a milder X-linked form (1). The term, "chondrodysplasia punctata"(CDP) denotes a pattern of abnormal punctate calcification of dystrophic epiphyseal cartilage

and certain other cartilaginous structures, such as the larynx. CDP occurs in a variety of genetic disorders associated with skeletal dwarfism and can also be caused by prenatal exposure to warfarin (1). Although the most studied clinical syndrome with CDP, rhizomelic chondrodysplasia punctata (RCDP), is known to be caused by several different abnormalities of plasmalogen biosynthesis, there are many other genetic disorders with CDP for which the biochemical cause is unknown. Because patients with Smith-Lemli-Opitz syndrome, a primary disorder of sterol biosynthesis, often have rhizomesomelic limb shortness and, less commonly, CDP, the group of Kelley in The Kennedy Krieger Institute and the Departments of Pediatrics and Neurology, Johns Hopkins University School of Medicine, assessed sterol levels and metabolism in patients with different clinical forms of CDP. By quantitative sterol analysis of a variety of tissues, they identified 5 patients with similar radiological findings and abnormally increased levels of 8-dehydrocholesterol and cholest-8(9)-en-3β-ol, suggesting a deficiency of 3β-hydroxysteroid-Δ^8,Δ^7-isomerase, a principal enzyme of cholesterol biosynthesis (52). Cultured cells available from one patient showed increased levels of the same two sterols, decreased synthesis of cholesterol, and a pattern of inhibition by triparanol and AY-9944 consistent with a deficiency of 3β-hydroxysteroid-Δ^8,Δ^7-isomerase. Clinical diagnoses among the 5 patients included X-linked dominant Conradi-Hünermann-Happle syndrome and nonspecific lethal CDP. They concluded that abnormal cholesterol biosynthesis is a characteristic of some clinical syndromes with rhizomesomelic dwarfing and CDP. (52)

1.5 *Gonzo* (goz) Zebrafish Mutant

In the late 1980s, Christiane Nüsslein-Volhard, a researcher at the Max Planck Institute for Developmental Biology in Tübingen, Germany and one of the fruit fly scientists who won the 1995 Nobel prize, convinced colleagues that they should conduct a large-scale mutant hunt in an attempt to find the genes, an estimated 2,000 to 5,000, involved in normal zebra fish embryogenesis.

That ambitious effort, undertaken in parallel by the groups in Tübingen and Satler in Boston, has now paid off. Though the screens fell quite short of hitting every gene,

researchers examined millions of embryos, ultimately identified mutations in about 600 specific genes, and have already described more than 300 of the most interesting mutants. The *Gonzo* (goz) mutant is one of them because it displays a chondrodysplasia phenotype.

Gonzo is a zebrafish mutant with defects in cartilage formation (53). The mutant displays phenotypes similar to human chondrodysplasias. They have smaller head skeleton than the wild-type and all cartilage elements, including Meckel's cartilage are smaller in the *goz* mutants (Figure 5). At 5 days post fertilization, all of the skeletal elements in *goz* homozygotes larvae are present but consist of chondrocytes that are smaller in size and align in an irregular way, unlike typical single cell rows seen in wild-type embryos (Figure 5). The *goz* homozygotes larvae at this stage also showed extracellular matrix defects. Unlike wild-type embryos that show homogeneous distribution of proteoglycans in the cartilage, proteoglycans in the *goz* homozygotes larvae are absent in the extracellular matrix of the mutant's cartilage and appear to accumulate ectopically next to cartilage elements (Figure 6). The *goz* mutant has irregular collagen type II aggregates accumulation that are located in the cartilage matrix of all cartilage elements, around the otic vesicle and the notochord (Figure 7). In the wild-type embryos, the cartilage matrix protein collagen II is distributed homogeneously around the chondrocytes, the otic vesicle and the notochord (Figure 7).

Although the collagen II protein is present in aggregate in *goz* mutant, the expression of the collagen II mRNA does not differ to that of the wild-type's, suggesting that collagen II defects in *goz* is caused post-transcriptionally (53).

Lipid metabolism is also affected in *goz* mutant. This is similar to Smith-Lemli-Opitz syndrome, a severe human chondrodysplasia, caused by deficiencies in cholesterol metabolism during embryogenesis. In wild-type zebrafish embryos, lipids were found in high concentrations aound the eye, the otic vesicle and the olfactory placodes at 48 hour post-fertilization (Figure 8). When the trabeculae of the neurocranium developed at this stage, high lipid concentrations were also observed in the head of the wild-type zebrafish

embryos (Figure 8). However in *goz* mutant, much lower lipid concentrations were observed around and in the areas mentioned above (Figure 8).

Positional cloning identified the mutated gene responsible for the *goz* mutant and this encodes zebrafish site-1 protease (S-1P)/subtilisin kexin isoenzyme-1 (SKI-1).

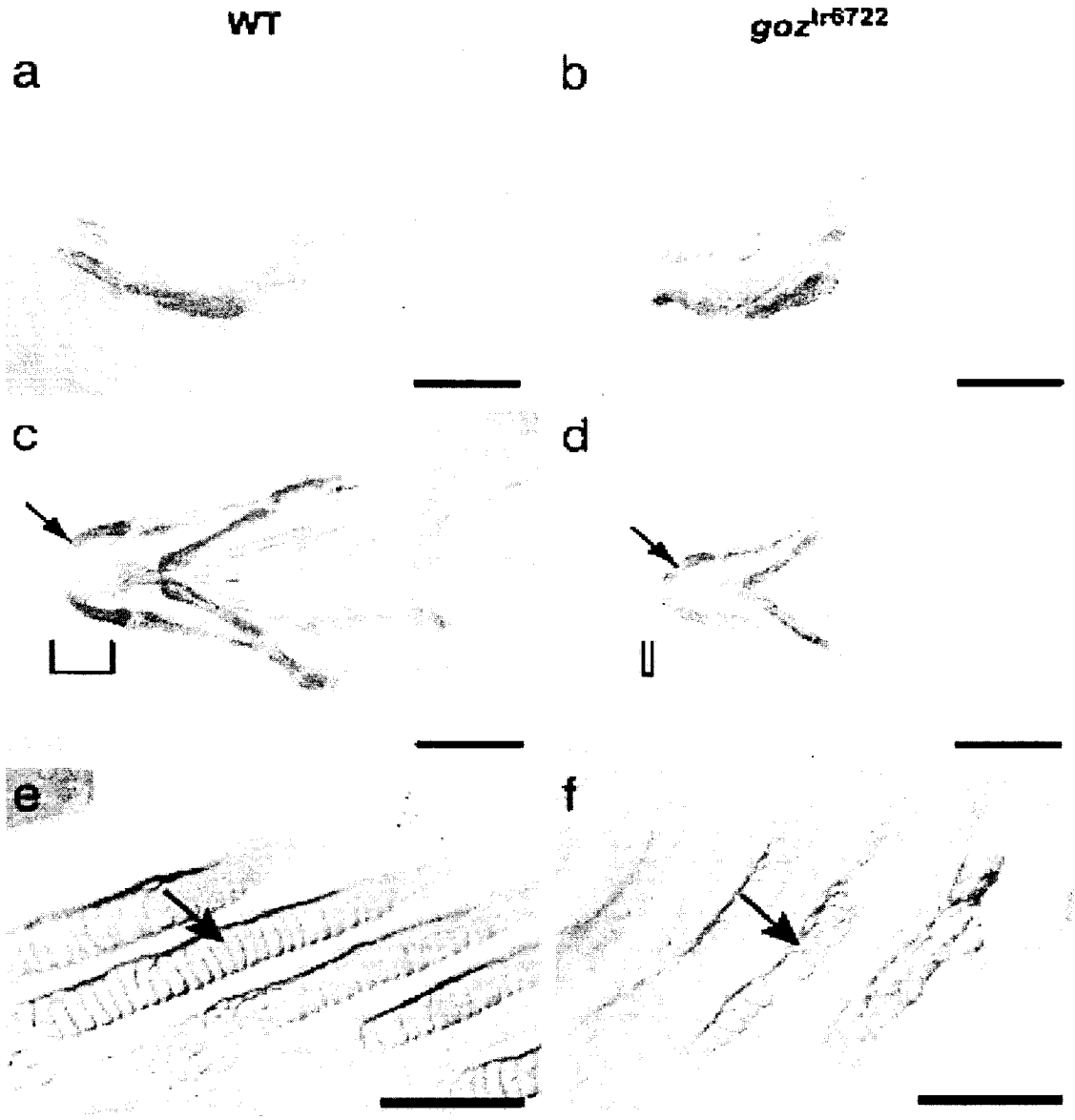

Figure 5: Cartilage defects in *goz*. Alcian Blue staining of sibling larvae (*a*, *c*, and *e*) and *goz* larvae (*b*, *d*, and *f*) at 5 days post fertilization (dpf) is shown. (*a* and *b*) Lateral view. (*c* and *d*) Ventral view of the head. (*e* and *f*) Enlargement of the branchial arches.

Cartilage matrix staining is slightly reduced in *goz* mutants. All cartilage elements, including Meckel's cartilage (arrows in *c* and *d*), are smaller in the mutant. Tissue anterior to the eyes is missing (bars in *c* and *d*). The columnar arrangement of chondrocytes in the branchial arches is disrupted in *goz* mutants (arrows in *e* and *f*). (Scale bars are 200 μmin *a–d* and 50 μmin *e* and *f*.) (Adapted from Schlombs, Kornelia et al. (2003) Proc. Natl. Acad. Sci. USA 100, 14024-14029)

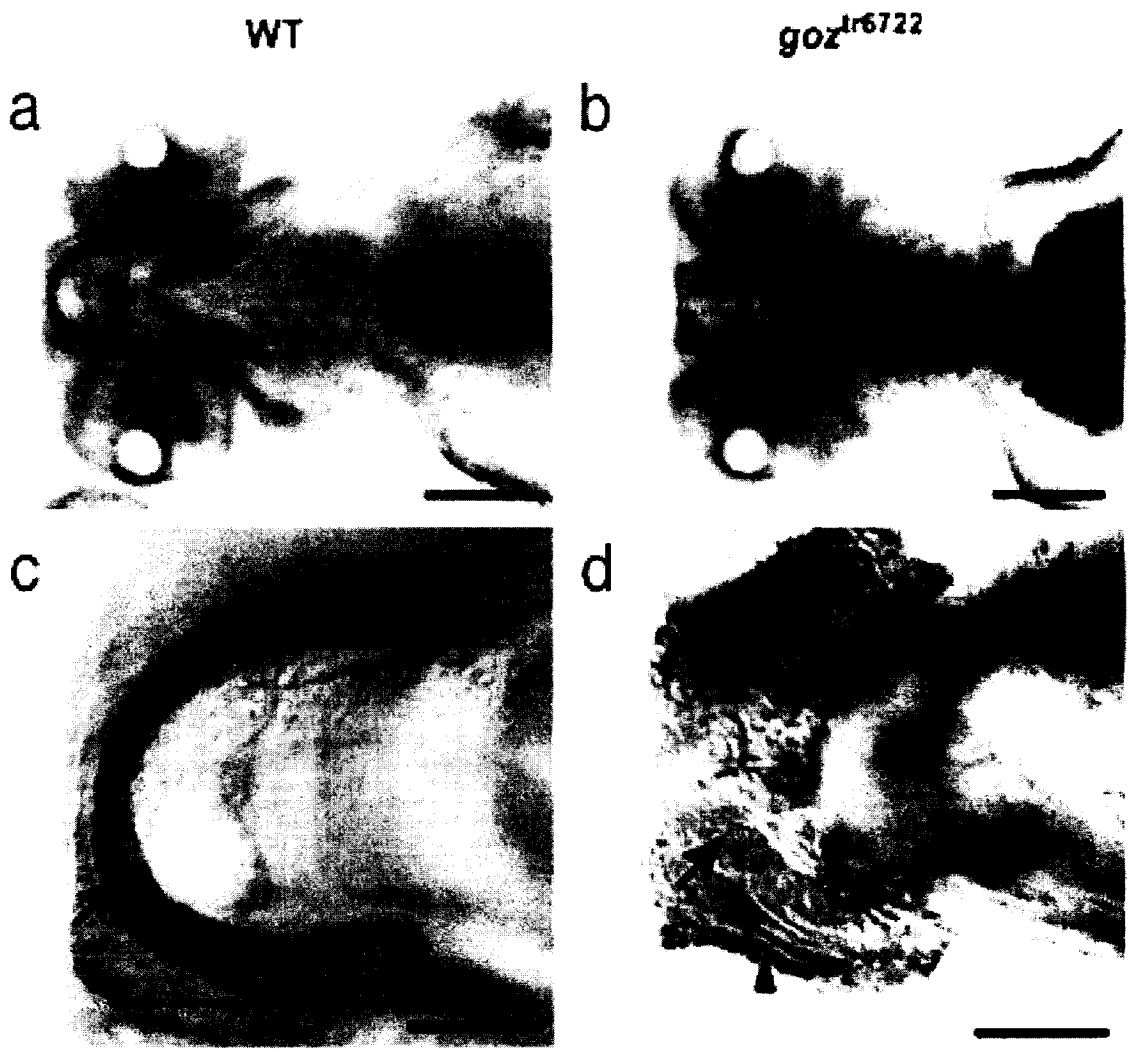

Figure 6: Proteoglycan phenotypes in *goz*. Wheat germ agglutinin staining of matrix proteoglycans in wild-type (WT) sibling larvae (*a* and *c*) and *goz* larvae (*b* and *d*) at 5 dpf. (*a* and *b*) Ventral view. (*c* and *d*) Enlargement of Meckel's cartilage. Proteoglycans

are homogeneously stained in the cartilage matrix of sibling larvae (*a* and *c*). This staining is absent in the cartilage matrix of *goz* (arrow in *d*) where proteoglycans seem to accumulate ectopically (arrowheads in *b* and *d*). (Scale bars are 200 μm in *a* and *b* and 50 μm in *c* and *d*.) (Adapted from Schlombs, Kornelia et al. (2003) Proc. Natl. Acad. Sci. USA 100, 14024-14029)

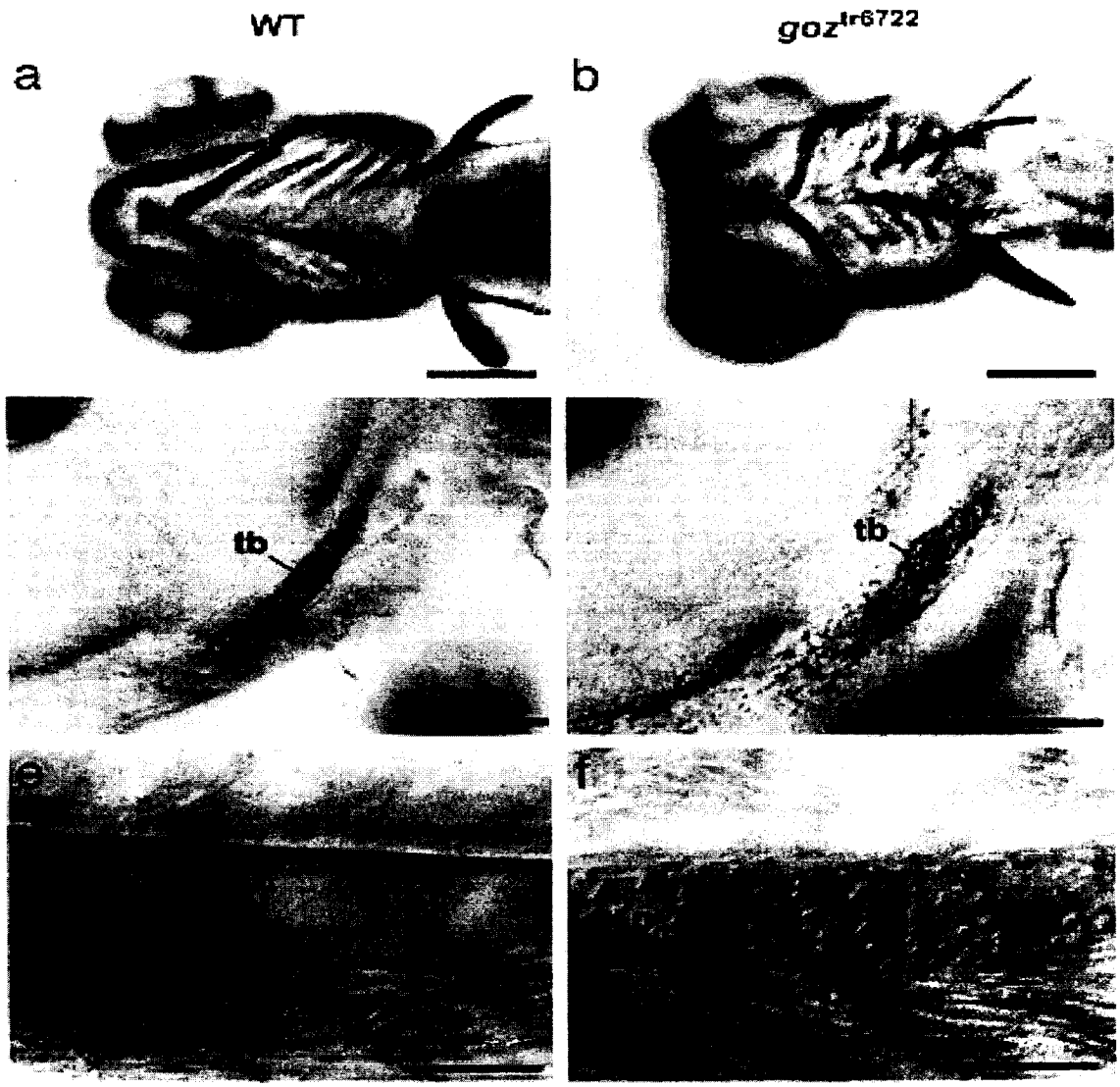

Figure 7: Col II defects in *goz*. Immunohistological staining of Col II in wild-type (WT) sibling larvae (*a*, *c*, and *e*) and *goz* larvae (*b*, *d*, and *f*) is shown. (*a* and *b*) Ventral view of the head 5 dpf. (*c* and *d*) Enlargement of the trabeculae (tb) of the neurocranium (lateral view) at 2 dpf. (*e* and *f*) Enlargement of the notochord (n) in the tail at 2 dpf. Cartilage matrix is homogeneously stained in sibling larvae (*a*, *c*, and *e*), whereas abnormal protein aggregates can be seen in the cartilage matrix and around the notochord in *goz* larvae (*d* and *f*). (Scale bars are 200 μm in *a* and *b* and 50 μm in *c–f*.) (Adapted from Schlombs, Kornelia et al. (2003) Proc. Natl. Acad. Sci. USA 100, 14024-14029)

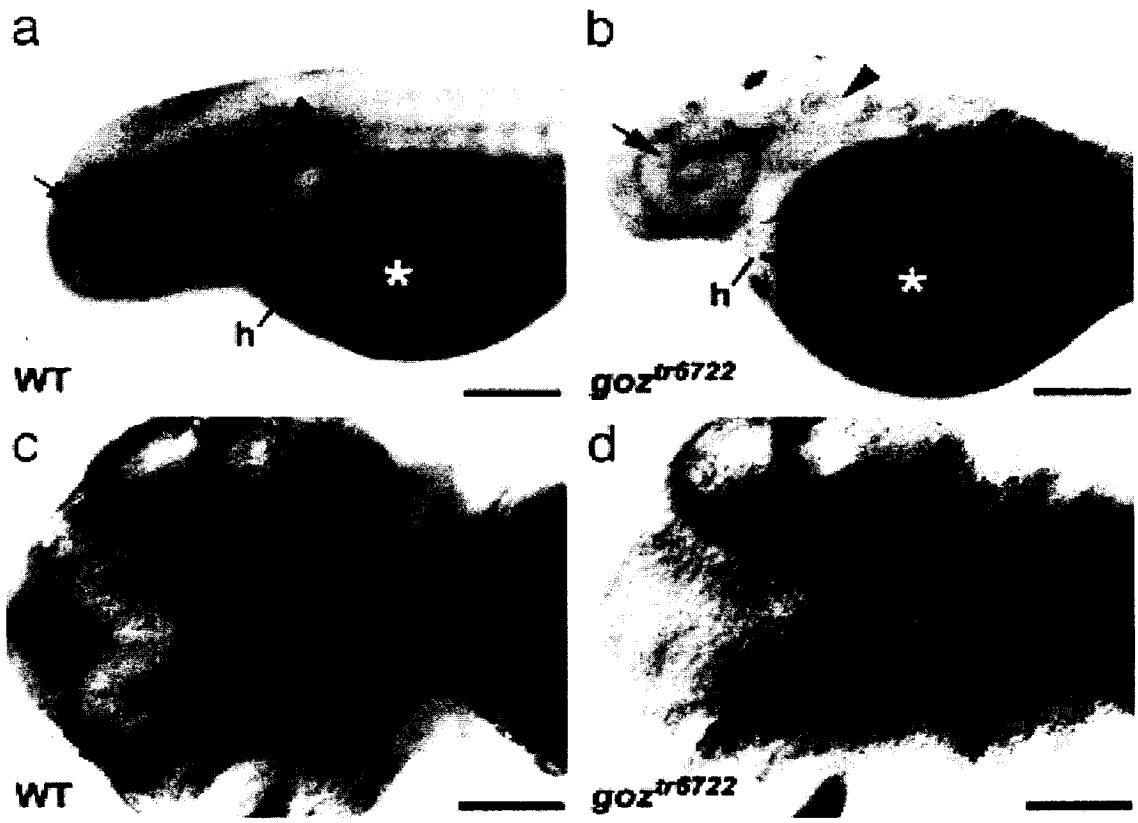

Figure 8: Lipid defects in zebrafish *S-1p* mutants. Oil red O staining of 48 hpf zebrafish larvae. (*a* and *b*) Lateral view. (*c*and *d*) Ventral view. *goz* (*b* and *d*) and sibling (*a* and *c*) larvae and larvae injected with 6 ng of *s2p2* (S-2P2 oligoneucleotide). Strong lipid staining can be observed around the eye (arrow), the otic vesicle (arrowhead), and in the heart (h) of sibling larvae (*a*), in addition to the region of developing trabeculae

(arrow in *c*). Both sibling and *goz* larvae show a strong lipid staining of the yolk (asterisks in *a* and *b*). Lipid deposit is severely reduced in all other tissues in *goz* larvae (*b*), especially around the eye (arrow) and the otic vesicle (arrowhead). No lipid can be detected around the developing trabeculae in *goz* (arrow in *d*). (Adapted from Schlombs, Kornelia et al. (2003) Proc. Natl. Acad. Sci. USA 100, 14024-14029)

1.6 Site-1 Protease (S-1P)/ Subtilisin kexin isoenzyme-1 (SKI-1)

Limited proteolysis at single and pairs of basic residues has now been recognized to be a fundamental process in living organisms. The major mammalian enzymes that catalyze this reaction, known as the proprotein convertases (PCs), are serine proteinases related to yeast kexin and bacterial subtilisins. Mammalian PCs are implicated in the processing of numerous precursors, ranging from polypeptide hormones to growth factors, receptors, and enzymes as well as viral surface glycoproteins. Seven members of the PC family have so far been identified and shown to process these various precursors usually within the consensus sequence **(R/K)**X_n**(R/K)**$\downarrow$, where X_n is the number of spacer amino acids (0, 2, 4, or 6) and X is any amino acid, but not Cys (54).

Cellular processing of precursors could also occur at sites not occupied by basic residues. The widely expressed, membrane-bound, type I subtilase known either as Site-1 Protease (S-1P) or Subtilisin kexin isoenzyme-1 (SKI-1) is one of them.

Site-1 Protease (S-1P) was simultaneously discovered by the group of Goldstein and Brown in Dallas, Texas and the group of Nabil Seidah in the Clinical Research Institute of Montreal where it was given the name Subtilisin kexin isoenzyme-1 (SKI-1). S-1P is a subtilisin-related serine endopeptidase in the secretory pathway which has been shown to activate proproteins. It is a multidomain enzyme composed of an amino propeptide, a subtilisin like catalytic domain, a middle domain and a unique growth factor cytokine receptor-like (GFCR) motif (Figure 9). The enzyme is synthesized as an inactive

precursor that is autocatalytically cleaved in the endoplasmic reticulum (ER) at two alternate B' and B sites RKVF^{133} ↓ and RKVFRSLK^{137}↓, respectively (55). The latter products are then transported to the *cis/medial* Golgi whereupon they are further autocatalytically processed into a C-form at RRLL^{186} ↓ (Table 1), generating the active S-1P enzyme devoid of its prosegment. The GFCR is essential for the autocatalytic process of S-1P. Both *goz* alleles result in truncated proteins lacking intact GFCR and expressed only inactive S-1P. Mutagenesis studies surmised that S-1P processes precursors exhibiting the consensus motif (R/K)*X* (hydrophobic)*Z*↓, where *Z* is any amino acid, preferentially Leu or Thr, but excluding Val, Pro, Glu, Asp or Cys (54).

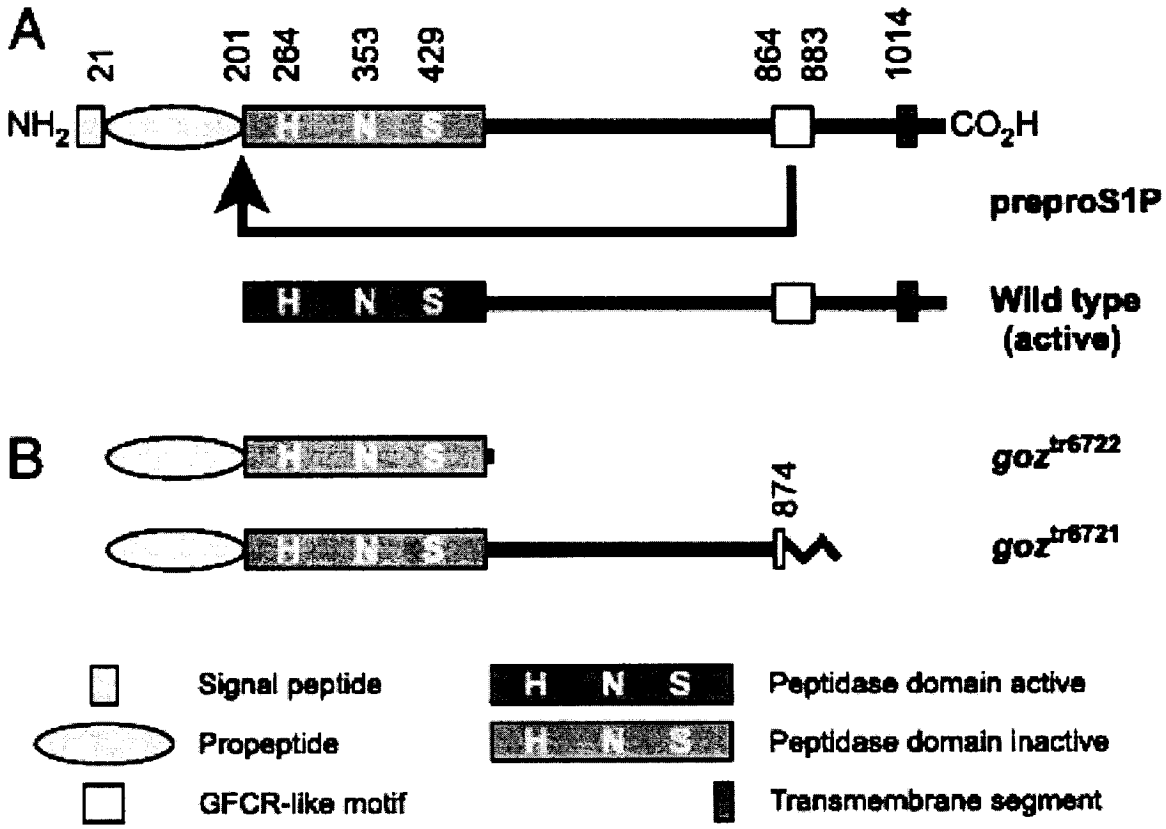

Figure 9: S-1P. (*A*) S1P is synthesized as preproprotein and activated through sequential cleavage. A growth factor cytokine receptor (GFCR)-like motif is essential for this autocatalytic process (arrow in *A*). (*B*) Both *goz* alleles result in truncated proteins lacking intact GFCR-like motifs and are predicted to express only inactive S1P. An

altered sequence caused by splice defects in *goz*^{tr6721} is shown in red. (Adapted from Schlombs, Kornelia et al. (2003) Proc. Natl. Acad. Sci. USA 100, 14024-14029)

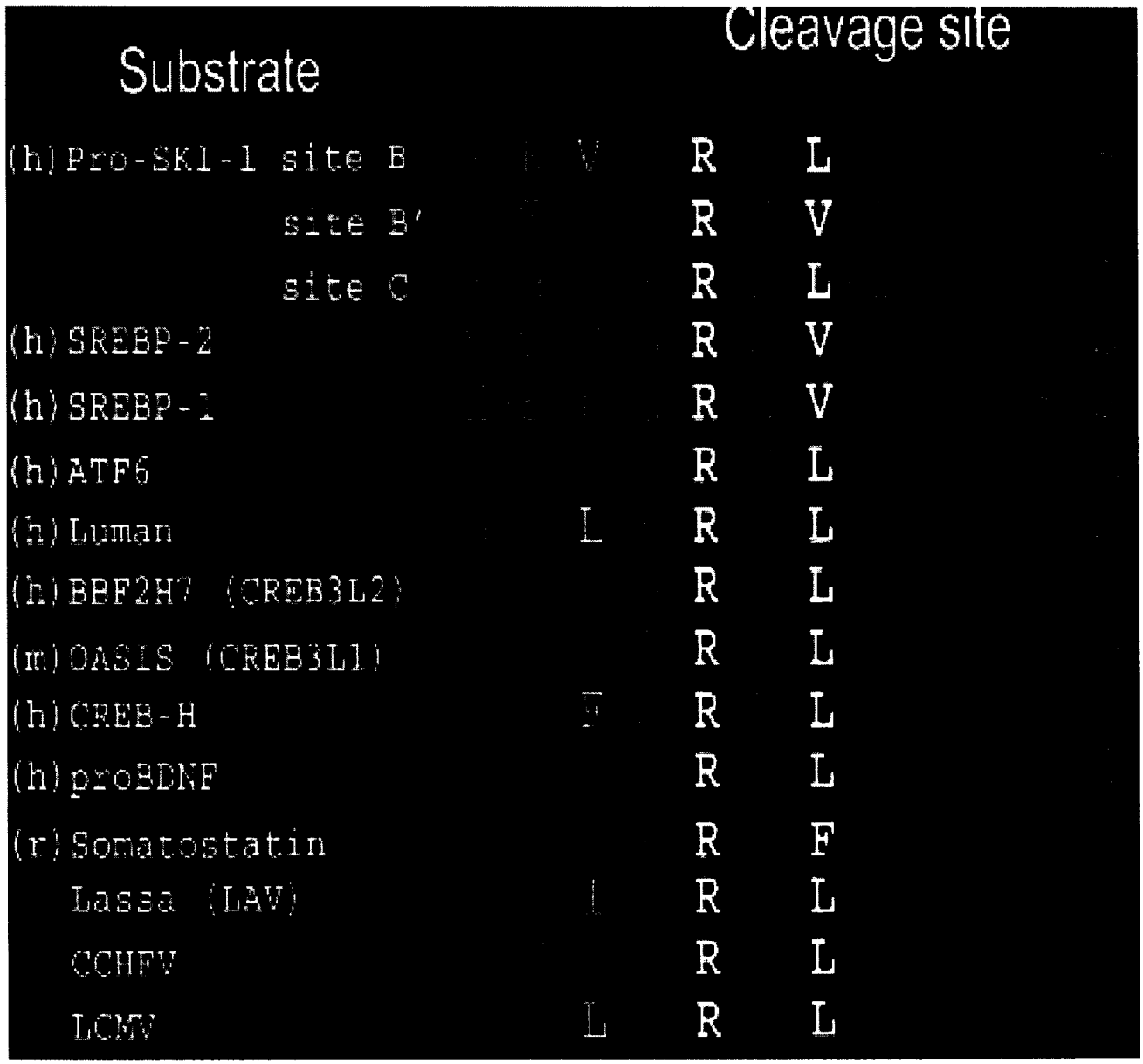

Table 1: Processing of protein precursors by S-1P (The table is kindly provided by Dr. Nabil Seidah)

S-1P plays a crucial role in the regulation of lipid metabolism and cholesterol homeostasis through the processing of the sterol regulatory element-binding proteins, SREBP-1 and SREBP-2, which occurs in the *cis/medial* Golgi.

SREBPs are a family of three proteins, each of ~1150 amino acids in length. Each SREBP is inserted into the membranes of the endoplasmic reticulum and nuclear envelope co-translationally in a hairpin orientation (56). The NH_2-terminal segment of ~480 amino acids is a transcription factor of the basic helix-loop-helix-leucine zipper family that projects into the cytoplasm. The middle segment of ~80 amino acids consists of two membrane-spanning helices separated by a luminal hydrophilic loop of ~30 amino acids. The COOH-terminal segment of ~590 amino acids extends into the cytoplasm, where it forms a complex with the COOH-terminal segment of a membrane-bound regulatory protein designated SREBP-cleavage activating protein (SCAP). The SREBP/SCAP complex is the true substrate for S-1P; disruption of this complex in intact cells abrogates the proteolytic reaction (57).

The precursors of the SREBPs are cleaved in SCAP and insulin-induced gene (INSIG)-dependent fashion. When cellular cholesterol levels are high, INSIG binds and retains the SCAP-SREBP complex in the ER. When cells are deprived of sterols, INSIG separates, allowing the transport of the SCAP-SREBP complex to the Golgi. Therein S-1P initiates the processing of SREBPs by cleaving at a site in the middle of the luminal loop. This reaction has been studied most extensively for human SREBP-2. S-1P cleaves this protein between the leucine and serine of the sequence RSVLS (58). The specificity of recognition has been studied by transfecting cDNAs encoding mutant forms of SREBP-2 into cultured cells. Cleavage of SREBP-2 absolutely requires arginine or lysine at the P4 position. Although the full range of residues at the P1 position was not studied, cleavage was markedly reduced when the leucine at P1 was replaced by alanine or by valine. The serine at the P1' position and the serine and valine at the P3 and P2 positions could be replaced by alanine with no effect on cleavage (58).

Cleavage by S-1P separates the SREBP into two fragments, each of which has a single membrane-spanning sequence. This separation allows a second protease, designated Site-

2 protease (S-2P), to cleave the NH_2-terminal fragment at a position within its membrane-spanning sequence (58). This cleavage releases the NH_2-terminal segment of SREBP, allowing it to enter the nucleus, where it binds to enhancers and activates transcription of more than 35 mRNAs coding for proteins/ enzymes required for the biosynthesis and uptake of low density lipoprotein (LDL) and cholesterol (57). When sterols accumulate in cells, the cleavage of SREBPs by S-1P is abolished; SREBPs remain attached to membranes; and transcription of the target genes declines. This regulation is mediated by the sterol-sensing domain of SCAP (57). The mechanism by which SCAP stimulates the Site-1 cleavage reaction and the mechanism by which sterols block this stimulation is unknown.

Similar to SREBPs, the ER- anchored type II membrane bound transcription actor ATF6 plays a major role in the unfolded protein response (UPR) to enhance the protein folding or refolding capacity of the secretory pathway (59). Cells cope with unfolded proteins accumulated in the ER primarily by transient attenuation of translation and by transcriptional induction of genes encoding ER-resident molecular chaperones (BiP/GRP78, GRP94 etc.) and folding enzymes (protein-disulfide isomerase, peptidyl-prolyl cis-trans isomerase, etc.), leading to augmenting the folding capacity in the ER. These processes are collectively termed the Unfolded Protein Response (UPR). ER chaperones commonly contain in their promoter regions a unique cis-acting element designated as the ER stress response element (ERSE), whose consensus sequence is CCAAT-N9-CCACG; the ERSE is necessary and sufficient for the transcriptional induction of ER chaperone genes (60). As the general transcription factor NF-Y (CBF) constitutively occupies the CCAAT part of the ERSE (61), the binding of ER stress response factor(s) to the ERSE requires a component that is capable of binding to the CCACG part of the ERSE and that is specifically activated during the UPR. The basic leucine zipper proteins ATF6α (encoded by the ATF6 gene) and ATF6β (encoded by the G13/cAMP response element-binding protein-related protein gene) are identified as CCACG-binding proteins (60). Both ATF6α and ATF6β are constitutively synthesized as type II transmembrane glycoproteins that are inserted in the ER membrane and are activated by proteolysis in response to ER stress (62). The N-terminal fragments thereby

released from the membrane (mature forms of ATF6α and ATF6β) enter the nucleus and activate the transcription of their target genes via direct binding to the CCACG part of the ERSE in a manner dependent on the binding of NF-Y to the CCAAT part (63).

Under normal conditions, both forms of ATF6 are held in the ER through mechanisms requiring the chaperon BiP (type II), with its N-terminal DNA binding domain facing the cytosol and its COOH terminus in the ER lumen (63). Accumulation of improperly folded proteins in the ER, which can be induced by calcium depletion (thapsigargin) or inhibition of N-glycosylation (tunicamycin), leads to an ER-stress response resulting in BiP dissociation from proATF6. The latter is then translocated in a SCAP dependent fashion to the Golgi where it is firstly cleaved by S-1P and then by S-2P. This releases the cytosolic N-terminal domain, which reaches the nucleus (nATF6) to activate ER stress target genes, this includes the transcription of BiP mRNA(60).

Other type-II membrane-bound substrates (Table 1) include the basic leucine zipper transcription factor Luman, the cellular counterpart of herpes simplex virus VP16 (64) and the CREB-like proteins. Brain-derived neurotrophic factor (BDNF) is a soluble substrate and the study of its processing led to the initial cloning of SKI-1 (55). S-1P was shown to play a major role in the processing of surface glycoproteins of infectious viruses such as Lassa (65), lymphocytic choriomeningitis (LCMV) (66) and Crimean Congo hemorrhagic fever (CCHF) (67) viruses.

SREBPs, ATF6 and their processing enzymes, S-1P and S-2P are certainly important targets for drug development. A sensitive S-1P-specific fluorogenic assay has been developed based on the processing of a quenched fluorogenic peptide mimicking the glycoprotein processing site of Lassa (65) and CCHF (67) viruses. It was shown *in vivo* that S-1P plays a crucial role in the processing of SREBPs in liver and is necessary for normal rates of triglyceride and sterol synthesis. Thus, whereas homozygote S-1P (-/-) results in a lethal phenotype, conditional knockout in mouse liver results in 64–83% decrease in the rates of cholesterol and fatty acid biosynthesis in hepatocytes (68).

The critical implication of S-1P in various cellular functions and in certain pathologies emphasizes the importance of understanding the function of this convertase and of developing specific inhibitors that could modulate its activity in disease states. Whereas S-1P inhibition was recently achieved using 300 μM of the serine protease inhibitor AEBSF (69), it was not a specific S-1P inhibitor. The group of Dr. Nabil Seidah introduced S-1P recognition motifs into the reactive site loop (RSL) of α_1-AT (P1-P4 positions) as one approach to the development of protein-based inhibitors. They also optimized the prosegment-based inhibition of S-1P and identified a unique R134E mutant (also called pro-SKI-1) (70) exhibiting a potent inhibitory activity. These inhibitors represent protein-based inhibitors designed to specifically block intracellular S-1P activity.

1.7ATDC5 Cells

In the formation of cartilage, mesenchymal cells pass through at least three distinct differentiation stages: 1) prechondrogenic cells 2) proliferating chondrocytes, and 3) hypertrophic and calcifying chondrocytes. During endochondral bone development, mesenchymal cells undergo an orderly series of events which involves the transitions of prechondrogenic cells to proliferating chondrocytes through cellular condensation (early phase differentiation). Chondrocytes at the proliferating stage then proceed to the hypertrophic stage (late phase differentiation). In permanent cartilage, e.g., normal articular cartilage on the joint surface, chondrocytes do not undergo the late phase conversion of phenotype. The late phase differentiation is characterized by a several-fold increase in cell volume and a marked increase in alkaline phosphatase (ALPase) activity (71). Hypertrophic chondrocytes eventually mineralize the surrounding cartilage matrix to allow invasion of blood vessels, leading to the replacement of cartilage by bone.

This biphasic transition of the cellular phenotype is accompanied by a change in collagen gene activation: prechondrogenic mesenchymal cells express type I collagen mRNA, and the early phase differentiation is characterized by inductive expression of type II and IX collagen genes as well as the aggrecan gene. The late phase differentiation is characterized by the onset of expression of the short-chain collagen type X gene, which

thus far has been found only in hypertrophic and calcifying chondrocytes (72). Hypertrophy of chondrocytes is also accompanied by reduction of aggrecan and type II collagen expression (72).

The clonal cell line, ATDC5, was isolated from the feeder-independent teratocarcinoma stem cell line AT805 on the basis of chondrogenic potentials in the presence of insulin (73). Murine teratocarcinoma AT805 cells can differentiate into a wide range of somatic cells including chondrocytes after their injection into a syngeneic host (73). They differentiated into chondrocytes in vitro hardly at all, but spontaneously, they differentiated into fibroblastic cells. ATDC5 cells exhibit a fibroblastic cell morphology at the subconfluent stage and the cells do not stop growing after confluence. Many studies showed that ATDC5 cells reproducibly undergo the early phase differentiation of chondrocytes to form numerous cartilage nodules in the presence of a high concentration of insulin (10 μg/mL) (73). This concentration is presumed to exert its effects through the insulin-like growth factor-I (IGF-I) receptor. Johnstone's group in Ohio (74) showed that with addition of ascorbate, chondrocyte diffeentiation was more extensive in ATDC5 cells. With the addition of ascorbate, the mRNA expression level of all chondrocyte markers including sox9, collagen type II and aggrecan was also many fold higher than the control culture conditions. The most well-documented effect of ascorbate is on collagen hydroxylation. This modification of prolyl and lysyl residues, necessary for the formation of stable, secreted triple-helical collagen, requires ferrous iron; ascorbate promotes hydroxylation by maintaining enzyme-bound iron in the reduced state (75). A major consequence of collagen underhydroxylation is impaired collagen secretion, which can be rapidly reversed by ascorbate addition (75).

After early phase differentiation of chondrocytes in ATDC5 cells, cartilage nodules increased in size due to the proliferation of chondrocytes and then spontaneously ceased to grow (76). After the cessation of growth, it was found that hypertrophic cells appeared in the center of cartilage nodules in association with type X collagen gene expression and a dramatic elevation of ALPase activity in culture. Matrix vesicles, Alkaline phosphatase (ALPase), and type X collagen are all implicated in the mineralization of cartilage (77).

Under the appropriate culture conditions, hypertrophic ATDC5 cells initiated mineral deposition via the matrix vesicle (MV)-mediated mechanism in the preformed cartilage matrix. Mineralization in the culture markedly propagated with time in culture.

β-glycerophosphate has been a culture supplement used for the stimulation of mineralization in vitro, although it sometimes gives artifactual mineralization. β-glycerophosphate supplementation was not required for mineralization of the differentiated ATDC5 cells (78).

Therefore, the ATDC5 cell line appears to be a good model for studying gene expression and morphological changes during the normal differentiation of mesenchymal precursor cells into terminally differentiated chondrocytes.

1.8 Aims of the Thesis

Studies done by Nusslein-Volhard and Schlombs, Kornelia et al. clearly showed that S-1P plays important roles in cartilage development in zebrafish. Positional cloning of zebrafish *S-1p* gene underlying the *goz* defect encodes a protein of 1,074 amino acids with 82% identity to human S-1P (53). It is therefore interesting to investigate the role of S-1P in mammalian cartilage development. The hypothesis was that the disruption of the expression of S-1P causes abnormal cartilage development in mouse (a mammalian model system). The very long term objective of this project is to determine the molecular mechanism underlying the role of S-1P in mammalian cartilage development, in particular its target substrate(s). However the objective of my Master's thesis is to study the expression of S-1P in cartilage development using ATDC5 cells as a mammalian model system.

Aims:

1. Investigate the expression of S-1P together with other cartilage related components in ATDC5 cells.
2. Investigate the effect of the inhibition of S-1P on the expression levels of cartilage related components in ATDC5 cells.

CHAPTER 2

Materials and Methods

2.1 Cell cultures

The ATDC5 cell line was obtained from the RIKEN cell bank (Tsukuba, Japan). The cells were maintained in a medium consisting of a 1:1 mixture of Dulbecco's modified Eagle's medium (DMEM) and Ham's F-12 medium (Invitrogen, Canada) containing 5% fetal bovine serum (Invitrogen, Canada.), 10 μg/ml bovine transferrin (Invitrogen, Canada), and 3×10^{-8} M sodium selenite (Sigma-Aldrich, Canada) at 37°C in a humidified atmosphere consisting of 5% CO_2 and 95% air.

The ATDC5 cells were seeded at a density of 6×10^3 cells/cm^2 in 24-well cell culture plates for cell-proliferation studies, or six-well plates for ECM-production and gene-expression studies. Three days after plating, when cultures had reached 90%–95% confluency, chondrogenesis was induced in half of the cultures by supplementing the maintenance medium with 10 μg/ml bovine insulin (Sigma-Aldrich). Cells were grown for another 17 days, with the medium being replaced every other day for the first week, and thereafter every 3 days. On days 4, 8, 16 and 20, the cell growth was determined by counting in a hemocytometer chamber, the cartilage-specific ECM production was assayed by staining with Alcian Blue, and the transcriptional expression of S-1P was assessed using RT-PCR.

In experiments on the induction of chondrogenesis using ascorbic acid, one experimental group of cells was induced with a combination of 10 μg/mL bovine insulin (Sigma-Aldrich) and 37.5 μg/mL of ascorbate 2-phosphate (Sigma-Aldrich). Cells were grown for another 17 days, with the medium being replaced every other day for the first week, and thereafter every 3 days. On days 4, 8, 16 and 20, 24, 28, 32 and 35 in the insulin-treated, insulin and ascorbate-treated and control cultures, the cell growth was determined by counting in a hemocytometer chamber, the cartilage-specific ECM production was assayed by staining with Alcian Blue, and the transcriptional expression of 5 selected genes (*aggrecan, collagen I, collagen II, collagen X and S-1P*) was analyzed by real-time RT-PCR. At least two independent experiments were carried out in duplicate.

2.2 Transfection of ATDC5 cells

The day before transfection, cells were plated at a density of 2 x10^5 cells/well in a 6-well plate. In a microfuge tube, 2 μg of plasmid was diluted in 375 μL of DMEM/F12. The plasmid DNA constructs used in the transfections were expressing either pIRES-EGFP alone, pIRES-EGFP-proSKI R134E, pIRES-EGFP-V5, or pIRES-EGFP-pro-PDGF-A*-V5 (mutant) (all these plasmids were provided by Dr. Nabil Seidah.) In another microfuge tube, 6 μL of FuGENE 6 (Roche, Canada) was diluted in 375 μL of DMEM/F12. The two solutions were combined, gently mixed and incubated at room temperature for 45 minutes. 750 μL of DMEM/F12 (without antibiotics) was added to the tube containing the DNA-FuGENE 6 complex. The solution was gently mixed and overlaid onto the washed cells. The cells were then incubated for 5 hours at 37° C in 5% CO_2 incubator. After 5 hours of incubation, 1.5 mL of DMEM/F12 with 20% FCS was added to each well without removing the transfection medium. After 24 hours of incubation at 37° C, the cells were rinsed with PBS and incubated in serum-free DMEM/F12 for another 24 hour. 48-hour post-transfection, the medium was resolved on a 12% SDS gel for the experiment set up for the study of the functional inhibition of S-1P. In this case, the cells were transfected with the plasmid DNA of pIRES-EGFP-V5 (control) and pIRES-EGFP-pro-PDGF-A*-V5 (mutant). Detection by Western blotting was done with monoclonal antibody directed against the V5 epitope fused to the C-terminal end of pro-PDGF-A (1:5000 dilution) (Invitrogen).

2.3 Generating Stable ATDC5 cell lines transfected with DNA of pIRES-EGFP and pIRES-EGFP-proSKI-1 (R134E)

ATDC5 cells were seeded in a 12 wells plate at a density of 90-100% confluency. Some wells were reserved for use as a control for transfection (i.e. nothing was being transfected into these wells). The purpose of the control well(s) is to give an indication of the time necessary to kill all cells that do not contain the neomycin-resistance DNA. 24 hours after the start of transfection, the DMEM/F12 medium was replaced with a regular medium containing 200-400 μg/mL (for selection) of the neomycin antibiotic (G418-Geneticin Sulfate, Gibco). The medium containing neomycin was replaced every day.

The concentration of neomycin was varied as required. The cells should not die quickly (i.e. lifting from the bottom of the well) in the first few days. Cells not containing the neomycin-resistance DNA should die after 7-14 days after the start of transfection. (control wells were used to be certain). Once all the transfected cells have died, there were only colonies of ATDC5 transfectants remaining. At this point, the neomycin-supplemented medium (reduced to 200 μg/mL neomycin) was replaced every two days until the colonies became dense. The cells were trypsinized after the colonies hadbecome dense. The cells were then reseeded in a new 12-well plate to evenly disperse the cells over the surface of the well. When the cells were confluent, or nearly confluent, they were trypsinized and transferred to 6-well plates preserving their distinctiveness. Much care was taken so that colonies from different wells did not mix together. Each colony was expanded to P60 and eventually P100 plates, with the medium always supplemented with neomycin.

2.4 Western Blotting

Cell culture media were collected from cell culture 48 hours post-transfection. Equal volumes of media (30 μL) collected from cell culture of cells transfected with plasmid DNA of pIRES-EGFP-V5 (control) and pIRES-EGFP-pro-PDGF-A*-V5 (mutant) were separated by 12% SDS-PAGE gel electrophoresis at 100 V for 2 hours and transferred to Hybond ECL nitrocellulose membranes (Amersham, Canada). 5% bovine serum albumin fraction V in Tris-buffered saline (Fisher, Canada) containing 0.1% Tween 20 (TBS-T) (Sigma, Canada) was used to block the membranes for 1 hour at room temperature. The membranes were then incubated at 4 °C overnight with mouse monoclonal anti-V5 (Invitrogen, Canada) antibody at 1:5000 dilution in 5% BSA/TBST. The blots were rinsed three times with PBST [PBS containing 0.1% Tween-20] for 20 min each. The transferred proteins were visualized using an enhanced chemiluminescence detection kit (Amersham Biosciences Corp.) and detected on Hyperfilm (Amersham Biosciences Corp).

2.5 Alcian Blue Staining and Glycosaminoglycan (GAG) Quantification

Alcian Blue, a group of polyvalent basic dyes that are water soluble, stains acid mucosubstances (sulfated and carboxylated mucopolysaccharides) and sialomucins (glycoproteins), both of which are cartilaginous elements. Since the synthesis of these extracellular macromolecules is increased during chondrogensis, staining with Alcian Blue is a fast and easy method to identify cells undergoing chondrogenesis.

To evaluate the synthesis of ECM, sulfated glycosaminoglycans were visualized by staining with Alcian Blue. Cells were washed twice with PBS, fixed with 90% methanol at −20°C for 2 min, stained with 0.1% Alcian Blue 8GX (Sigma-Aldrich) in 0.1 N HCl overnight, and rinsed repeatedly with distilled water. The preparations were evaluated by phase-contrast microscopy. For quantitative analysis, the Alcian Blue-stained cultures were extracted with 200 μl of 6 M guanidine-HCl overnight at room temperature. The optical density of the extracted dye was measured at 620 nm in a spectrophotometer.

2.6 DAPI Staining

4'-6-Diamidino-2-phenylindole (DAPI) is known to form fluorescent complexes with natural double-stranded DNA, showing a fluorescence specificity for AT, AU and IC clusters. Because of this property DAPI is a useful tool in various cytochemical investigations.

ATDC5 cells were grown in slide chamber. On forty-eight hours post-transfection, the cells were washed once with PBS then fixed in 4% paraformaldehyde for 20 minutes. The cells were washed 2X with PBS again and incubated in 10 µg/ml 4'6-diamidino-2-phenylindole (DAPI, Sigma) for 10 minutes. After incubation with 0.1 microgram/mL of DAPI, the cells were washed 3 times with distilled water and observed using a fluorescence microscope. Nuclei are considered to have the normal phenotype when glowing bright in blue and homogenously. Apoptotic nuclei can be identified by the condensed chromatin gathering at the periphery of the nuclear membrane or a total fragmented morphology of nuclear bodies.

2.7 RNA isolation and Reverse Transcription Polymerase Chain Reaction (RT-PCR)

Total RNA from ATDC5 cells was extracted with standard protocols using the TRIzol® total RNA isolation system (Invitrogen, Canada). Approximately 5mL of TRIzol® was added into a tube of cells collected from each 6-well plate. The mixture was incubated at room temperature for 5 min. two-hundred microliters of chloroform per 1 ml TRIzol® are added and shaken for 15 sec. The mixture was then incubated at room temperature for 2-3 min. The tubes were centrifuged at 10, 000g, 2-8 °C for 15 min. The colorless upper aqueous phase (containing RNA) was transferred to a fresh tube. 500 microliters of isopropanol per 1 ml TRIzol® in the initial step were added in to the tubes. The mixture was then incubated at room temperature for 10 min and was centrifuged at > 8,000g, 2-8°C for 10 min. The supernatant was removed and discarded. The tube was washed in 1 ml of 75% (v/v) ethanol/DEPC-treated water per 1 ml TRIzol®. The pellet was vortexed to resuspend and centrifuged at > 8 000g, 2-8°C for 5 min. The RNA pellet was allowed to dry (briefly) and resuspended in 100 μL RNAse free water. The solution was then incubated at 55°C for 10 min. to ensure total resuspension. After isolation, total RNA was quantified by ultraviolet spectrophotometry by measuring the OD260 and was purity assessed by measuring the OD260/OD280 ratio. Oligo (dT) (Invitrogen, Canada) primers were used for the reverse transcription reaction to synthesize cDNA from total RNA. RNA was linearized at 95–98 °C for 5 min, and reverse transcription was carried out in a total volume of 15 µL containing oligo dT, 0.5 µL 40 U/µL RNase in, 0.75 µL 10 mM dNTP and 0.75 µL 200 U/µL Molony murine leukaemia virus (M-MLV) reverse transcriptase in 3 µL 5× buffer (250 mM Tris-HCl, pH 8.3, 375 mM KCl, 15 mM $MgCl_2$) and diluted in distilled water. The reaction was allowed to proceed at 37 °C for 1 h, terminated by heating to 95 °C for 3 min, and then the sample (cDNA) was cooled on ice. The 20 µL PCR reaction solution contained 1 µL of cDNA sample, 2 µL of 10× PCR buffer with 2.0 mM $MgCl_2$ (Invitrogen, Canada), 200 µM dNTPs, 0.3 µm each of forward and reverse primer, 0.4 U Taq polymerase (Invitrogen, Canada), and 13.7 µL of double distilled water. The cycling parameters were 95 °C for 5 min followed by 30 cycles of 95 °C for 30 s, 56 °C for 30 s, 72 °C for 40 s, and finally 72 °C for 7 min.

The following sequences of forward and reverse primers were used in this study. For GAPDH (mouse) mRNA:5'-TTCTTGTGCAGTGCCAGCCT-3' (forward primer) and 5'-GCCCTTGAACTTGCCGTGGG-3' (reverse primer) generate a 223 bp amplicon. For S-1P(mouse) mRNA: 5'-GGGCCGTCACCTTGTTAGTA-3' (forward primer) and 5'-GCGGTTTATAGCTGCTGAGG-3' (reverse primer) generate a 177 bp amplicon. Since the DNA of pro-SKI-1 transfected in to the ATDC5 cells is one derived from human, the pro-SKI-1 primer designed for RT-PCR reaction is also one derived from human, and at the site specific to human pro-SKI-1: 5'-CCCCAACGAAAAGTCTTTGA-3' (forward primer) and 5'-TACTGCAGTGTCTGGGCAAC-3' (reverse primer) generate a 218 bp amplicon.

2.8 Quantitative Real-time PCR

Quantitative Real-time PCR analysis was performed in a total volume of 25 μL containing 11.25 μL template cDNA (1μg), 1.25 μL of unlabeled primers for amplifying the sequence of interest (containing TaqMan Minor Groove Binder (MGB) probe (6-FAM dye-labeled) for detecting the sequence of interest), 12.5 μL of TaqMan Universal Master Mix (Applied Biosystems). The mixtures were subjected to 40 amplification cycles (15 seconds at 95° C for denaturation and 1 min for annealing and extension at 60° C). Incorporation of TaqMan MGB probes into PCR products was monitored in real time using a GeneAmp 7500 Sequence detection system (Applied Biosystems) allowing determination of the threshold cycle (C_T) at which exponential amplification of PCR products begins. After PCR, the dissociation curves were generated with one peak, indicating the specificity of the amplification. A threshold cycle (C_T value) was obtained from each amplification curve using the software provided by the manufacturer (Applied Biosystems).

Relative amounts of mRNA in non-induced, non-transfected ATDC5 cells; induced, non-transfected ATDC5 cells; induced ATDC5 cells that were stably tansfected with DNA of pIRES-EGFP and induced ATDC5 cells stably transfected with DNA of pIRES-EGFP-proSKI-1(R134E) were determined using the comparative C_T method using β-actin as an endogenous control. Relative mRNA expression in the ATDC5 cells was determined

using the $\Delta\Delta$ C_T method, as detailed in the manufacturer's guidelines (Applied Biosystems). A Δ C_T value was first calculated by subtracting the C_T value for the housekeeping gene β-actin from the C_T value from each sample. A $\Delta\Delta$ C_T value was then calculated by subtracting the Δ C_T value of the control (non-induced, non transfected ATDC5 cells) from the Δ C_T value of each treatment. Fold changes compared with the control were then determined by raising 2 to the $\Delta\Delta$ C_T power. Each PCR was performed in duplicate on 3 separate occasions for each independent experiment.

CHAPTER 3

Results

3.1 Effects of various concentrations of insulin on ATDC5 differentiation

Many studies showed that ATDC5 cells reproducibly undergo the early phase differentiation of chondrocytes to form numerous cartilage nodules in the presence of high concentration of insulin (10μg/mL). My first task in this project was to verify this finding by studying the effects of various concentrations of insulin on ATDC5 cells differentiation. ATDC5 cells were seeded in 6-multiwell dish and were cultured in DMEM/F12 medium containing 5% fetal bovine serum, 10 μg/ml bovine transferrin, and 3×10^{-8} M sodium selenite, and various concentrations of insulin were inoculated into the wells. After 14 days, the cells stained with Alcian Blue. Photographs of the wells were then taken with a digital camera (Figure 10). Figure 10 shows Alcian Blue staining of wells of ATDC5 cells supplemented with different concentration of insulin (indicated on the top left of each well). The results showed that ATDC5 cells started stain more Alcian Blue when 10 μg/mL of insulin was supplemented into the culture media. Supplementing the cells with higher concentration of insulin did not increase the level of glycosaminoglycan accumulation in these cells as the cells did not seem to stain more Alcian Blue (Figure 10). This finding was later confirmed and supported by glycosaminoglycan quantification (Figure 11).

To quantitatively assess the extent glycosaminoglycan accumulation, stained ATDC5 cells were extracted with 6M guanidine-HCl overnight at room temperature. The optical density of the extracted dye was measured at 620 nm in a spectrophotometer (Figure 11). When at least 0.1 μg/mL of insulin was supplemented in the cell culture media, a significant promotion of differentiation was observed. The highest incidence of glycosaminoglycan accumulation was observed with the addition of 10 to 50 μg/mL of insulin. Glycosaminoglycan accumulation in ATDC5 cells declined when 100 μg/mL of insulin was added to culture the cells. My results agreed with those of others (72, 73) have found: that 10 μg/mL of insulin is the optimum concentration to be used to induce differentiation in ATDC5 cells. Higher concentration of insulin did not increase glycosaminoglycan accumulation in the cells.

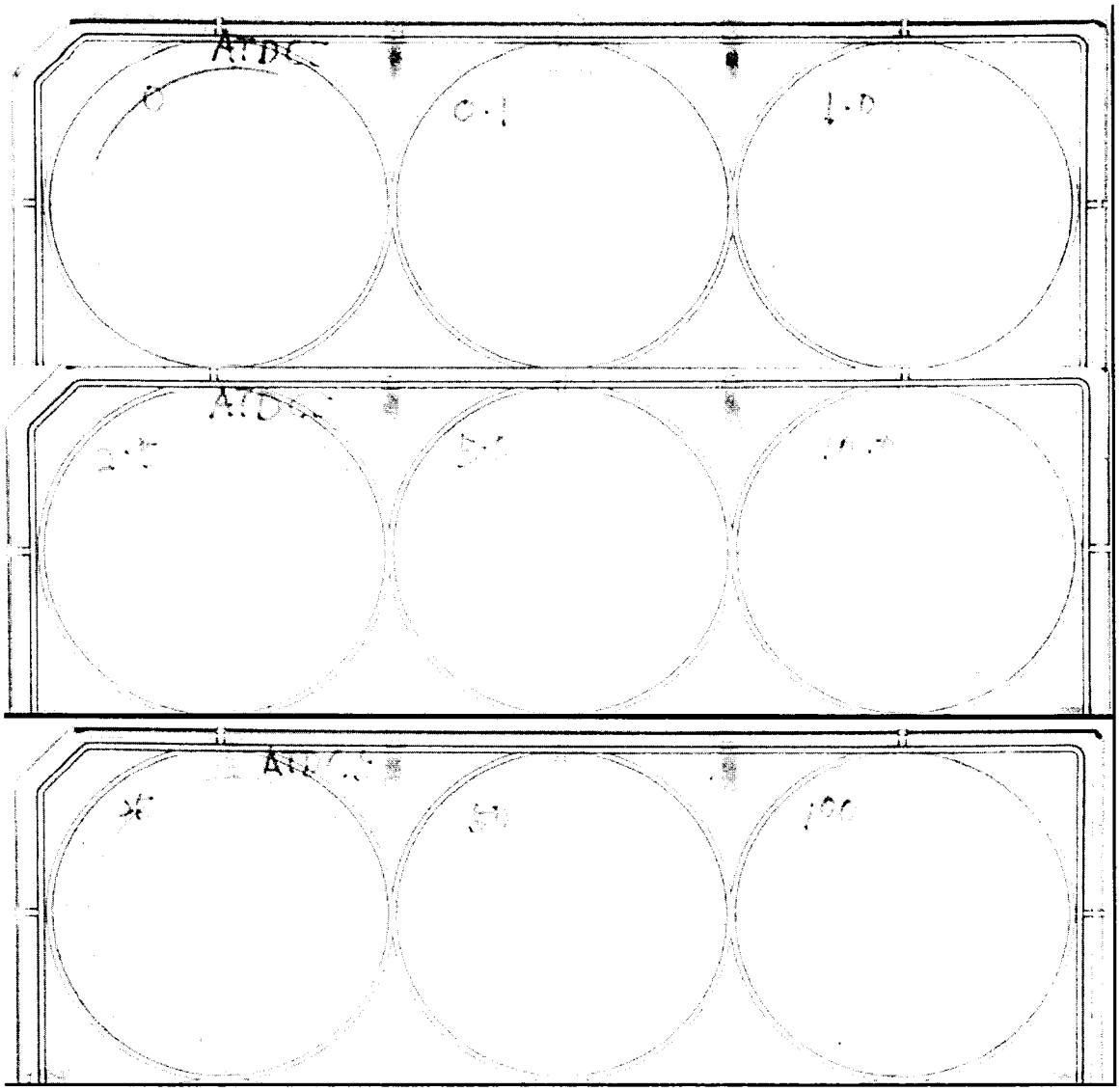

Figure 10: Photographs of Alcian Blue staining of ATDC5 cells on day 14. These cells were cultured in DMEM/F12 media supplemented with various concentration of insulin (indicated on the top of the wells). The cells were washed with PBS, fixed and stained with Alcian Blue on day 14 of culture. Significant increase of glycosaminoglycan accumulation occured when cells were supplement with 10 μg/mL of insulin. ATDC5 cells did not seem to accumulate more glycosaminoglycan when cultured in higher concentration of insulin as they did not stain more Alcian Blue in this case.

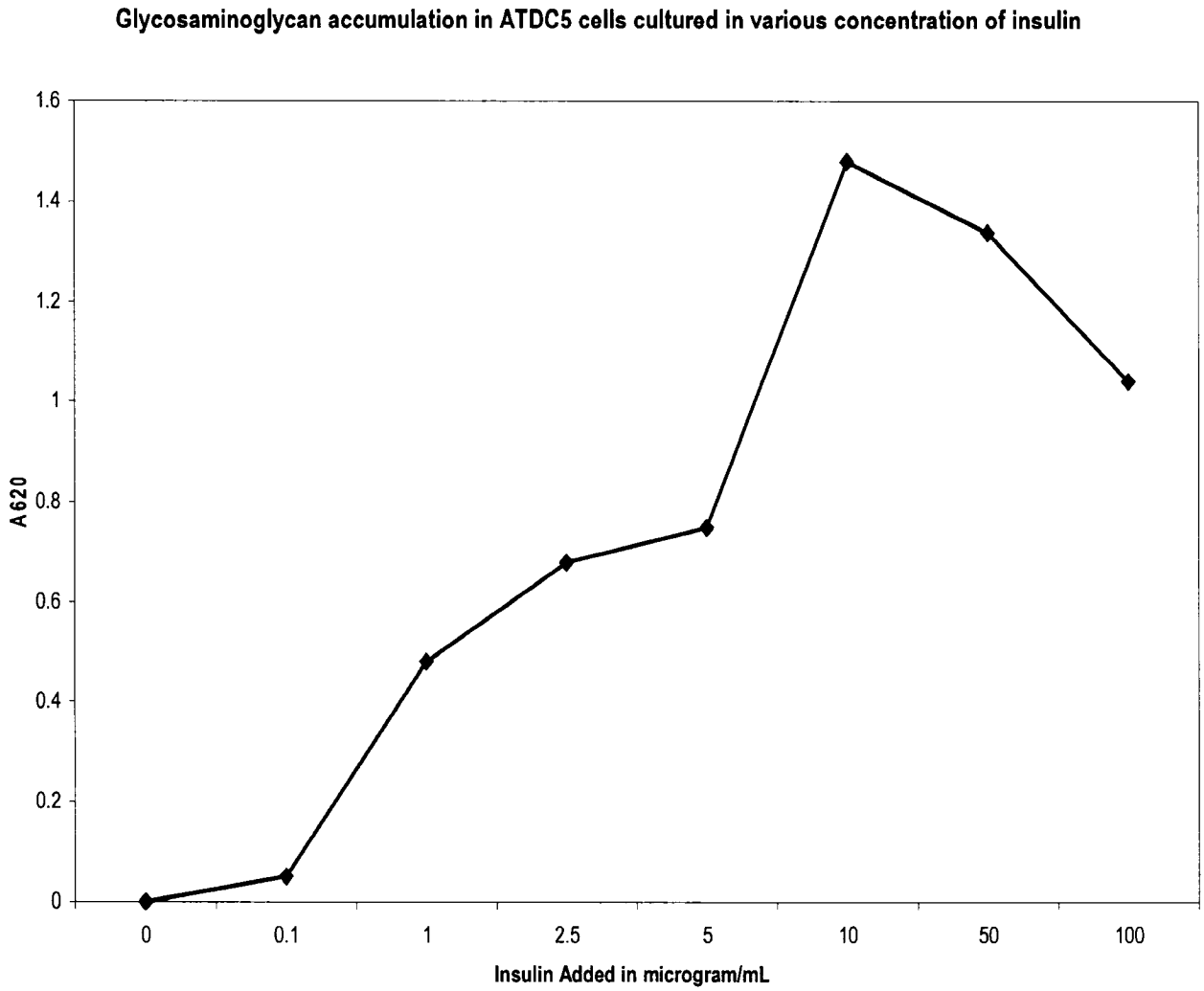

Figure 11: Effects of various concentrations of insulin added to the medium on the cartilage specific glycosaminoglycan accumulation of ATDC5 cells. Cells were cultured for 14 days in DMEM/F12 medium supplemented with 5% FCS and the indicated concentration of insulin. The cells were washed with PBS, fixed with 90% methanol and stained with Alcian Blue on day 14 of culture. The bound bye was extracted with 6 M guanidine-HCl. The concentration of extracted dye was measure at 620 nm and designated A_{620}.

3.2 Optimal insulin-dependent accumulation of Alcian Blue-positive matrix.

I started to induce differentiation in the ATDC5 cells with 10 μg/mL of insulin after verifying that 10 μg/mL of insulin is the optimum concentration for this purpose. Cells were cultured as indicated earlier and photomicrographs were taken on day 4, day 8, day 12, day 16 and day 20. As expected, ATDC5 cells treated with insulin underwent progressive differentiation from day 4 to day 20 compared with cultures untreated with insulin.

Undifferentiated ATDC5 cells rapidly proliferated (Figure 12a) and ceased to grow at confluence. In the presence of 10 μg/mL of insulin, the cells reentered the growth state through a cellular condensation (Figure 12b) followed by formation of cartilage nodules (early phase differentiation) (Figure 12c and 12d). The cells formed cartilage nodules that exhibited a round morphology (Figure 12d). The cells progressively formed more cartilage nodules by day 20. These cartilage nodule-like aggregates were intensely stained with Alcian Blue on day 20 of culture (Figure 13). However, it was observed that ATDC5 culture at this stage also contained undifferentiated cells (Figure 12e).

3.3 Expression of S-1P in ATDC5 cells

To investigate the expression and the role of S-1P in chondrocyte differentiation, I used ATDC5 cells as an in vitro model for cell differentiation. The first question I asked was whether or not ATDC5 cells expressed S-1P. If ATDC5 cells expressed S-1P, do they express the protease constitutively--when they are not induced with insulin, i.e. when they are still fibroblastic and not differentiated? And do they express S-1P when they are induced with insulin? Or does the induction with insulin inhibit the expression of S-1P in non-induced ATDC5 cells?

To answer these questions, RT-PCR analyses are performed. The ATDC5 cells were seeded at a density of 6×10^3 cells/cm^2 in 24-well cell culture plates for cell-proliferation studies, or six-well plates for ECM-production and gene-expression studies. Three days after plating, when cultures reached 90%–95% confluency, chondrogenesis was induced in half of the cultures by supplementing the maintenance medium with 10 μg/ml bovine

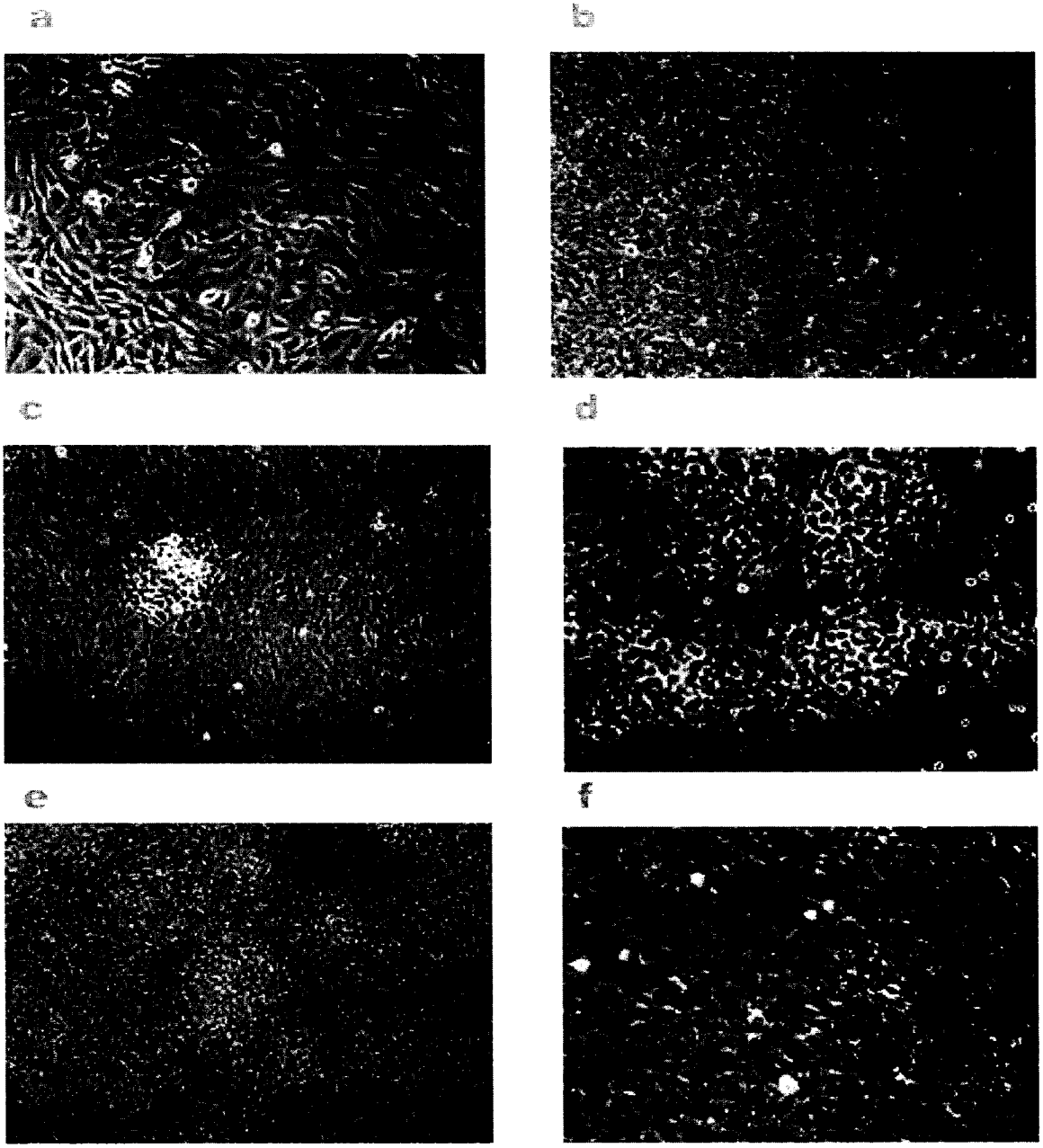

Figure 12: Phase contrast photomicrographs of ATDC5 cells cultured in DMEM/F12 supplemented with 10 μg/mL of insulin. a) Cells at subconfluent stage on day 4. b) Cells that have reached condensation stage on day 8. c) Cells formed cartilage cartilage aggregates nodules exhibited round morphology on day 12. d) Cells on day 16 that have formed. e) Cartilage nodules that have reached hypertrophy stage on day 20. Not all cells formed cartilage nodules. f) Control cells (cultured in media not supplemented with insulin) on day 20. These cells did not form cartilage nodules. Scale bar: 0.25 μm

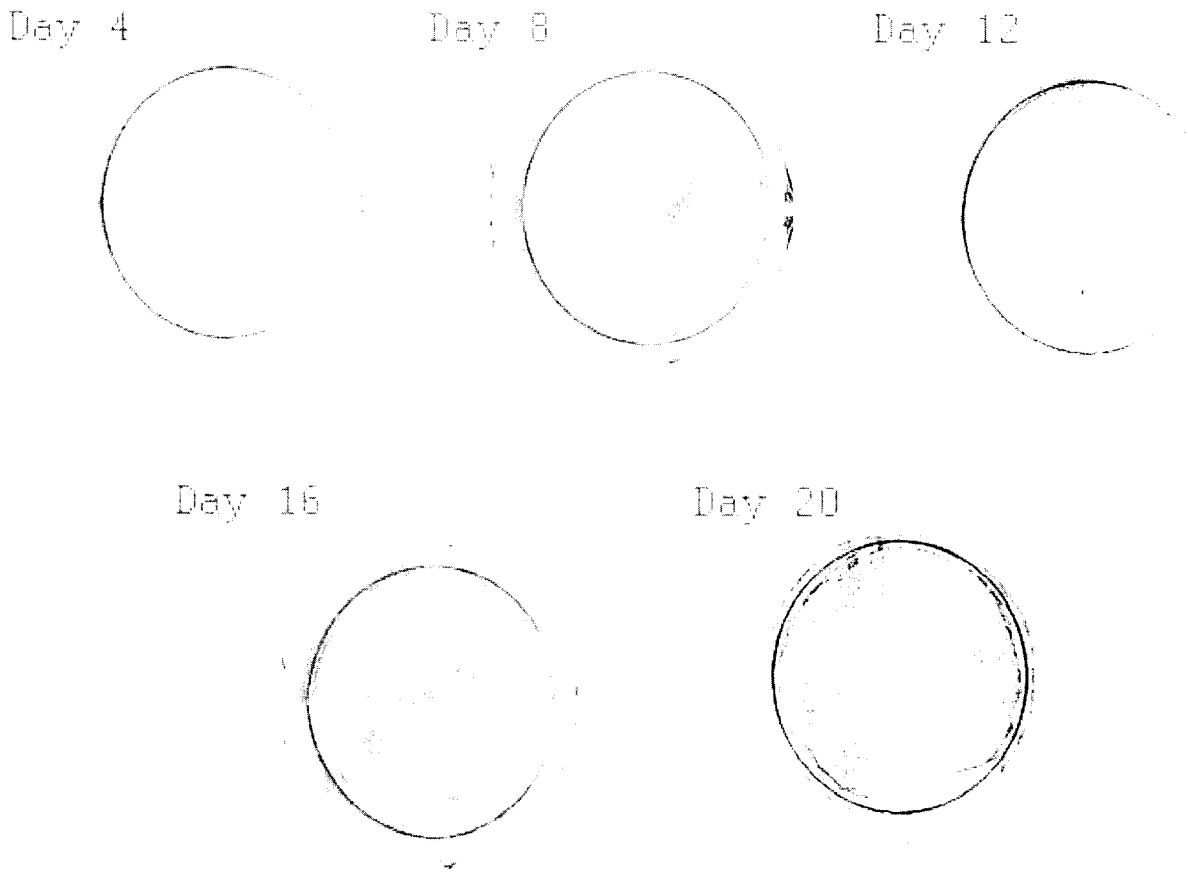

Figure 13: Alcian Blue Staining of ATDC5 cells induced with 10 μg/mL of insulin. ATDC5 cells progressively stained more Alcian Blue when cultured in media supplemented with 10 μg/mL of insulin typically on/after day 8 of culture when the cells have reached condensation stage. This is an indicative sign that the cells are forming glycosaminoglycan, an important cartilage matrix.

insulin. Another experimental group of cells served as control group and were cultured without the supplementation of insulin. Cells were grown for another 17 days, with the medium being replaced every other day for the first week, and thereafter every 3 days. On days 4, 8, 12, 16 and 20, total RNA from ATDC5 cells was extracted with standard protocols using the TRIzol® total RNA isolation system. GAPDH was used as endogenous control for RT-PCR.

Results showed that S-1P mRNA is expressed in ATDC5 cells at all time points (days 4, 8, 12, 16 and 20) when they are not induced with insulin (Figure 14). This indicated that S-1P is expressed in the cells when they are fibroblastic, not differentiated.

S-1P mRNA is also expressed at all time points tested (days 4, 8, 12, 16 and 20) in the experimental group of ATDC5 cells that are supplemented with 10 μg/mL bovine insulin in the maintenance medium (Figure 15). This indicated that S-1P is expressed in ATDC5 cells when the cells become chondrogenic. The fact that S-1P mRNA is expressed in ATDC5 cells at all time points tested indicated that the mRNA of the protease is expressed when ATDC5 cells were subconfluent (on day 4), when the cells have reached condensation stage (on day 8), when the cells have formed cartilage nodules (on day 12) and when the cells have reached hypertrophy stage (on day 16 and 20). In other words, S-1P mRNA is expressed in ATDC5 cells in all stages of chondrogenesis when the cells were induced with insulin.

Taken together, my results showed that S-1P is constitutively expressed in ATDC5 cells. Also, according to Figure 14 and 15, insulin treatment may change/modulate S-1P expression levels.

3.4 Chondrogenesis induction of ATDC5 cells with ascorbic acid

The questions I next sought to answer were whether chondrogenesis of ATDC5 cells depends on the differentiation inducers?

To answer this question, I induced chondrogenesis in ATDC5 cells using ascorbic acid. Johnstone's group in Ohio showed that ascorbic acid also enhanced chondrogenesis in ATDC5 cells. They showed that 37.5μg/mL of ascorbic acid was the optimum concentration to induce differentiation and mineralization in ATDC5 cells (results not published).

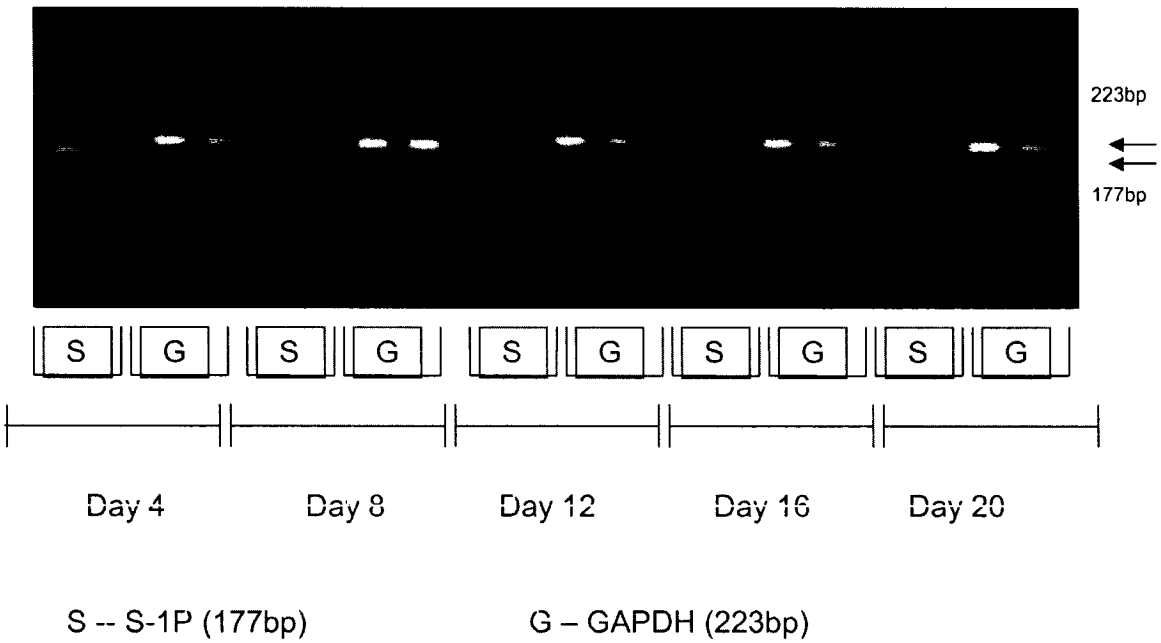

Figure 14: RT-PCR of ATDC5 cells not induced with insulin. mRNA of S-1P is expressed in ATDC5 cells cultured in DMEM/F12. Total RNA of ATDC5 cells was extracted on day 4, day 8, day 12, day 16 and day 20 with standard protocols using the TRIzol® total RNA isolation system (refer to Materials and Methods). GAPDH was used as endogenous control for RT-PCR.

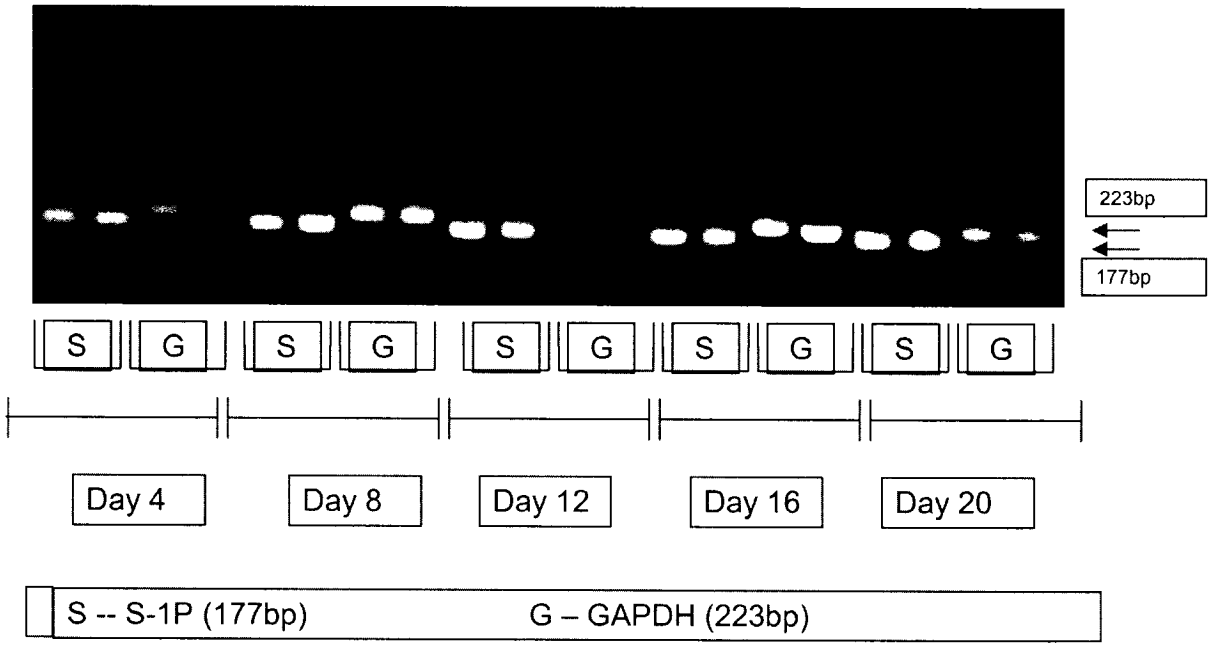

Figure 15: RT-PCR of ATDC5 cells induced with insulin. mRNA of S-1P is expressed in ATDC5 cells cultured in DMEM/F12 supplemented with 10 μg/mL bovine insulin. Total RNA of ATDC5 cells was extracted on day 4, day 8, day 12, day 16 and day 20 with standard protocols using the TRIzol® total RNA isolation system (refer to Materials and Methods). GAPDH was used as endogenous control for RT-PCR.

The ATDC5 cells were seeded at a density of 6×10^3 cells/cm^2 in 24-well cell culture plates for cell-proliferation studies, or six-well plates for ECM-production and gene-expression studies. Three days after plating, when cultures reached 90%–95% confluency, chondrogenesis was induced in a group of the cultures by supplementing the maintenance medium with 10 μg/ml bovine insulin. One experimental group of cells was induced with 37.5 μg/mL of ascorbate 2-phosphate. Another experimental group of cells was induced with a combination of 10 μg/mL bovine insulin and 37.5 μg/mL of ascorbate 2-phosphate. And one group of ATDC5 cells were cultured in DMEM/F12, not induced with either insulin or ascorbic acid. This group of cells was the control of the experiment. Cells were grown for another 17 days, with the medium being replaced every other day for the first week, and thereafter every 3 days. On days 4, 8, 16 and 20, 24, 28, 32 and 35 in the insulin-treated, insulin and ascorbate-treated and control cultures, the cell growth was determined by counting in a hemocytometer chamber, the cartilage-specific ECM production was assayed by staining with Alcian Blue, and the transcriptional expression of 5 selected genes (*aggrecan, collagen I, collagen II, collagen X and S-1P*) was analyzed by real-time RT-PCR. At least two independent experiments were carried out in duplicate.

Glycosaminoglycan quantification (Figure 16) showed that ATDC5 cells were chondrogenic when they were induced with 10 μg/mL bovine insulin. A significant promotion in glycosaminoglycan accumulation was observed from day 8 of culture when the cells have reached condensation stage at this point. At any time point after day 10 of culture, it was also observed that ATDC5 cells induced with ascorbic acid accumulated higher amount of glycosaminoglycan compared to the cells induced with insulin. However, the highest incidence of glycosaminoglycan accumulation was observed in the group of ATDC5 cells induced with a combination of 10 μg/mL of bovine insulin and 37.5 μg/mL of ascorbic acid. A combination of insulin and ascorbic acid seemed to have an additive effect in chondrogenesis induction in ATDC5 cells.

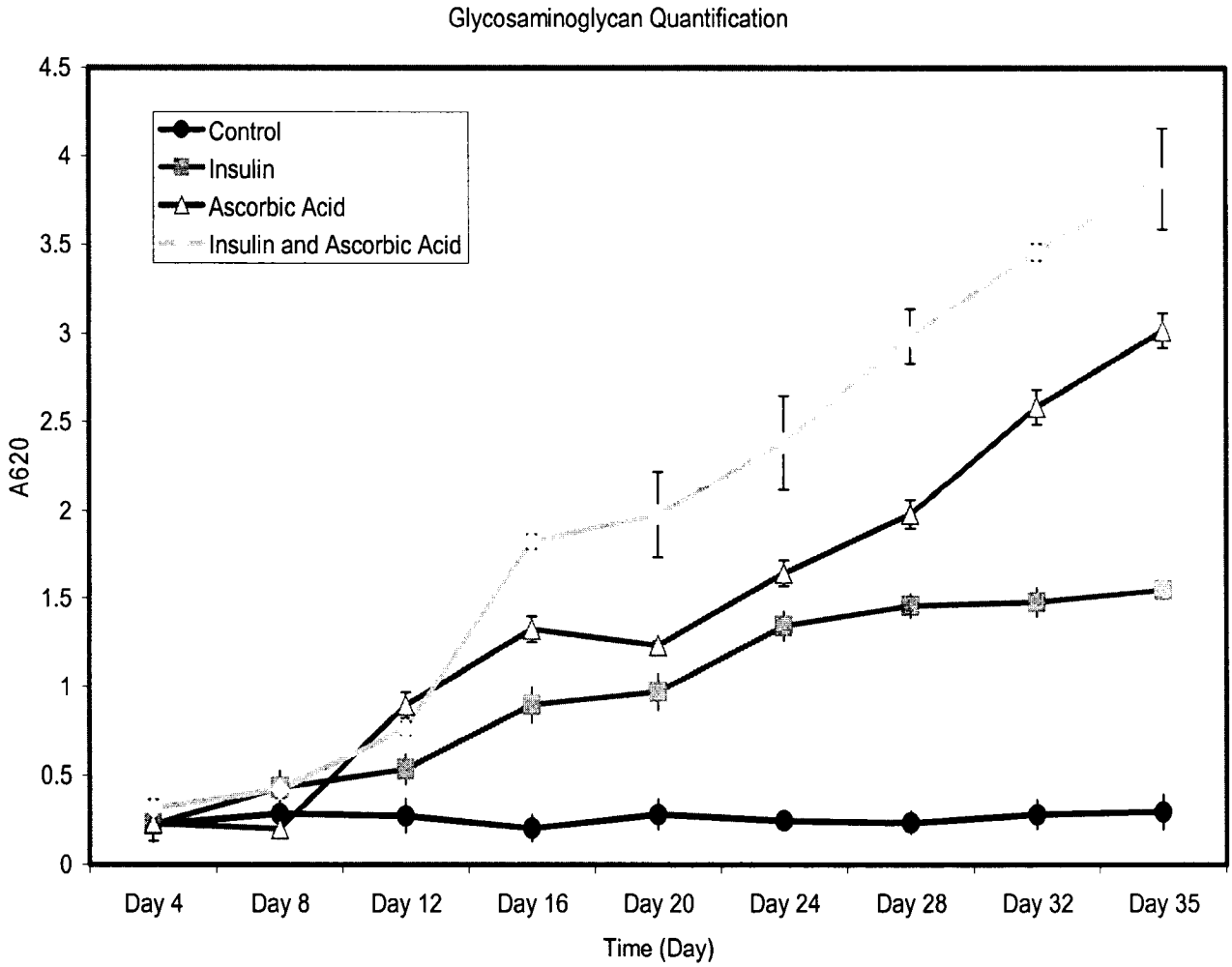

Figure 16: Glycosaminoglycan quantification of ATDC5 cells induced with different inducers. To evaluate the synthesis of ECM, sulfated glycosaminoglycans were visualized by staining with Alcian Blue. The Alcian Blue-stained cultures were extracted guanidine-HCl overnight at room temperature. The optical density of the extracted dye was measured at 620 nm in a spectrophotometer. ATDC5 cells were chondrogenic when induced with insulin. Ascorbic acid is more efficient in inducing choondrogenesis in ATDC5 cells compared to insulin. A combination of insulin and ascorbic acid seemed to have an additive effect in chondrogenesis induction in ATDC5 cells.

3.5 Expression of S-1P, aggrecan, collagen I, collagen II and collagen X in ATDC5 cells induced with different inducers

Does expression level of S-1P differ in the control and induced ATDC5 cells? Does the expression level of S-1P depend on the differentiation inducers? And does the expression level of S-1P related to the progression of chondrocyte differentiation?

To answer these questions, quantitative Real-time PCR analysis was performed. Results showed that *S-1P* is constitutively expressed in ATDC5 cells. However its expression level does depend on the differentiation inducers and the progression of chondrocyte differentiation in ATDC5 cells. On day 4 when the cells were at subconfluent stage (Figure 12a), the expression level of *S-1P* in ATDC5 cells induced with insulin alone, ascorbic acid alone or the combination of ascorbic acid and insulin was not higher in the control cells that were not induced with differentiation inducers (Figure 17a). *S-1P* expression peaked on day 12 at the early phase differentiation when ATDC5 cells formed cartilage nodules with round morphology (Figure 12c), especially in the experimental group of cells induced with a combination of 10 μg/mL bovine insulin and 37.5 μg/mL of ascorbic acid. The differentiation was also quantitatively characterized by increased in glycosaminoglycan accumulation (Figure 16). Similarly to glycosaminoglycan accumulation, the use of combination of insulin and ascorbic acid seemed to have additive effect of the expression S-1P (Figure 17a). The expression of the protease in ATDC5 cells declined in all experimental groups after day 12, especially after day 20 when the cells had reached the stage of hypertrophy and mineralization (Figure 16).

The differentiation of ATDC5 cells was further quantitatively illustrated by sequential increases in aggrecan, collagen I, collagen II, collagen X mRNAs from days 4 to days 35. The pro-condensation marker, *collagen I*, began to increase on day 4, peaked at day 8 and gradually declined after that (Figure 17b). The highest incidence of *collagen I* expression occurred on day 8 in the ATDC5 cells induced with a combination of 10 μg/mL bovine insulin and 37.5 μg/mL of ascorbic acid (Figure 17b).

The early and mature chondrocyte marker, *collagen II,* began to increase at day 4, peaked at day 12 and gradually declined after reaching its peak (Figure 17c).The expression profile of *aggrecan*(Figure 17d) mimicked that of *collagen II* but with a higher fold

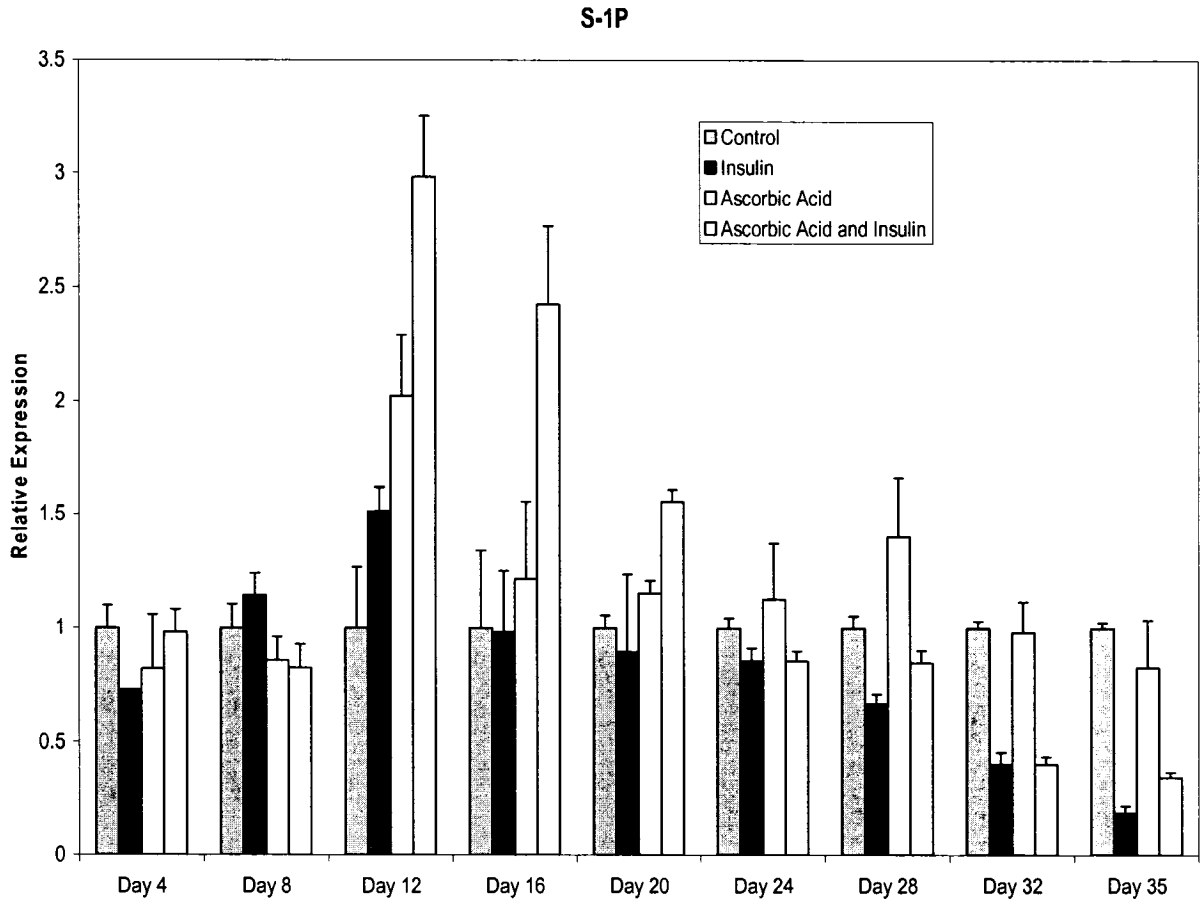

Figure 17a: Expression of *S-1p* in ATDC5 cells on day 4, 8, 12, 16, 20, 24, 28, 32 and 35. Total RNA was extracted from ATDC5 cells and the relative expression of *S-1p* was determined by TaqMan quantitative real-time PCR. A ΔC_T value was first calculated by subtracting the C_T value for the housekeeping gene β-actin from the C_T value from each sample. A $\Delta\Delta C_T$ value was then calculated by subtracting the ΔC_T value of the control (non-induced, non transfected ATDC5 cells) from the ΔC_T value of each treatment. Fold changes compared with the control were then determined by raising 2 to the $\Delta\Delta C_T$ power. *S-1p* expression peaked on day 12 and gradually declined after that. The expression of *S-1p* on day 12 is highest in the group of ATDC5 cells induced with a combination of 10 μg/mL bovine insulin and 37.5 μg/mL of ascorbic acid

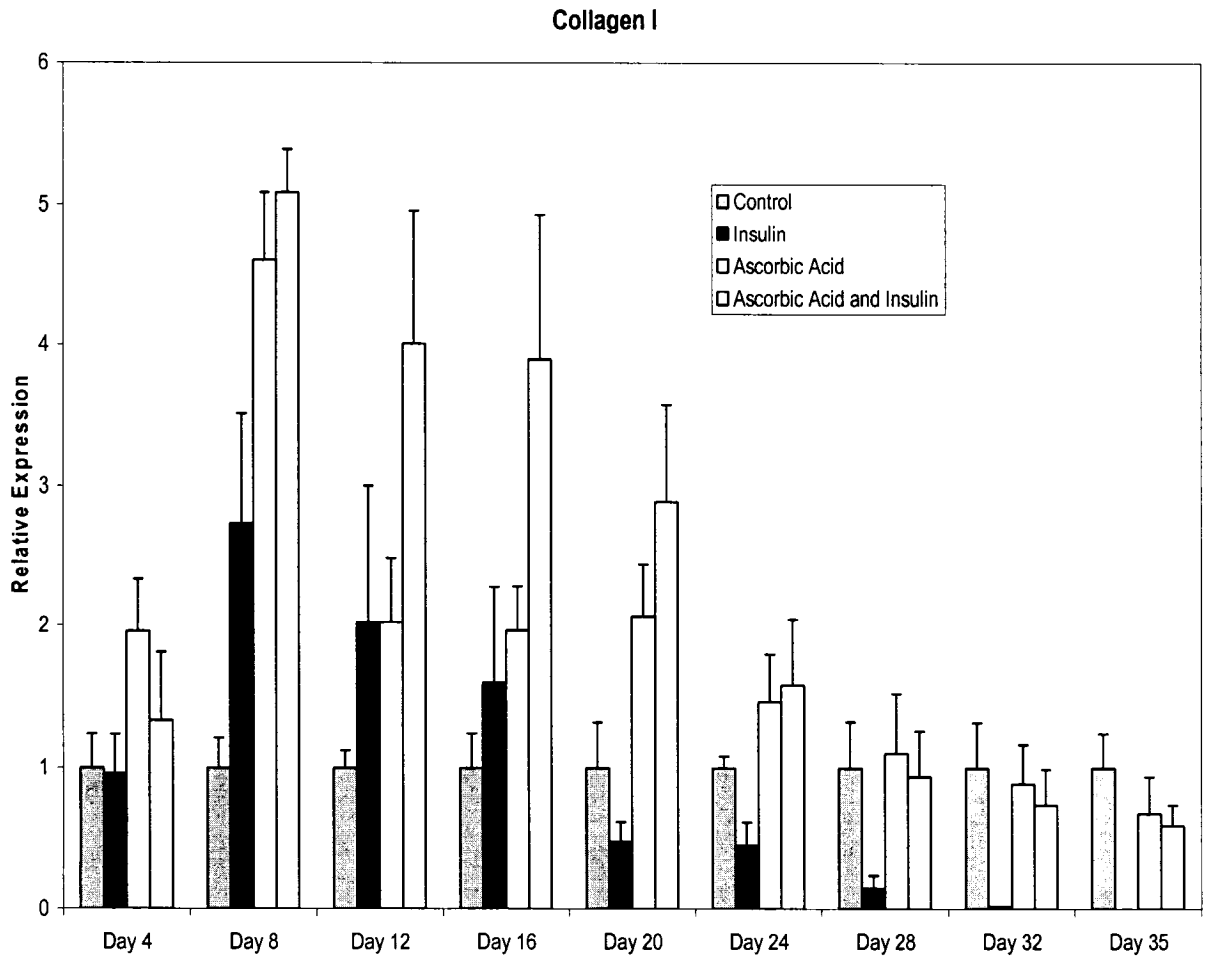

Figure 17b: Expression of *collagen I* in ATDC5 cells on day 4, 8, 12, 16, 20, 24, 28, 32 and 35. Total RNA was extracted from ATDC5 cells and the relative expression of *collagen I* was determined by TaqMan quantitative real-time PCR. *collagen I* , the pro-condensation chondrocyte marker, began to increase on day 4, peaked on day 8 and gradually decline after reaching its peak. The expression of *collagen I* during its peak is highest in the group of ATDC5 cells induced with a combination of 10 μg/mL bovine insulin and 37.5 μg/mL of ascorbic acid.

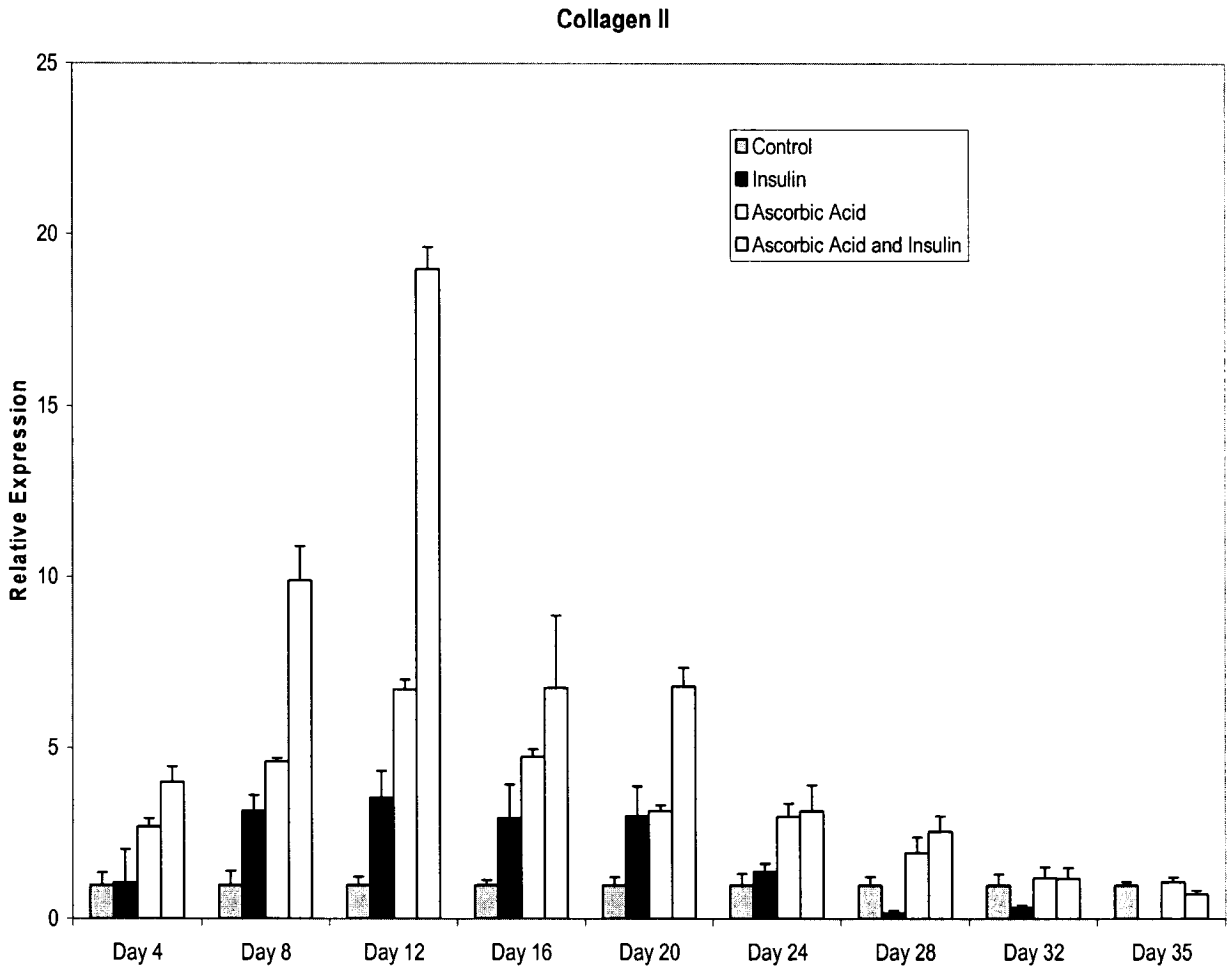

Figure 17c: Expression of *collagen II* in ATDC5 cells on day 4, 8, 12, 16, 20, 24, 28, 32 and 35. Total RNA was extracted from ATDC5 cells and the relative expression of *collagen II* was determined by TaqMan quantitative real-time PCR. *collagen II*, the early phase and mature chondrocyte marker started to increase on day 4 and was markedly upregulated on day 12. The combination of 10 μg/mL bovine insulin and 37.5 μg/mL of ascorbic acid showed the highest inducing effect in *collagen II* expression in ATDC5 cells.

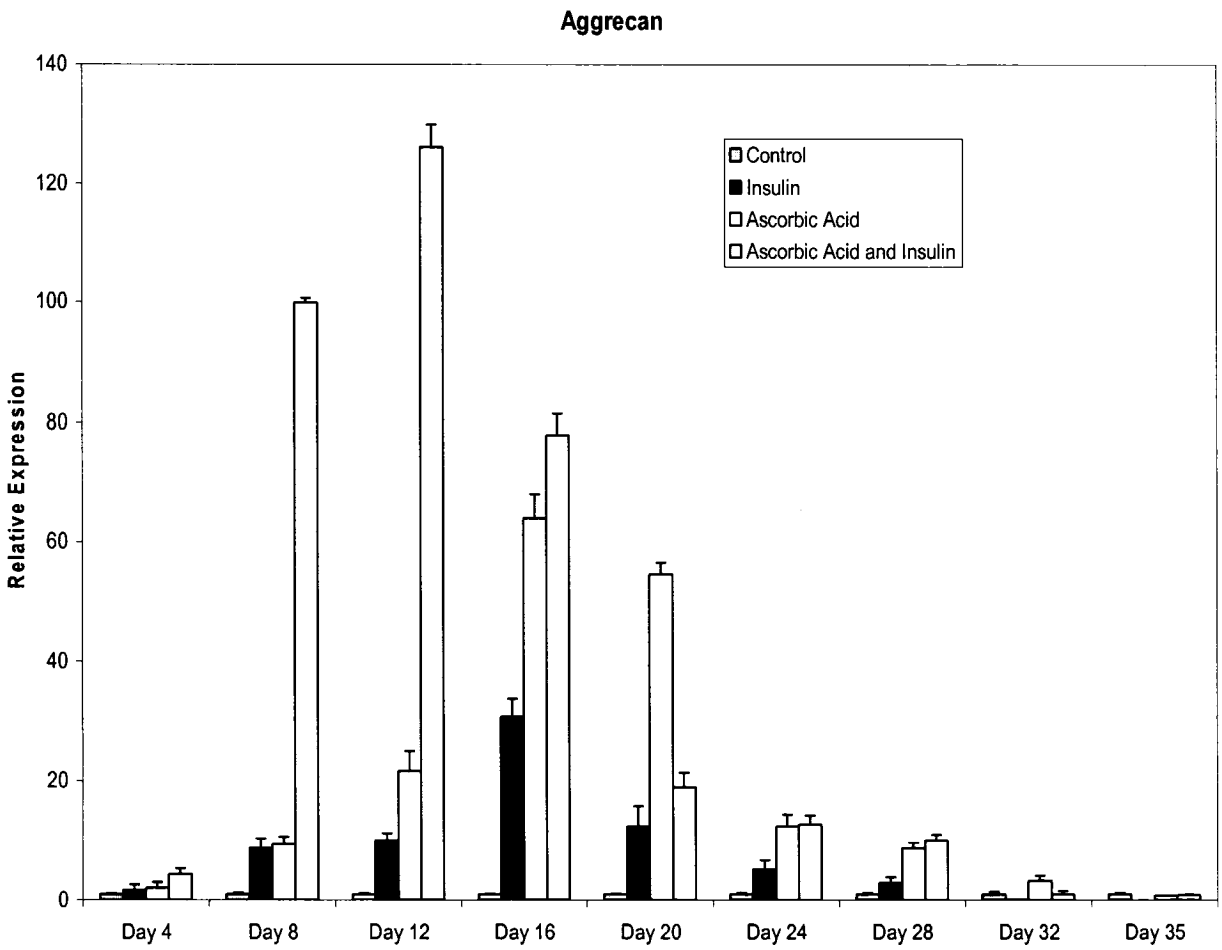

Figure 17d: Expression of *aggrecan* in ATDC5 cells on day 4, 8, 12, 16, 20, 24, 28, 32 and 35. Total RNA was extracted from ATDC5 cells and the relative expression of *aggrecan* was determined by TaqMan quantitative real-time PCR. *aggrecan*, the early phase and mature chondrocyte marker mimicked that of *collagen II*. *aggrecan* started to increase on day 4 and was markedly upregulated on day 12. The combination of 10 μg/mL bovine insulin and 37.5 μg/mL of ascorbic acid showed the highest inducing effect in *aggrecan* expression in ATDC5 cells.

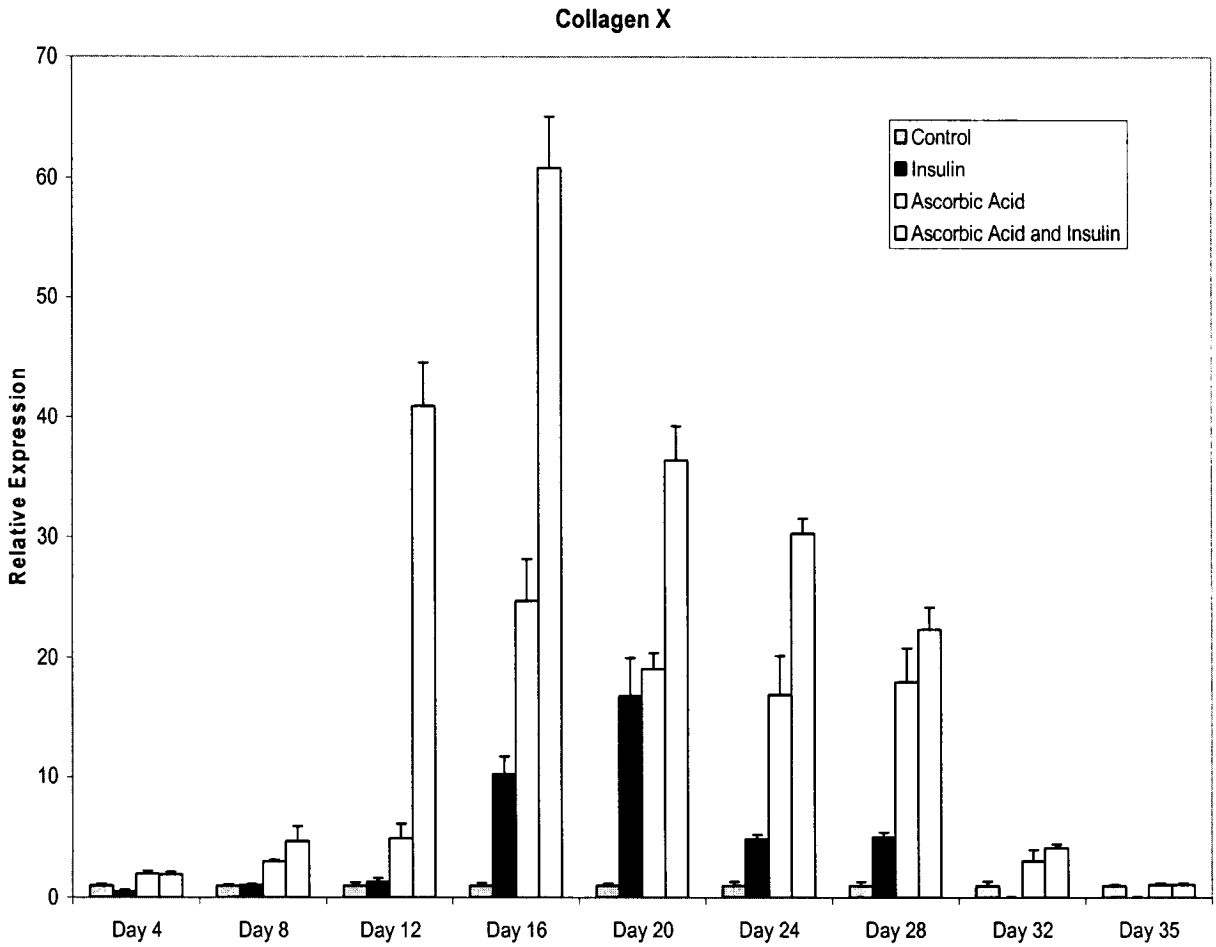

Figure 17e: Expression of *collagen X* in ATDC5 cells on day 4, 8, 12, 16, 20, 24, 28, 32 and 35. Total RNA was extracted from ATDC5 cells and the relative expression of *collagen X* was determined by TaqMan quantitative real-time PCR. *collagen X* is a hypertrophic chondrocyte marker. Its expression peaked on day 16. The combination of 10 μg/mL bovine insulin and 37.5 μg/mL of ascorbic acid showed the highest inducing effect in *collagen X* expression in ATDC5 cells.

increase. The decline in expression of *aggrecan* and *collagen II* coincided with the onset of the late stage of chondrocyte differentiation. The message of the hypertrophic chondrocyte marker, *collagen X*, began to increase on day 12 and reached its peak on day 16 (Figure 17e). The expression patterns of these early and late chondrocyte markers described here were consistent with previous findings using ATDC5 cells and in vivo chondrocyte differentiation (79-81).

It was observed that *S-1p* expression mimicked that of *collagen II* and *aggrecan*—reaching its peak on day 12 when the cells have formed cartilage nodules and its declination coincided with hypertrophy of ATDC5 cells, with the increase of hypertrophic chondrocyte marker, *collagen X*.

It was also observed that the use of a combination of 10 μg/mL of bovine insulin and 37.5 μg/mL of ascorbic acid shown to have the highest effects in inducing chondrogenesis in ATDC5 cells. Results showed that the expression of all the early and late chondrocyte markers tested here were highest in the cells induced with the combination of both chondrogenic inducers.

3.6 The effect of the inhibition of S-1P on ATDC5 cells

Real-time PCR results showed that S-1P expression in ATDC5 cells does depend on differentiation inducers and its expression level also related to the progression of chondrocyte differentiation in ATDC5 cells. Since the combination of 10 μg/mL bovine insulin and 37.5 μg/mL of ascorbic acid shown to have the highest effects in inducing chondrogenesis in ATDC5 cells, the cells were cultured in the maintenance media supplemented with a combination of both differentiation inducers in the following experiments.

In order to study the effect of the inhibition of S-1P on ATDC5 cells, I attempted an experiment to inhibit S-1P in ATDC5 cells. Inhibition of S-1P in the cells was performed using the R134E prosegment mutant of S-1P (pro-SKI-1) which has been shown to be a potent cellular inhibitor of S-1P. ATDC5 cells were stably transfected using a construct for pro-SKI-1 that had been subcloned into pIRES2. The vector contains the enhanced green fluorescent protein (EGFP) coding region linked to the internal ribosome entry site

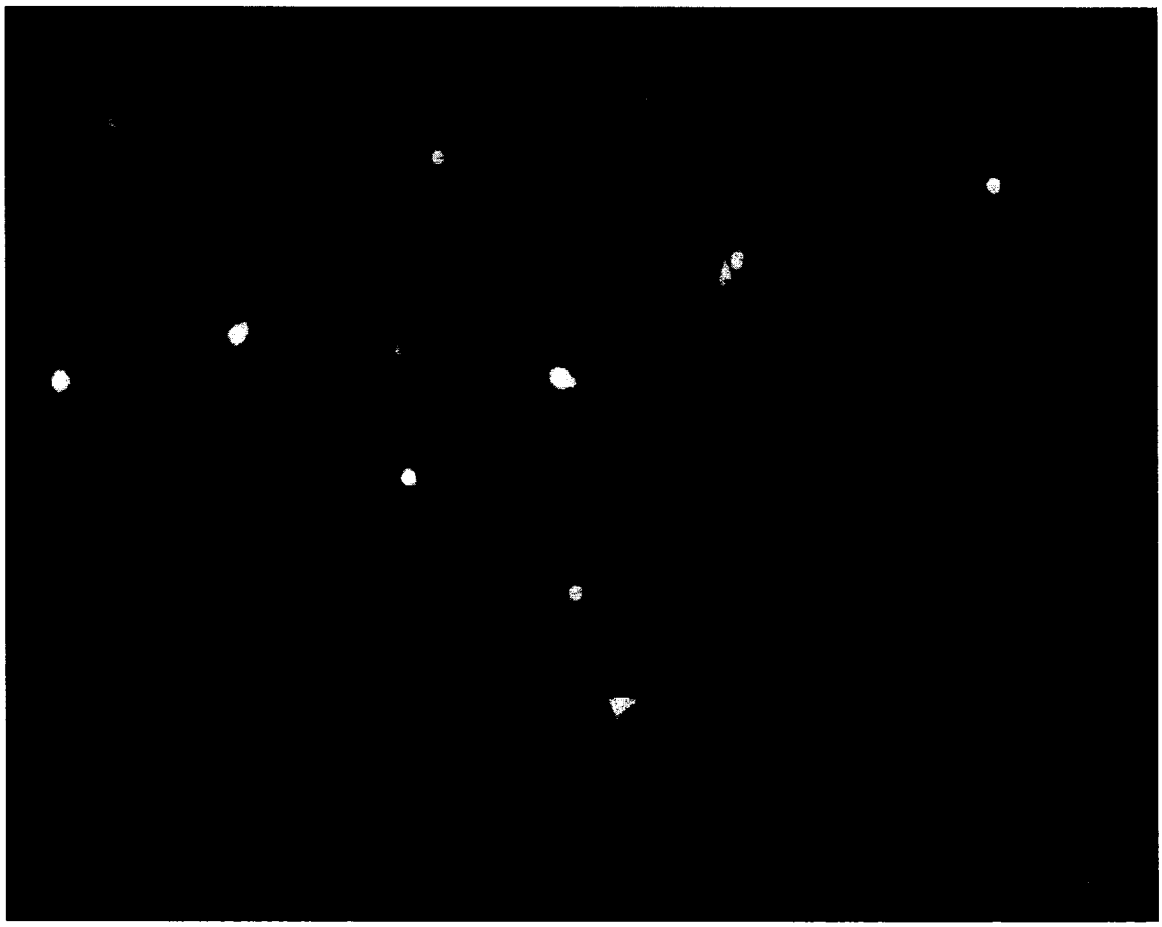

Figure 18a: Superimposed image of ATDC5 cells transfected with the DNA of the control (pIRES-EGFP) on 48 hours post-transfection. All cells took up DAPI and were glowing bright in blue when viewed under UV light. And the cells with DNA of pIRES-EGFP integrated were glowing in fluorescent green.

Figure 18b: Superimposed image of ATDC5 cells transfected with the DNA of pIRES-proSKI-EGFP on 48 hours post-transfection. All cells took up DAPI and were glowing bright in blue when viewed under UV light. And the cells with DNA of pIRES-proSKI-EGFP integrated were glowing in fluorescent green.

(IRES;1,2) of the encephalomyocarditis (ECMV) between the multiple cloning site (MCS) and the enhanced protein (EGFP) coding region. This permits both the gene of interest (cloned into the MCS) and the EGFP gene to be transcribed and translated from a bicistronic mRNA driven by a CMV promoter. The plasmid DNA used in the transfection was expressing either pIRES-EGFP alone (as a control of the transfection) or pIRES-EGFP-proSKI R134E.

Forty-eight hours post-transfection, ATDC5 cells were stained with DAPI and photomicrographs were taken. It was observed that ATDC5 cells that took up the plasmid DNA appeared fluorescent green when viewed with fluorescence microscope as a result of the presence of the EGFP in the construct (Figure 18a and b).

ATDC5 cells were very healthy after transfection, as shown in DAPI staining. Nuclei of the cells had the normal phenotype because they were glowing bright in blue and homogenously (Figure 18a and b). Transfection efficiency was however very low in both group of cells transfected with plasmid DNA expressing either pIRES-EGFP alone (Figure18a) or pIRES-pro-SKI-EGFP(R134E) (Figure18b).

Stable clones were isolated after 1 ½ months of culture in G418 (neomycin). Alcian Blue staining was performed on the cells. Cell-bound Alcian Blue was extracted using 6 M guanidine-HCl after staining and washing. Glycosaminoglycan accumulation was assayed quantitatively by spectroscopy.

On day 4 of culture, control ATDC5 cultures did not bind Alcian Blue dye, indicating the cells were not chondrogenic at this stage (Figure 19a). Three clones were selected from ATDC5 cells that were stably transfected with DNA of pIRES-EGFP. All 3 clones did not bind Alcian Blue dye on day 4 of culture, so as the 7 clones of ATDC5 cells that were stably transfected with DNA of pIRES-pro-SKI-EGFP, indicating the cells were not chondrogenic on day 4 despite the fact that they were induced with 10 μg/mL bovine insulin and 37.5 μg/mL of ascorbic acid. Results were consistent with glycosaminoglycan quantification.

On day 16 of culture, cells in the control group that were not induced with the supplementation of 10 μg/mL bovine insulin and 37.5 μg/mL of ascorbic acid did not bind Alcian Blue dye (Figure 19b), and indicative sign that the cells were not chondrogenic and did not form cartilage specific extracellular matrix at this stage. This

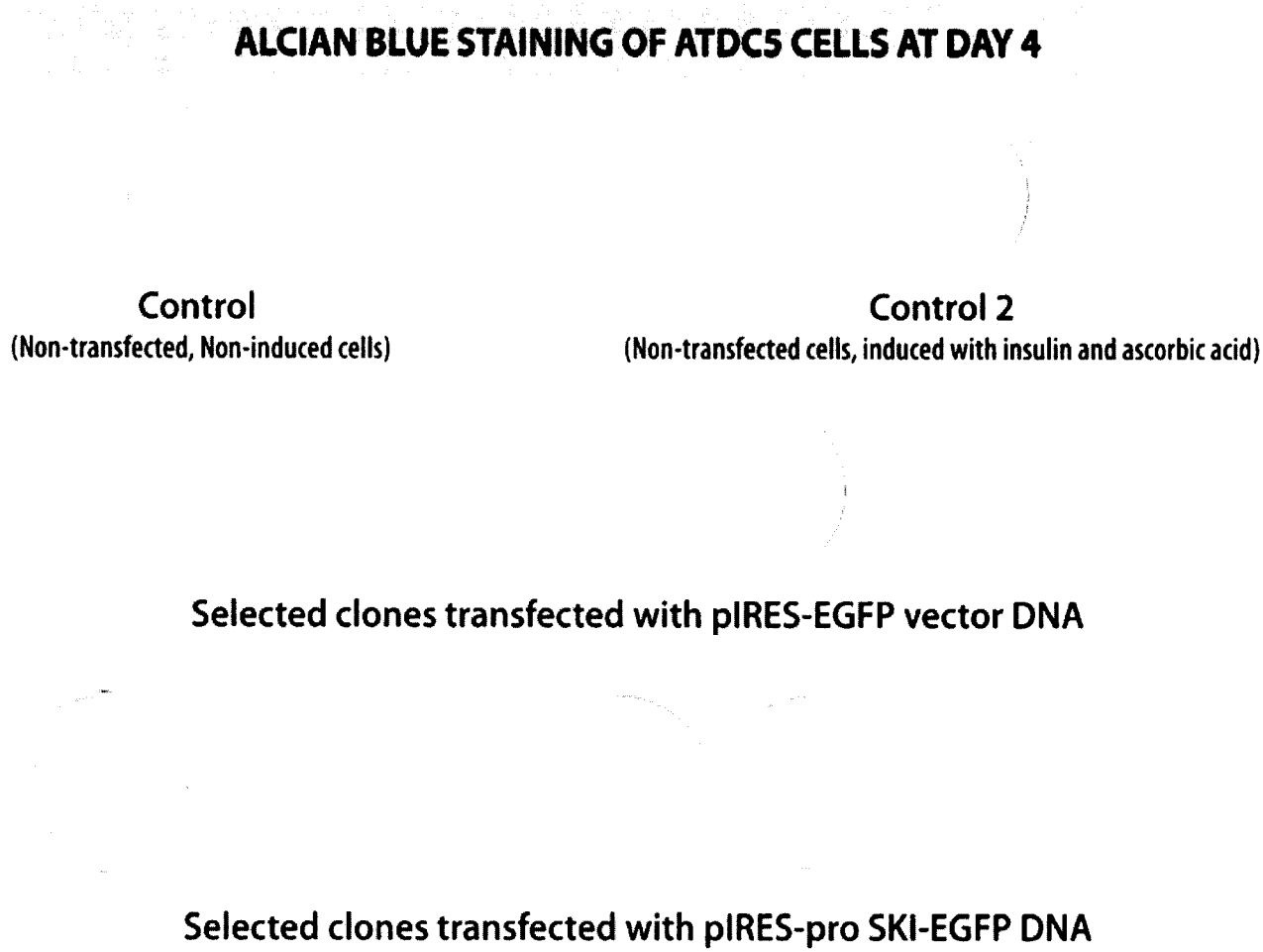

Figure 19a: Alcian Blue Staining of ATDC5 cells on day 4. Except for cells of control group that were non-transfected and non-induced, cells of all other groups were supplemented with 10 μg/mL bovine insulin and 37.5 μg/mL of ascorbic acid in the maintenance media. The cells hardly bound Alcian Blue at this point, indicating they were not chondrogenic on day 4.

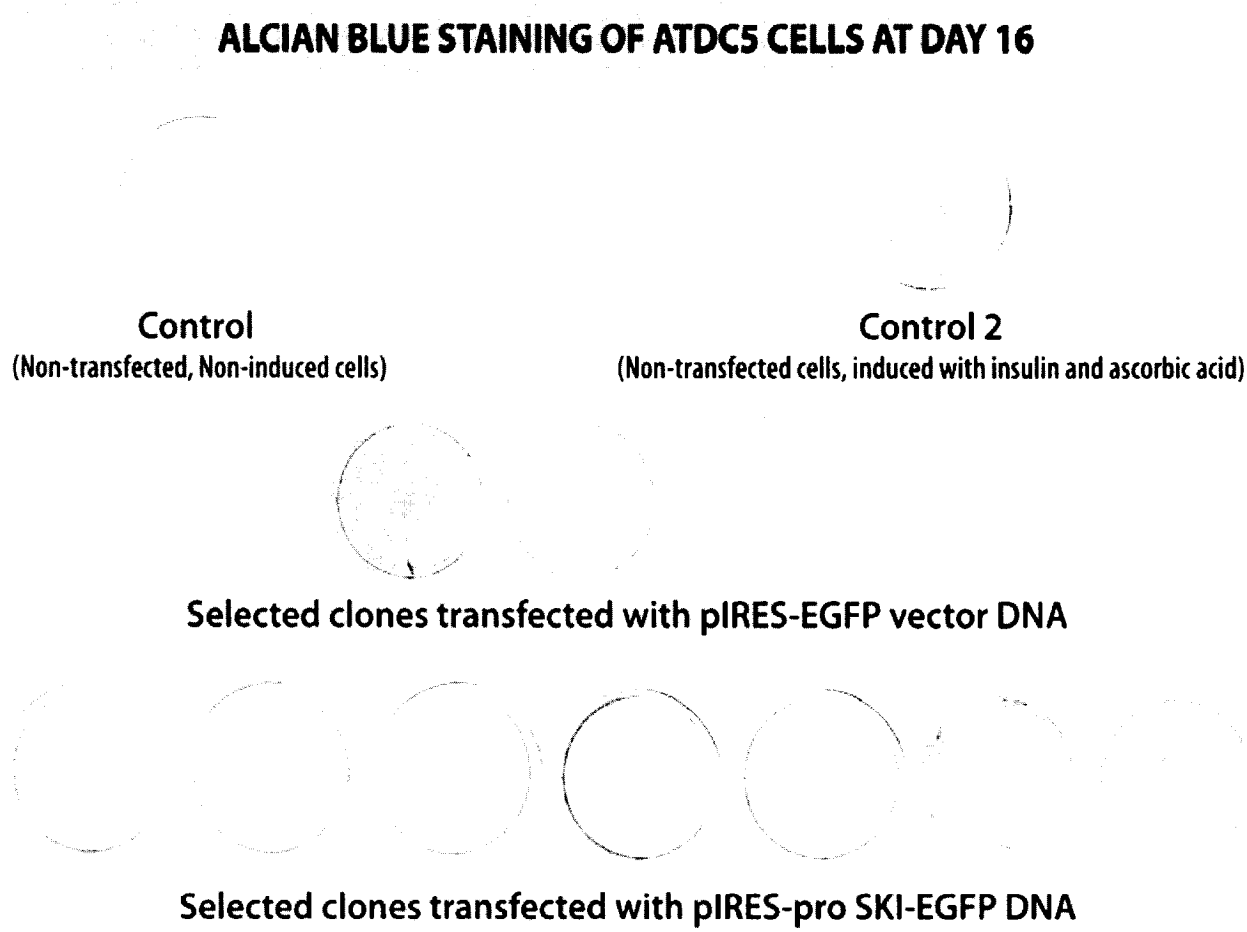

Figure 19b: Alcian Blue staining of ATDC5 cells on day 16. Except for cells of control group that were non-transfected and non-induced, cells of all other groups were supplemented with 10 μg/mL of bovine insulin and 37.5 μg/mL of ascorbic acid in the maintenance media. Cells of control group (control 2) that were non-transfected but were induced with insulin and ascorbic acid showed enhanced staining in Alcian Blue dye. The 3 selected clones that were stably transfected with the DNA of pIRES-EGFP also intensely stained Alcian Blue dye at this stage. 5 clones out of 7 of the ATDC5 cells that were stably transfected with the DNA of pIRES-pro-SKI-EGFP were not chondrogenic as they bound very little Alcian Blue. 2 of the clones from this experimental group of cells were highly chondrogenic at this point as they were intensely stained with Alcian Blue dye.

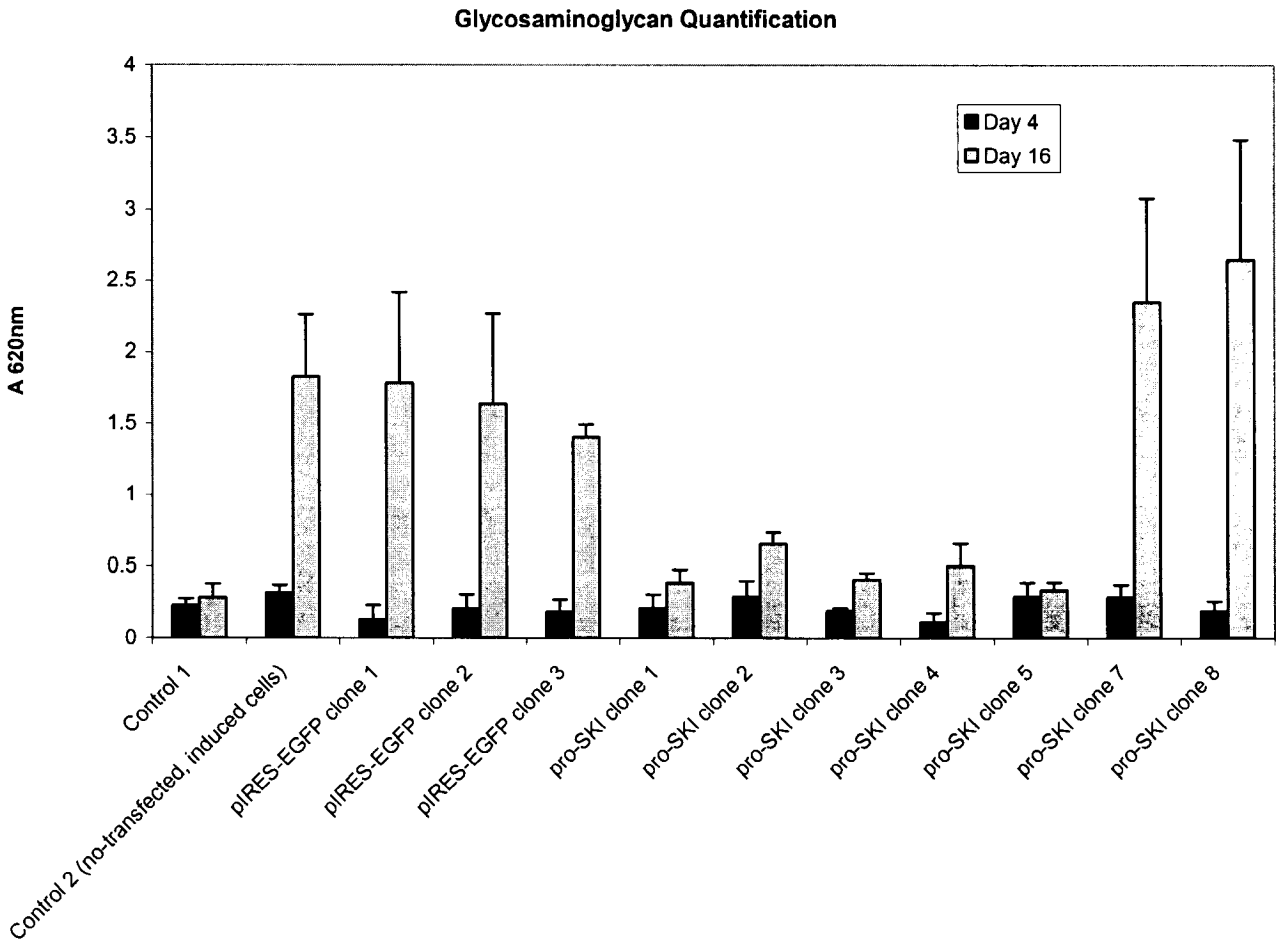

Figure 20: Glycosaminoglycan quantification of ATDC5 cells on day 4 and day 16 of culture. On day 4 of culture, cells of all control and experimental groups showed very low amount of glycosaminoglycan accumulation. On day 16, control cells that were non-transfected but were induced with insulin and ascorbic acid showed increased amount of glycosaminoglycan accumulation. The 3 selected clones that were stably transfected with the DNA of pIRES-EGFP also showed increased in glycosaminoglycan accumulation. 5 clones out of 7 of the ATDC5 cells that were stably transfected with the DNA of pIRES-pro-SKI-EGFP showed very low level of glycosaminoglycan accumulation even on day 16 of culture. However 2 of the clones (clone 6 and clone 7) from this experimental group of cells showed highest amount of glycosaminoglycan accumulation.

was consistent with result of glycosaminoglycan quantification. This group of control cells showed very low level of glycosaminoglycan accumulation at this stage (Figure 20). However, the group of control cells (Control 2) that were not transfected with either the DNA of pIRES-EGFP or pIRES-EGFP-proSKI R134E but were induced with 10 μg/mL bovine insulin and 37.5 μg/mL of ascorbic acid showed enhanced staining with Alcian Blue dye (Figure 19b), and increased level of glycosaminoglycan accumulation (Figure 20). All 3 clones that were selected from ATDC5 cells that were stably transfected with the DNA of pIRES-EGFP and induced with 10 μg/mL bovine insulin and 37.5 μg/mL of ascorbic acid were chondrogenic on day 16 of culture evidenced by enhanced Alcian Blue staining (Figure 19b) and increased glycosaminoglycan accumulation (Figure 20). On day 16, 5 clones out of 7 of the ATDC5 cells that were stably transfected with the DNA of pIRES-pro-SKI-EGFP were not chondrogenic as they bound very little Alcian Blue (Figure 19b) and showed very low level of glycosaminoglycan accumulation (Figure 20). However 2 of the clones (clone 6 and clone 7) from this experimental group of cells were highly chondrogenic at this point as they were intensely stained with alcian bue dye (Figure 19b) and also showed highest amount of glycosaminoglycan accumulation (Figure 20) compared to cells of control and other experimental groups.

Stably transfected ATDC5 cells were selected and the consequences of S-1P inhibition on the expression of cartilage related components were analyzed by performing real-time PCR.

The expression of *collagen I,* the early, pro-condensation marker was high on day 4 and lowered by day 16 (Figure 21a) in ATDC5 cells of all control and experimental groups. Expression level of *collagen I* of ATDC5 cells that were stably transfected with the DNA of pIRES-EGFP was similar to the cells of the control group that were non-transfected but were induced with insulin and ascorbic acid, which was 3-4 fold higher than cells of the control group that were non-transfected and non-induced. However, the expression of *collagen I* was lower in clones 1-5 of ATDC5 cells transfected with the DNA of pIRES-pro-SKI-EGFP compared to cells of the experimental group that were transfected with the DNA of pIRES-EGFP and the cells that were induced but not transfected. This could be an indication that the inhibition of S-1P inhibited the

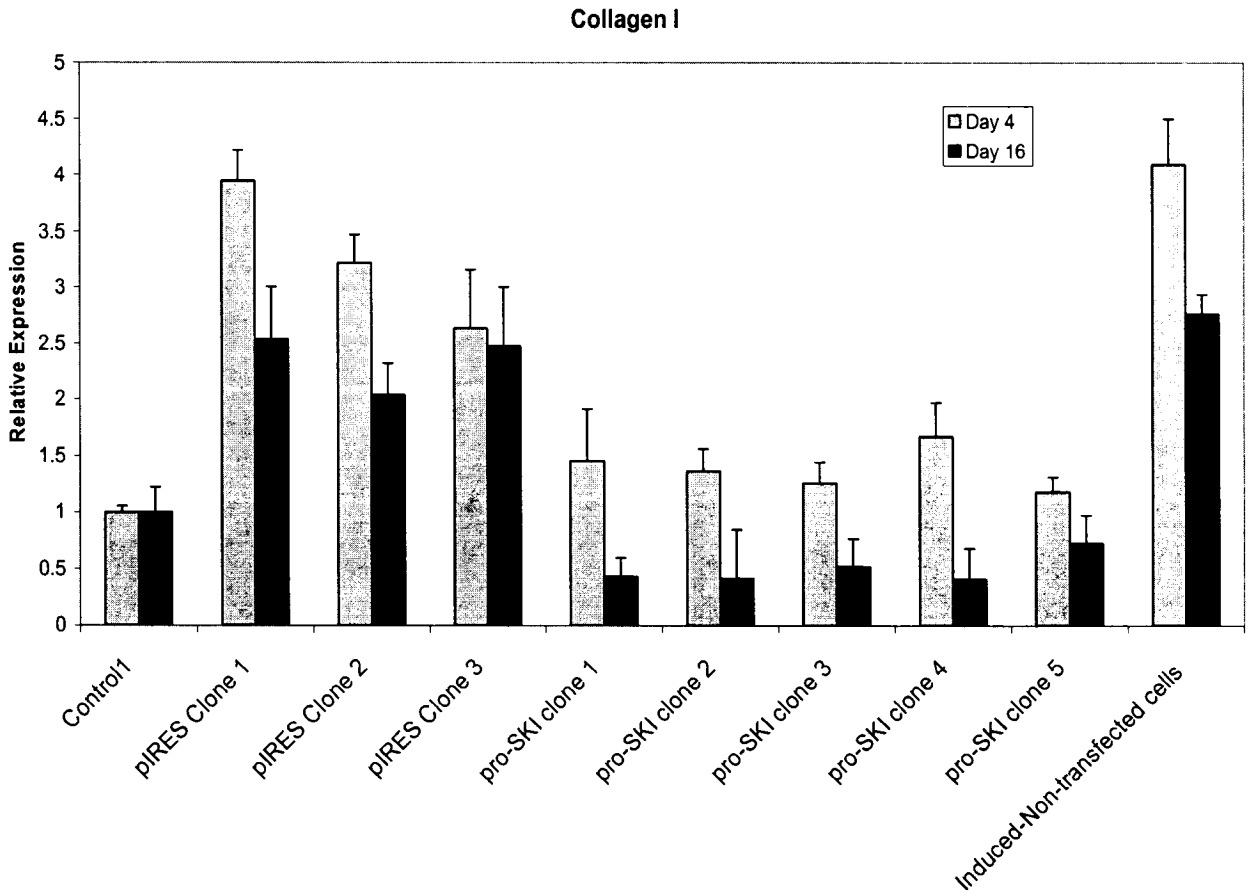

Figure 21a: Expression of *collagen I* in ATDC5 cells on day 4 and day 16 of culture. Except for cells of control 1, cells of all experimental groups were cultured in maintenance media and supplemented with 10 μg/mL of bovine insulin and 37.5 μg/mL of ascorbic acid. Total RNA was extracted from ATDC5 cells on day 4 and day 16; and the relative expression of *collagen I* was determined by TaqMan quantitative real-time PCR. *collagen I* , the pro-condensation chondrocyte marker of ATDC5 cells that were stably transfected with the DNA of pIRES-EGFP was similar to the cells of the control group that were non-transfected but were induced with insulin and ascorbic acid, which was 3-4 fold higher than cells of the control group that were non-transfected and non-induced. Clones 1-5 of ATDC5 cells transfected with the DNA of pIRES-pro-SKI-EGFP showed lowest expression level of *collagen I* compared to ATDC5 cells that were stably transfected with the DNA of pIRES-EGFP and cells that were induced but non-transfected.

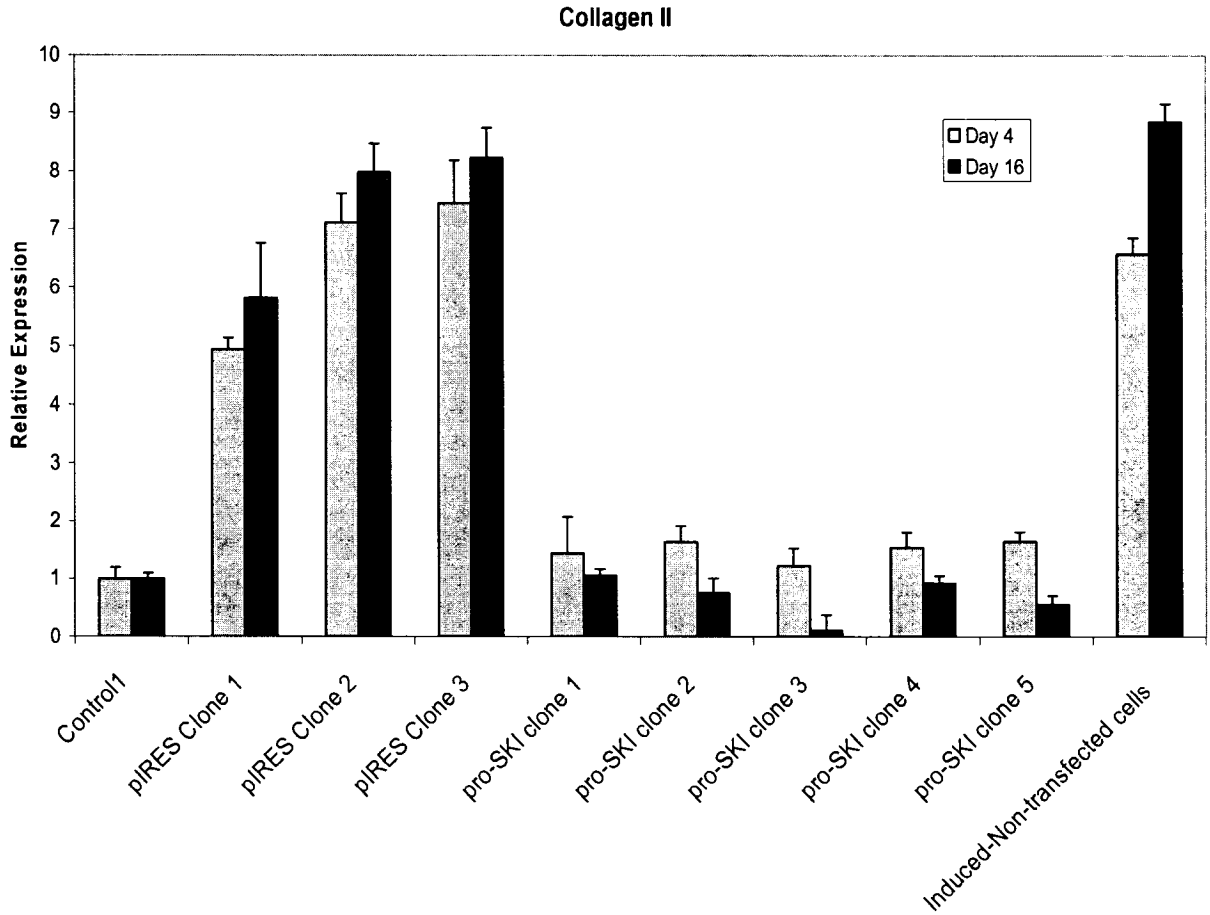

Figure 21b: Expression of *collagen II* in ATDC5 cells on day 4 and day 16 of culture. Except for cells of control 1, cells of all experimental groups were cultured in maintenance media and supplemented with 10 μg/mL of bovine insulin and 37.5 μg/mL of ascorbic acid. Total RNA was extracted from ATDC5 cells on day 4 and day 16; and the relative expression of *collagen I* was determined by TaqMan quantitative real-time PCR. *collagen II* expression was highest in the ATDC5 cells stably transfected with the DNA of pIRES-EGFP and cells of the control group that were non-transfected but induced with insulin and ascorbic acid. The expression of *collagen II* was highest on day 16 in these cells. Clones 1-5 of ATDC5 cells that were transfected with the DNA of pIRES-pro-SKI-EGFP showed much lower *collagen II* expression compared to the formers, and the expression of *collagen II* was higher on day 4 than on day 16.

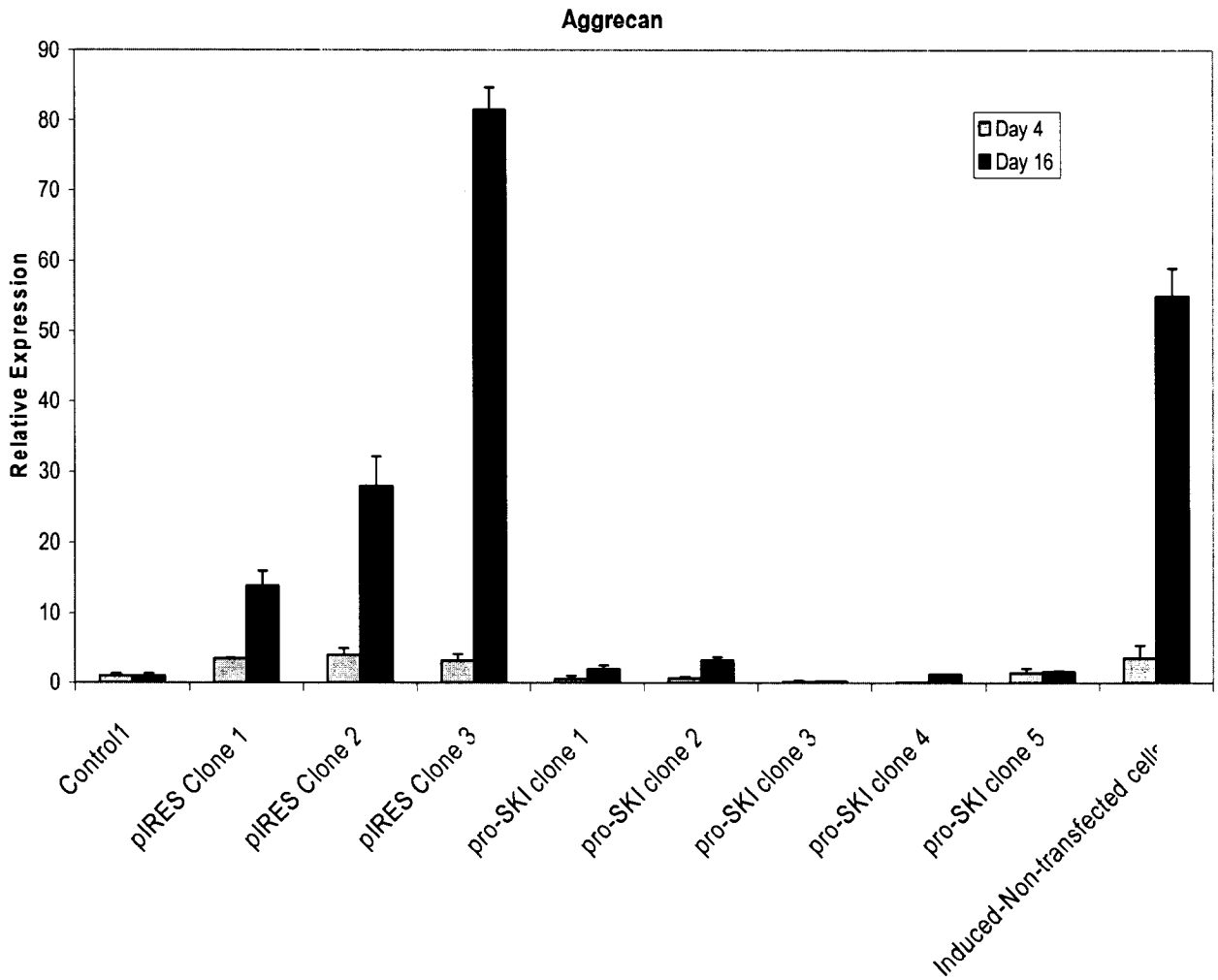

Figure 21c: Expression of *aggrecan* in ATDC5 cells on day 4 and day 16 of culture. The expression of *aggrecan* peaked on day 16, and its expression is highest in the cells stably transfected with the DNA of pIRES-EGFP and cells of the control group that were non-transfected but induced with insulin and ascorbic acid. The expression of *aggrecan* was significantly suppressed on both day 4 and day 16 in ATDC5 cells transfected with the DNA of pIRES-pro-SKI-EGFP.

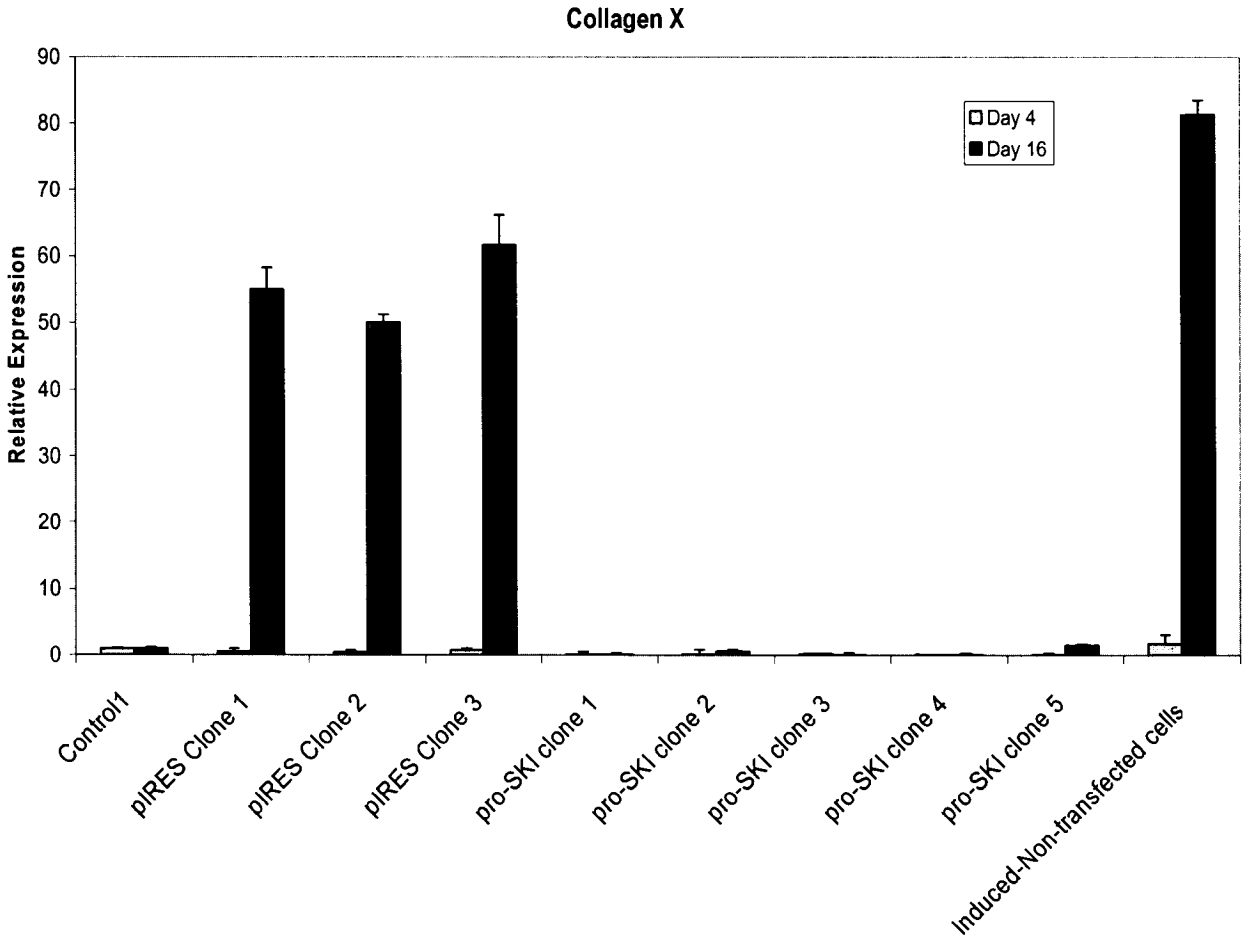

Figure 21d: Expression of *collagen X* in ATDC5 cells on day 4 and day 16 of culture. The expression of *collagen X* reached its peak on day 16 of culture in the control cells that were induced but non-transfected, and also in the ATDC5 cells stably transfected with the DNA of pIRES-EGFP. There expression of *collagen X* was severely suppressed in ATDC5 cells that were stably transfected with the DNA of pIRES-pro-SKI-EGFP on both day 4 and day 16.

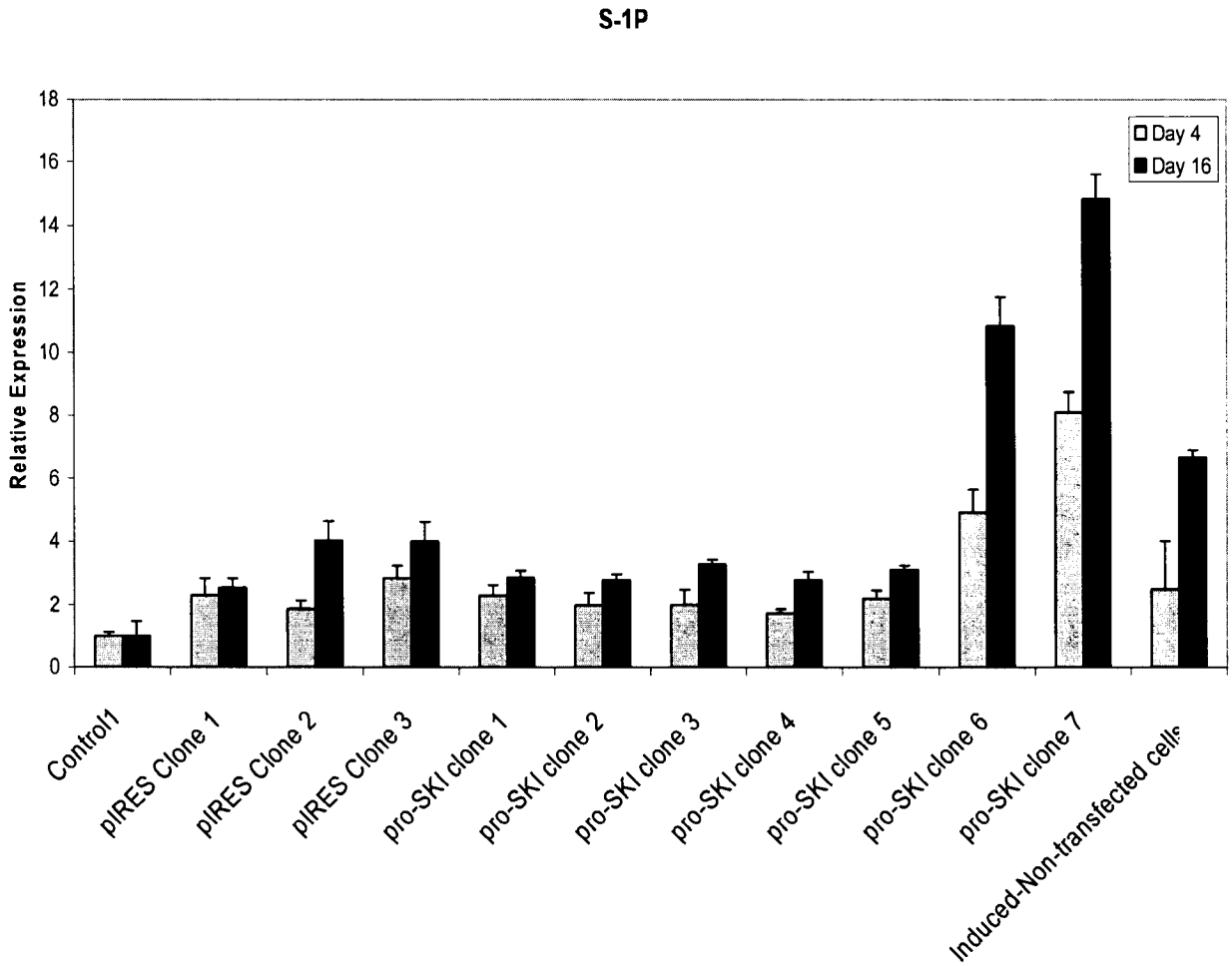

Figure 21e: Expression of *S-1p* in ATDC5 cells on day 4 and day 16 of culture.

The expression level of *S-1p* in ATDC5 cells on day 4 and day 16 were similar in cells stably transfected with the DNA of pIRES-EGFP and clones 1-5 of the group that were transfected with the DNA of pIRES-pro-SKI-EGFP. However clone 6 and clone 7 in this experimental group showed 3-5 fold higher in *S-1p* expression on day 4 and 7-11 fold higher in its expression on day 16.

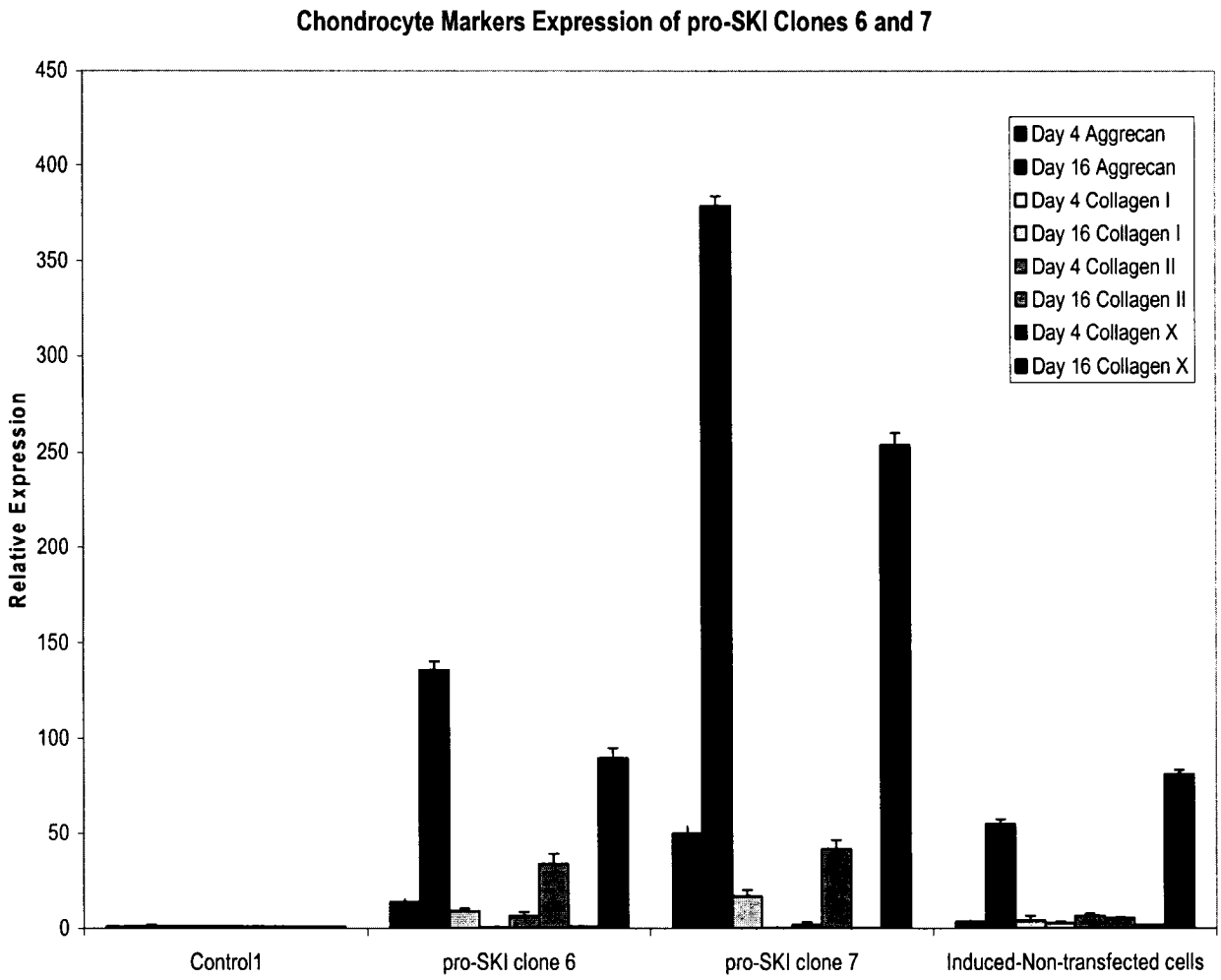

Figure 21f: Expression of aggrecan, collagen I, II and X in clones 6 and 7 of ATDC5 cells stably transfected with the DNA of pIRES-pro-SKI-EGFP. Clones 6 and 7 expressed high mRNA level of chondrocyte differentiation markers tested—more than a hundred folds higher than cells of the control group that were induced but non-transfected.

expression of *collagen I*, and perturbed chondrogenesis of ATDC5 cells as early as in the pro-condensation stage when collagen I was the prominent marker. S-1P inhibition also shown to have an inhibition effect on *collagen I* expression on day 16.

collagen II expression (Figure 21b) was highest in the ATDC5 cells stably transfected with the DNA of pIRES-EGFP and cells of the control group that were non-transfected but induced with insulin and ascorbic acid. The expression of *collagen II* was highest on day 16 in these cells. The expression of *collagen II* was lower in clones 1-5 of ATDC5 cells that were transfected with the DNA of pIRES-pro-SKI-EGFP compared to the formers, and the expression of *collagen II* was higher on day 4 than on day 16. The inhibition of S-1P in these cells seemed to have perturbed the expression of *collagen II* in both early and late stage of chondrogenesis, but with more pronounced effect when the cells have reached mature, condensation stage.

The expression pattern of *aggrecan* (Figure 21c) was similar to that of *collagen II.* Its expression was highest in the ATDC5 cells stably transfected with the DNA of pIRES-EGFP and cells of the control group that were non-transfected but induced with insulin and ascorbic acid. The expression of *collagen II* was highest on day 16 in these cells. However the expression of *aggrecan* seemed to be significantly suppressed in clones 1-5 of ATDC5 cells that were transfected with the DNA of pIRES-pro-SKI-EGFP on both day 4 and day 16 of culture.

The expression of the hypertrophic chondrocyte marker, *collagen X*, was very low on day 4 of culture in ATDC5 cells of the control and in all experimental groups. The mRNA of the collagen reached its peak on day 16 of culture in the control cells that were induced but non-transfected, and also in the ATDC5 cells stably transfected with the DNA of pIRES-EGFP. There expression of *collagen X* was severely suppressed in ATDC5 cells that were stably transfected with the DNA of pIRES-pro-SKI-EGFP on both day 4 and day 16. Since the inhibition of S-1P suppressed the expression of *collagen X*, this indicated that the inhibition of S-1P might perturb chondrogenesis in ATDC5 cells at late stage of chondrocyte differentiation -- when the cells were at the stage of hypertrophy and mineralization.

The expression level of *S-1P* in ATDC5 cells did not differ much in ATDC5 cells that were stably transfected with the DNA of pIRES-EGFP (control) and the clones 1-5 that

were transfected with the DNA of pIRES-pro-SKI-EGFP (Figure 21e). This is expected because the inhibition of S-1P by stable transfection happens at a post-transcriptional level and in theory should not affect the mRNA level of S-1P. However, the expression of S-1P mRNA in clone 6 and clone 7 of ATDC5 cells that were transfected with the DNA of pIRES-pro-SKI-EGFP was 3-5 fold higher than the other clones of the same experimental group on day 4 and 7-11 fold higher on day 16 of culture. Clones 6 and 7 of the ATDC5 cells that were transfected with the DNA of pIRES-pro-SKI-EGFP also showed enhanced Alcian Blue staining (Figure 19b) and highest amount of glycosaminoglycan accumulation (Figure 20), which was different from the results obtained from the same experimental group.

Clones 6 and 7 of the ATDC5 cells that were transfected with the DNA of pIRES-pro-SKI-EGFP not only showed enhanced Alcian Blue staining and high amount of glycosaminoglycan accumulation, they also expressed high mRNA level of chondrocyte differentiation markers tested—a few hundred folds higher than cells of the control group that were induced but non-transfected. This may be attributed to the higher expression of *S-1P* in these clones compared to the other clones of the same experimental group. The reason that these cells had higher *S-1P* remained elucidated. It could be that the DNA of pIRES-pro-SKI-EGFP integrated to the enhancer region of the genome of the cells and hence enhanced the expression of *S-1P*.

3.7 Confirmation of the functional inhibition of S-1P

RT-PCR was first carried out to determine the expression of the mRNA of the inhibitor construct—the pro-SKI (R134E)—in cells of the control and all experimental groups (Figure 22). The housekeeping gene, GAPDH, was used as an endogenous control in the RT-PCR reaction (Figure 22ai). The DNA of pro-SKI-1 was used as a positive control in the RT-PCR reaction (Figure 22bi, bii, ci and cii). ATDC5 cells that were stably transfected with the DNA of pIRES-pro-SKI-EGFP expressed *pro-SKI-1* on day 4 and day 16. However the cells that were stably transfected with the DNA of pIRES-EGFP did not show any *pro-SKI-1* expression on day 4 and day 16. This was also the case for both non- transfected controls, one of which was non-induced; the other one was induced with insulin and ascorbic acid. To ensure that it was the genomic *pro-SKI-1* that has integrated

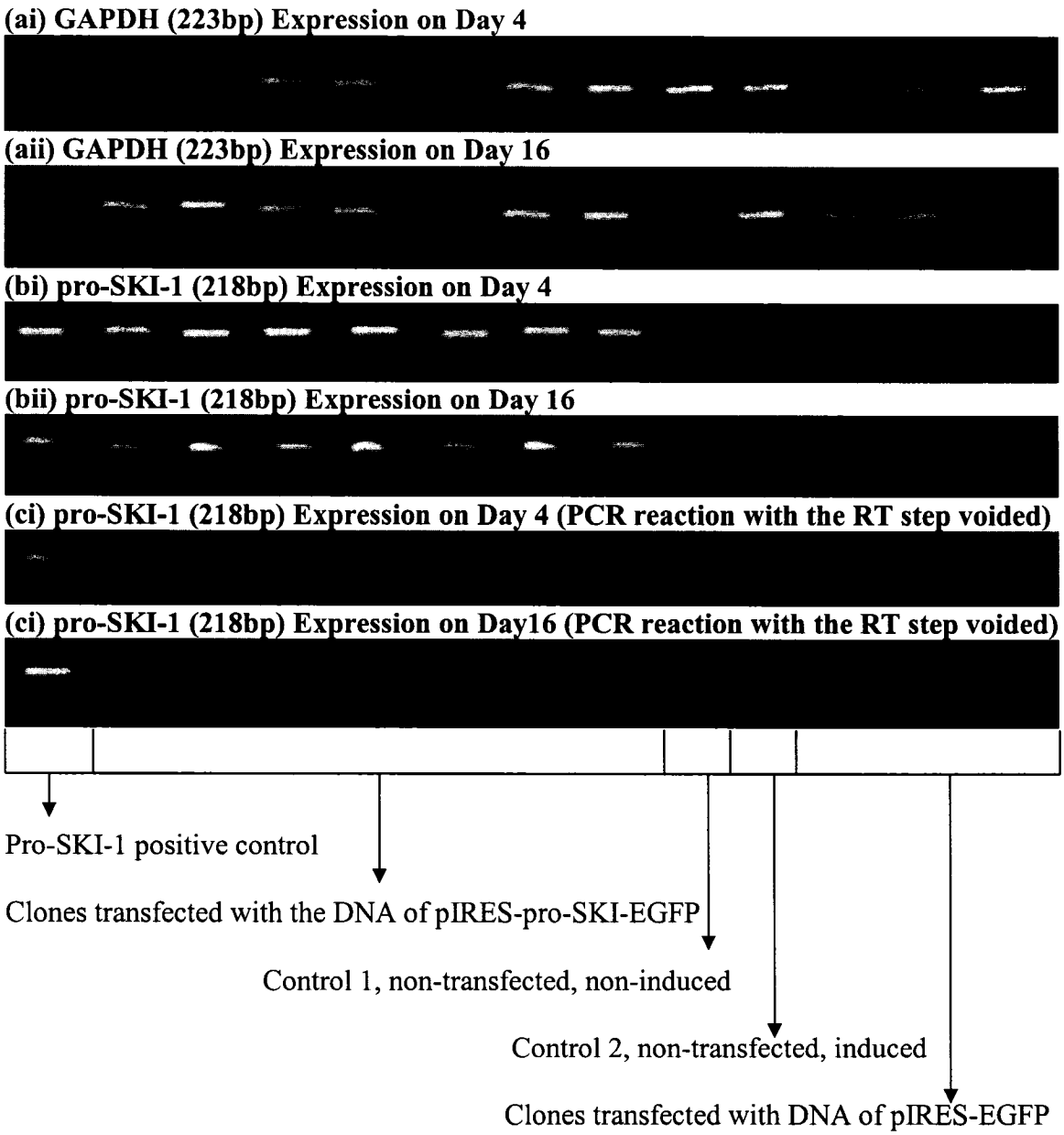

Figure 22: RT-PCR of ATDC5 cells on day 4 and day 16 of culture. Panel (ai) and (aii) showed GAPDH (endogenous control) expression in all cells on day 4 and day 16. Panel (bi): *pro-SKI-1* expression in ATDC5 cells on day 4. Only cells that were stably transfected with the DNA of pIRES-pro-SKI-EGFP expressed *pro-SKI-1* on day 4. Panel (bii): *pro-SKI-1* expression in ATDC5 cells on day 16. Only cells that were stably transfected with the DNA of pIRES-pro-SKI-EGFP expressed *pro-SKI-1* on day 16. Panel (ci) and (cii): PCR reaction with RT step voided in. *pro-SKI-1* plasmid DNA was not present, and hence not amplified in the PCR reaction.

into the genome of ATDC5 cells via stable transfection that was being amplified in the RT-PCR reaction, a control PCR reaction was performed whereby the RT step was voided. Results showed that *pro-SKI-1* plasmid DNA was not present in the stably transfected cells (Figure 22ci and cii) on both day 4 and day 16.

To confirm the functional inhibition of S-1P in ATDC5 cells in the stable transfection experiment, Real-Time PCR was performed to determine the expression of *HMG co-A reductase* in ATDC5 cells of the control and all experimental groups. HMG Co-A reductase is the rate-controlling enzyme in the mevalonate pathway, through which cholesterol is synthesized. The enzyme is a downstream target of active SREBP. The cleavage of SREBP by active S-1P releases the NH_2-terminal segment of SREBP, allowing it to enter the nucleus, where it binds to enhancers and activates transcription of more than 35 mRNAs coding for proteins/ enzymes required for the biosynthesis and uptake of low density lipoprotein (LDL) and cholesterol (57), and HMG co-A reductase is one of them.

Real-Time PCR result (Figure 23) showed that the expression of *HMG co-A reductase* was highest in all cells on day 16 of culture. Its expression was lowest in clones 1-5 of ATDC5 cells stably transfected with the DNA of pIRES-pro-SKI-EGFP compared to cells of the control groups on both day 4 and day 16. Even though all clones 1-7 of ATDC5 cells that were stably transfected with the DNA of pIRES-pro-SKI-EGFP expressed *pro-SKI-1* on day 4 and day 16 (Figure 22), the inhibitory effect was more evident only in clones 1-5 (Figure 23). Clones 6 and 7, however, behaved more like the control cells transfected with the DNA of pIRES-EGFP, and the control cells that were non-transfected but were induced with insulin and ascorbic acid (Figure 23). The expression level of *HMG co-A reductase* in clones 6 and 7 of the same experimental group was about 2 fold higher than clones 1-5, and slightly higher than the control groups on both time points. These two clones also expressed highest level of *S-1p* (Figure 21e). Higher level of *S-1p* in these clones would lead to higher expression level of the protease in the functional protein level and hence higher expression of *HMG co-A reductase* compared to clones of the same experimental group and of the controls.

An artificial substrate reporter construct adapted for specific cleavage by this protease was used to further confirm the functional inhibition of S-1P in ATDC5 cells. Mutation

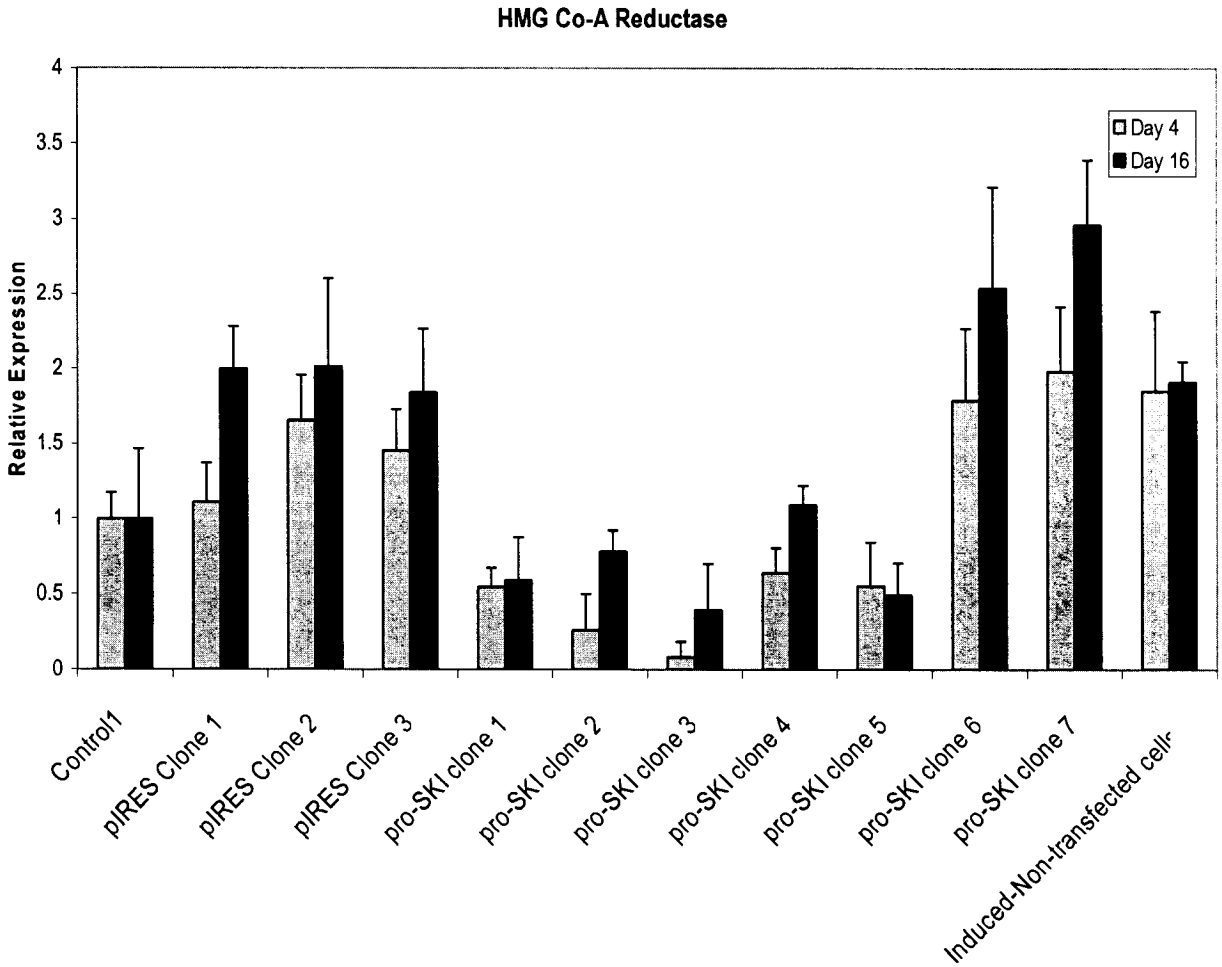

Figure 23: Real-time PCR of *HMG co-A reductase* of ATDC5 cells on Day 4 and Day 16. The expression of *HMG co-A reductase* was highest in all cells on day 16 of culture. Its expression was lower in clones 1-5 of ATDC5 cells stably transfected with the DNA of pIRES-pro-SKI-EGFP compared to cells of the control groups on both day 4 and day 16.

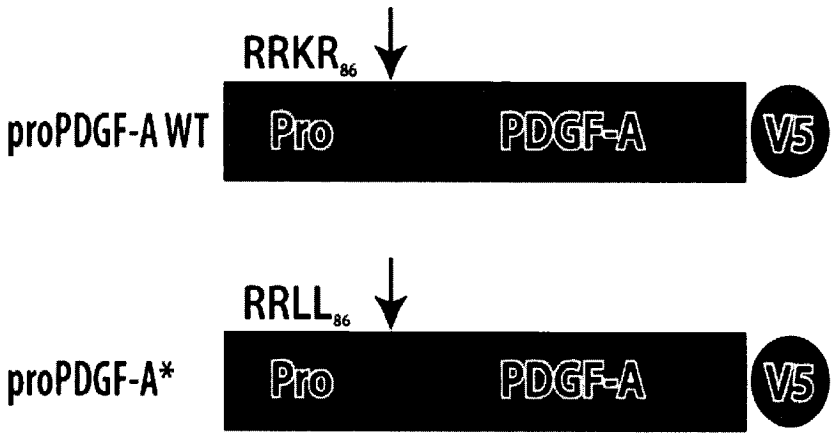

Figure 24: Pro-PDGF-A processing. A structure of pro-PDGF-A wild type and pro-PDGF-A* mutant with respective processing sites.

of proplatelet-derived growth factor A (pro-PDGF-A) at its furin-cleavage site (RRKR ^{86}) into RRLL^{86} (pro-PDGF-A*) resulted in a S-1P artificial substrate (Figure 24). It was previously (80) shown that S-1P can process intracellularly an RRLL ^{86} mutant of pro- PDGF-A (pro-PDGF-A*) into PDGF-A, paving the way for a convenient ex-vivo assay of S-1P using an anti-V5 Western blot analysis of secreted PDGF-A (Figure 24). Detection by Western blotting was done with a monoclonal antibody directed against the V5 epitope fused to the C-terminal end of pro-PDGF-A.

In cells transfected with the DNA of pIRES-EGFP, the 24-kDa pro-PDGF-A* was very efficiently processed into a 16-kDa PDGF-A product (Figure 25). This process is completely inhibited in clones 1-5 that were transfected with the DNA of pIRES-pro-SKI-EGFP. However, in clones 6 and 7 of the same experimental group pro-SKI-1 (R134E) did not seem to have any inhibitory effect, for the 24-kDa pro-PDGF-A* was processed into a 16-kDa PDGF-A product, reflecting that S-1P was still active in these clones.

Taken together, *pro-SKI-1 (R134E)* was present in all clones of ATDC5 cells transfected with the DNA of pIRES-pro-SKI-EGFP (Figure 22bi and bii). However, it seemed that only in clones 1-5 that S-1P was efficiently inhibited, and the protease was still active in clones 6 and 7. This was evidenced by real-time PCR result in determining the mRNA level of *HMG co-A Reductase* (Figure 23) and Western blotting on the processing of pro-PDGF-A* to PDGF-A in the cells (Figure 25).

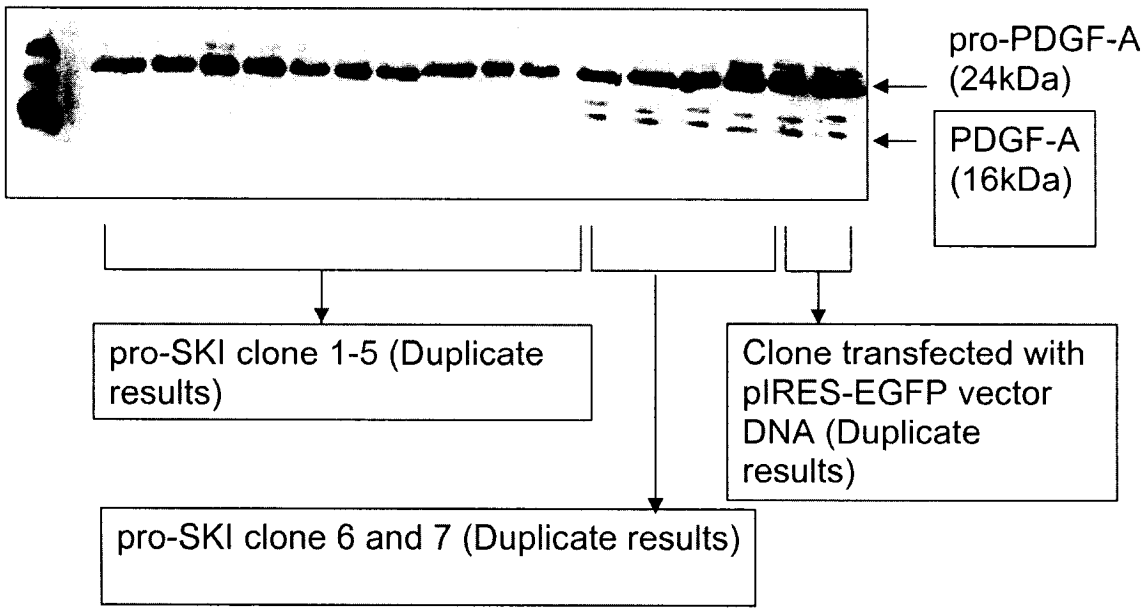

Figure 25: Western Blot analysis showing the processing of pro-PDGF-A*. The 24-kDa pro-PDGF-A* was processed into a 16-kDa PDGF-A product in cells transfected with the DNA of pIRES-EGFP. The process was inhibited in clones 1-5 of the cells transfected with the DNA of pIRES-pro-SKI-EGFP. Clones 6 and 7 of the same experimental group also showed efficient processing of pro-PDGF-A* to PDGF-A.

CHAPTER 4
Discussion

4.1 Discussion and overall conclusions

The overall results of my project showed that the ATDC5 cells are a good model system to study cartilage development. The cells recapitulate the steps of cartilage development when cultured in the presence of insulin. Results showed that 10 μg/mL of insulin is the optimum concentration to be used to induce chondrogenesis in ATDC5 cells. Using RT-PCR, it was shown that S-1P is constitutively expressed in ATDC5 cells both induced and non-induced with insulin. S-1P is also expressed in ATDC5 cells induced by ascorbic acid and combination of ascorbic acid and insulin. Real-time PCR results showed that S-1P mRNA expression levels in ATDC5 cells depended on chondrogenesis inducers. Ascorbic acid was a more effective chondrogenesis inducer in ATDC5 cells and a combination of both insulin and ascorbic acid had additive effect in inducing chondrogenesis in ATDC5 cells. S-1P expression was highest in the cells induced with the combination of both insulin and ascorbic acid. These cells were also the most chondrogenic as they accumulate the highest amount of glycosaminoglycan and the expression of all cartilage marker genes (*aggrecan, collagen I, collagen II and collagen X*) were also highest compared to cells induced with insulin or ascorbic acid alone. Results also showed that *S-1P* expression was related to the progression of chondrogenesis in ATDC5 cells. During the course of chondrogenic differentiation in ATDC5 cells, the *S-1P* expression profile mimicked that of *collagen II* with a slight delay. Since the induction of ATDC5 cells showed elevation in *S-1P* expression and *S-1P* expression was shown to correlate to the progression of chondrocyte differentiation, these preliminary results pointed toward the hypothesis that S-1P is involved in chondrogenesis.

Even though ATDC5 cells were shown to be a good model system to study cartilage development, there are drawbacks using these cells: First of all, the time required to follow the whole developmental program is long and hence there is a higher possibility of contamination during the culture period. The time scale of the experiment also prevented my effort to starve the cells of sterols in order to analyze the effect of the inhibition of S-1P in the expression level of HMG co-A reductase mRNA. The cleavage of SREBP by active S-1P in the absence of sterols releases the NH_2-terminal segment of SREBP, allowing it to enter the nucleus, where it binds to enhancers and activates transcription of

more than 35 mRNAs coding for proteins/ enzymes required for the biosynthesis and uptake of low density lipoprotein (LDL) and cholesterol (57), and HMG co-A reductase is one of the downstream targets of SREBP. The effect of the inhibition of S-1P on the expression levels of HMG co-A reductase was anticipated to be more pronounced if the stably transfected ATDC5 cells were cultured in the absence of sterols. HMG co-A reductase might also not be the best candidate to study the phenotype severity in S-1P inhibition because other studies showed that farnesyl diphosphate synthase, another enzyme required for cholesterol synthesis, reacted more sensitively to S-1P disruption (68). Studies have also showed that some functional SREBPs were present in the nucleus of the S-1P knockout mice (82). It is also likely that S-1P is present in great excess and that SREBP processing is not reduced severely until the amount of S-1P declines below 5% of the wild-type value (83). Previous studies of enzyme deficiency states revealed that as little as 5% of residual activity can prevent abnormal phenotypes in some diseases (84).

It is also not known whether ATF6 is cleaved during ATDC5 cell differentiation. The role of Unfolded Protein Response (UPR) in ATDC5 differentiation should be studied in more detail because UPR has been shown to occur during cellular developmental processes such as the transition of B-lymphocytes into antibody-secreting plasma cells (84).

The duration of cell culture ATDC5 cells required had also hampered our proposed attempt to inhibit *S-1P* of the cells using siRNA methods since the double-stranded RNA would disintegrate during long period of culture hence losing its effects. Transfection efficiency of ATDC5 cells was very low (only about 5-10%) which made them an unfavorable choice for transient transfection to study gene expression. Therefore selection of stable transfectants, which was very time consuming, seemed to be the most reasonable way to study gene expression and the course of cartilage development in ATDC5 cells.

Results showed that S-1P clearly plays important roles in cartilage development in ATDC5 cells. The effect of the inhibition of S-1P on the expression levels of cartilage related components was studied by inhibiting S-1P using the R134E prosegment mutant of S-1P, which has been shown to be a potent cellular inhibitor of S-1P. The DNA of the

pro-SKI-1 was subcloned into pIRES-EGFP and transfected into ATDC5 cells. Clones 1-5 of ATDC5 cells that were transfected with the DNA of pIRES-pro-SKI-EGFP showed severe suppression in chondrogenesis. Functional inhibition experiments confirmed that S-1P was effectively inhibited in these clones, since the expression level of *HMG co-A Reductase* was lower than in the controls and Western blotting showed that the processing of pro-PDGF-A* to PDGF-A was effectively inhibited in these clones. The cultures hardly bound Alcian Blue dye and had lower glycosaminoglycan accumulation. The clones also showed suppressed chondrogenesis marker expression. The expression of levels of type I collagen (early-phase chondrocyte differentiation expressing gene), type II collagen and aggrecan (mature chondrocyte matrix genes) and type X collagen (hypertrophic chondrocyte matrix gene) were lower in clones 1-5 of the ATDC5 cells that were transfected with the DNA of pIRES-pro-SKI-EGFP, reflecting that the inhibition of S-1P prohibited chondrogenesis in ATDC5 cells from early pro-condensation stage to late hypertrophy stage.

Clone 6 and 7 of ATDC5 cells that were transfected with the DNA of pIRES-pro-SKI-EGFP did not behave like clones 1-5 of the same experimental group. Real-time PCR result showed that clones 6 and 7 expressed higher level of *S-1P* mRNA than clones of the same experimental group and of the controls. Although the reason for the high *S-1P*expression in these clones remains elucidated, it could be attributed to the integration of the DNA of pro-SKI-1 into an enhancer region of the genome of these clones and hence the enhance transcription of *S-1P* and all other cartilage markers tested (*collagen I,, collagen II, aggrecan and collagen X*). Consistent with the high expression of cartilage markers, clones 6 and 7 also showed enhanced Alcian Blue staining and elevated glycosaminoglycan accumulation compared to controls and clones 1-5 of the same experimental group, indicating that these clones were highly chondrogenic. Functional inhibition experiments showed that S-1P was still active in clones 6 and 7: these clones showed higher expression of HMG co-A reductase and Western blot analysis showed that pro-PDGF-A* in these clones were effectively processed into PDGF-A.

The results clearly showed that the inhibition of S-1P activity (as in clones 1-5 of ATDC5 cells transfected with the DNA of pIRES-pro-SKI-EGFP) in ATDC5 cells prevented the chondrogenic process in these cells. This conclusion is supported by the results of Alcian

Blue staining, glycosaminoglycan quantification and Real-time PCR of the cartilage marker genes. Results of clones 6 and 7 also pointed to the hypothesis that the elevated *S-1p* expression and the fact the protease being active were the reasons of these cells being highly chondrogenic compared to the controls and clones 1-5 of the same experimental group.

Overall inhibition of the activity of S-1P in ATDC5 cells led to the inhibition in chondrogenesis. Recently, Sandell's group (Washington University, St. Louis) generated *S-1p* cartilage-specific knockout mice using the Col2-Cre system. Cartilage-specific S-1P disruption results in animals that died shortly after birth and also showed signs of chondrodysplasia with abnormally short and deformed limbs as compared to wild type mice (Figure 26a). The mice also showed a smaller skull size which causes the tongue to protrude from the mouth (Figure 26b).

So far the importance of S-1P in cartilage development is seen by studies in zebrafish where the *gonzo* mutation, which resulted in abnormal and disorganized cartilage assembly, was credited to a disruption of the S-1P gene. The studies of Sandell's with cartilage-specific S-1P knockout mice (85) showed that gene disruption of S-1P resulted in mice that showed signs of severe chondrodysplasia with abnormally short and deformed limbs. The results of my study showed that S-1P plays important role in cartilage development *in vitro*. These observations emphasized the general importance of S-1P in cartilage development in most species. It is therefore very important to identify the molecular target(s) of S-1P with respect to cartilage development.

The activation of SREBPs by S-1P is known to coordinate expression of key enzymes of cholesterol and fatty acid biosynthesis. Defects in cholesterol metabolism during embryogenesis affect the function of the growth regulator, Indian hedgehog, and have been shown to lead to severe skeletal abnormalities. Since 1998, five disorders involving enzyme defects in post-squalene cholesterol biosynthesis have been identified—desmosterolosis, X-linked dominant chondrodysplasia punctata, congenital hemidysplasia with ichthyosiform erythroderma and limb defects (CHILD) syndrome, lathosterolosis, and hydrops-ectopic calcification-moth-eaten skeletal dysplasia (87). They join the most common cholesterol biosynthetic disorder, Smith–Lemli–Opitz syndrome, whose underlying defect was identified in 1993. All are associated with major developmental

a)

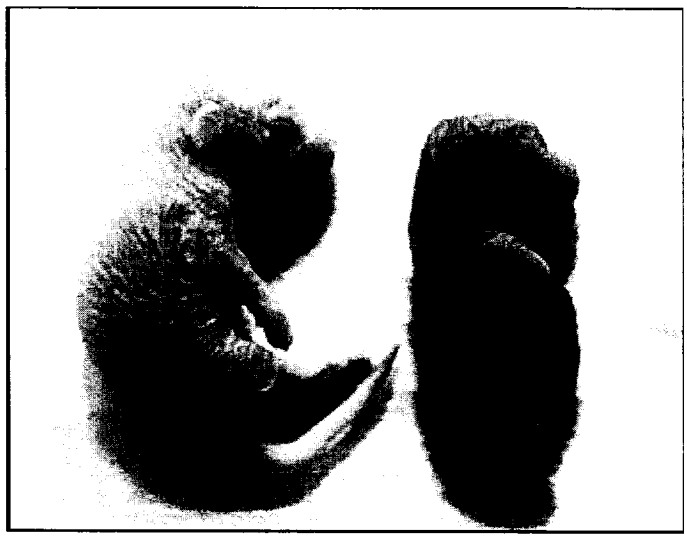

b)

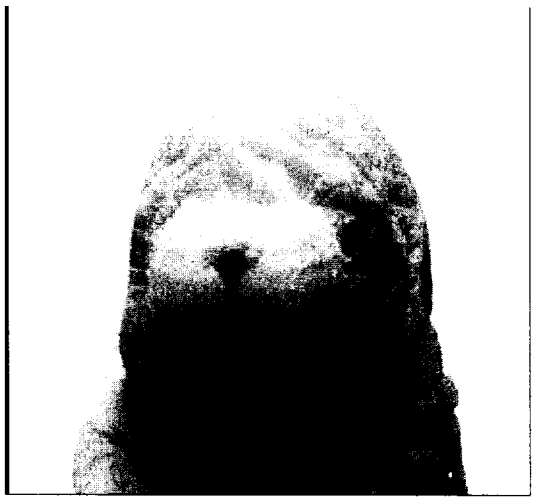

Figure 26: Wild-type and S-1P cartilage-specific knockout mouse. a) The wild-type P1 mouse is on the left-hand side. The S-1P knockout P1 mouse on the right-hand side is smaller and not fully developed (The tail from the mutant mouse has been cut off for genotyping). b) The tongue in case of the S-1P knockout mouse protrudes out of the mouth due to a smaller skull size. (Adapted from 52nd Annual Meeting of the Orthopaedic Research Society, Patra, D; Sandell, L)

malformations that are unusual for metabolic disorders and all showed skeletal defects (86).

Other suspected molecular targets of S-1P with respect to cartilage development would be the ATF6 and ATF6-related bZip factors: CREB4, CREB-H, Luman and OASIS.

CREB4 is a recently discovered transmembrane transcription factor whose localization is regulated by the unfolded protein response and that it can be a substrate for S-1P after the removal of the C-terminal of the protein (87). So far CREB-H is shown to be liver specific. Its expression in cartilage is yet to be determined. In response to ER stress, CREB-H is cleaved by S-1P and S-2P to liberate an N-terminal fragment that transits to the nucleus to activate the transcription of the genes encoding serum amyloid P-component (SAP) and C-reactive protein (CRP) (88). Luman/CREB3 is a ATF6-related bZip transcription factor and is demonstrated to be a substrate of S-1P but unlike ATF6, induction of the unfolded protein response did not result in relocation of Luman from the ER (87), and the signals that induce Luman trafficking to the Golgi remain to be identified. OASIS was induced at the transcriptional level during ER stress in astrocytes of the central nervous system (89), and is demonstrated to play pivotal roles in modulating unfolded protein response in astrocytes. OASIS is also shown to be expressed in osteoblast during osteogenesis (90) even though its role in osteogenesis remained to be elucidated. It is also likely that there are tissue or cell-type specific UPR or ER stress responses to be discovered.

Taken together, present study demonstrated that S-1P plays important role cartilage development. Understanding S-1P regulation of its transcription factors and determining the molecular target(s) of S-1P with respect to cartilage development should enable the discovery of novel signaling pathways involved in cartilage development.

4.2 Suggestion for future work

Investigate the molecular target(s) of S-1P with respect to cartilage development using a rescue of phenotype study, microarrays, proteomic and bioinformatics approaches.

CHAPTER 5

References

1. **Wakitani, S., Goto,T., Pineda, S., Young, R., Mansour, J., A. Goldberg, V.** Cartilage. *The Journal of Bone and Joint Surgery* (American Volume) **4** (1994) pp.579-592.

2. **Knudson, CB and Knudson, W.** Cartilage proteoglycans. *Semin Cell Dev Biol.* **12** (2001) pp: 69-78

3. **Eyre, D.** Collagen of articular cartilage. *Arthritis Res.* **4** (2002) pp.30-35

4. **Cancedda, R., Descalzi-Cancedda, F., and Castagnola, P.** Chondrocyte differentiation. *Int. Rev. Cytol.* **159** (1995) pp. 265–358

5. **Quarto, R., Dozin, B., Bonaldo, P., Cancedda, P. and Colombatti, A.** Type VI collagen expression is upregulated in the early events of chondrocyte differentiation. *Development* **117** (1993) pp. 245–251

6. **Erlebacher, A., Filvaroff, E.H., Gitelman, S.E., and Derynck, R.** Toward a molecular understanding of skeletal development. *Cell* **80** (1995) pp. 371–378.

7. **Johnson, R.L., and Tabin, C.J.** Molecular models for vertebrate limb development. *Cell* **90** (1997) pp. 979–990

8. **Vortkamp, A., Pathi, S., Peretti,G.M., Caruso, E.M., Zaleske D.J., and Tabin, C.J.** Recapitulation of signals regulating embryonic bone formation during postnatal growth and in fracture repair. *Mech. Dev.* **71** (1998) pp. 65–76

9. **Wallis, G.** Bone growth: Coordinating chondrocyte differentiation. *Curr. Biol.* **6** (1996) pp. 1577–1580

10. **Karp, S.J., Schipani, E., St-Jacques, B., Hunzelman, J., Kronenberg, H., McMahon, A.P.** Indian Hedgehog coordinates endochondral bone growth and morphogenesis via parathyroid hormone related-protein-dependent and -independent pathways. *Development* **127** (2000) pp.543–48

11. **Vortkamp, A., Gessler, M., Grzeschik, KH.** GLI3 zinc-finger gene interrupted by translocations in Greig syndrome families. *Nature* **273** (1996) pp.539–40

12. **Karaplis, A.C., Luz, A., Glowacki, J., Bronson, R.T., Tybulewicz, V.L., et al.** Lethal skeletal dysplasia from targeted disruption of the parathyroid hormone-related peptide gene. *Genes Dev.* **8** (1994) pp.277–89

13. **Schipani, E., Kruse, K., Juppner, H.** A constitutively active mutant PTH-PTHrP receptor in Jansen-type metaphyseal chondrodysplasia. *Science* **268** (1995) pp.98–100

14. **Jobert, A.S., Zhang, P., Couvineau, A., Bonaventure, J., Roume, J., et al.** Absence of functional receptors for parathyroid hormone and parathyroid hormone-related peptide in Blomstrand chondrodysplasia. *J. Clin. Invest.* **102** (1998) pp.34–40

15. **Chen, L., Adar, R., Yang, X., Monsonego, E.O., Li, C., et al.** Gly369Cys mutation in mouse FGFR3 causes achondroplasia by affecting both chondrogenesis and osteogenesis. *J. Clin. Invest.* **104** (1999) pp.1517–25

16. **Naski, M.C., Colvin, J.S., Coffin J.D., Ornitz, D.M.** Repression of hedgehog signaling and BMP4 expression in growth plate cartilage by fibroblast growth factor receptor 3. *Development* **125** (1998) pp.4977–88

17. **Pathi, S., Rutenberg, J.B., Johnson, R.L., Vortkamp, A.** Interaction of Ihh and BMP/Noggin signaling during cartilage differentiation. *Dev. Biol.* **209** (1999) pp.239–53

18. **Bouillet, P., Sapin, V., Chazaud, C., Messaddeq, N., Decimo, D., et al.** Developmental expression pattern of Stra6, a retinoic acid-responsive gene encoding a new type of membrane protein. *Mech. Dev.* **63** (1997) pp.173–86

19. **Chuang, P.T., McMahon, A.P.** Vertebrate Hedgehog signalling modulated by induction of a Hedgehog-binding protein. *Nature* **397** (1999) pp.617–21

20. **Burke, D., Wilkes, D., Blundell, T.L., Malcolm, S.** Fibroblast growth factor receptors: lessons from the genes. *Trends Biochem. Sci.* **23** (1998) pp.59–62

21. **Bellus, G.A., Hefferon, T.W., Ortiz de Luna, R.I., Hecht, J.T., Horton, W.A., et al..** Achondroplasia is defined by recurrent G380R mutations of FGFR3. *Am. J. Hum. Genet.* **56** (1995) pp.368–73

22. **Meyers, G.A., Orlow, S.J., Munro, I.R., Przylepa, K.A., Jabs, E.W.** Fibroblast growth factor receptor 3 (FGFR3) transmembrane mutation in Crouzon syndrome with acanthosis nigricans. *Nat. Genet.* **11**(1995) pp.462–64

23. **Shiang, R., Thompson, L.M., Zhu, Y.Z., Church, D.M., Fielder, T.J., et al.** Mutations in the transmembrane domain of FGFR3 cause the most common genetic form of dwarfism, achondroplasia. *Cell* **78** (1994) pp.335–42

24. **Tavormina, P.L., Shiang, R., Thompson, L.M., Zhu, Y.Z., Wilkin, D.J., et al.** Thanatophoric dysplasia (types I and II) caused by distinct mutations in fibroblast growth factor receptor 3. *Nat. Genet.* **9** (1995) pp.321–28

25. **Colvin, J.S., Bohne, B.A., Harding, G.W., McEwen, D.G., Ornitz, D.M.** Skeletal overgrowth and deafness in mice lacking fibroblast growth factor receptor 3. *Nat. Genet.* **12** (1996) pp. 390–97

26. **Bandtlow, C.E. and Zimmermann, D.R.** Proteoglycans in the developing brain: new conceptual insights for old proteins. *Physiol. Rev.* **80** (2000) pp. 267–1290

27. **Ruoslahti, E.** Structure and biology of proteoglycans. *Annu. Rev. Cell. Biol.* **4** (1988) pp. 229–255

28. **Oldberg, A., Antonsson, P., Hedbom, E., and Heinegard, D.** Structure and function of extracellular matrix proteoglycans. *Biochem. Soc. Trans.* **18** (1990) pp.789–792

29. **Kimata, K., Oike, Y., Tani, K., Shinomura, T., and Yamagata, M.** A large chondroitin sulfate proteoglyan (PG-M) synthesized before chondrogenesis in the limb bud of chick embryo. *J. Biol. Chem.* **261**(1986) pp.13517–13525

30. **Shinomura, T., Nishida, Y., Ito, K., and Kimata, K.** cDNA cloning of PG-M, a large chondroitin sulfate proteoglycan expressed during chondrogenesis in chick limb buds. Alternative spliced multiforms of PG-M and their relationship to versican. *J. Biol. Chem.* **19** (1993) pp.14461–14469

31. **Schwartz, N.B., Hennig, A.K., Krueger, R.C., Krzystolik, M., Li, H., and Mangoura, D.** Developmental expression of S103L cross-reacting proteoglycans in embryonic chick. In Fallon, J.F., Goetinck, P.F., Kelley, R.O., and Stocum, D.L. *Limb development and regeneration. Wiley-Liss, N.Y.* (1993) pp. 505–514

32. **Knudson, C.B.** Hyaluronan receptor-directed assembly of chondrocyte pericellular matrix. *J. Cell Biol.* **120** (1993) pp.825–834

33. **Solursh, M. and Jansen, K.L.** The accumulation of basement membrane components during the onset of chondrogenesis and myogenesis in the chick wing bud. *Development* **104** (1988) pp.41–49

34. **Solursh, M., Reiter, R.S., Jensen, K.L., Kato, M., and Bernfield, M.** Transient expression of a cell surface heparan sulfate proteoglycan (syndecan) during limb development. *Dev. Biol.* **140** (1990) pp.83–92

35. **French, M.M., Smith, S.E., Akanbi, K., Sanford, T., Hecht, J., Farach-Carson, M.C., and Carson, D.D.** Expression of the heparan sulfate proteoglycan, perlecan, during mouse embryogenesis and perlecan chondrogenic activity *in vitro. J. Cell Biol.* **145**(1999) pp. 1103–1115

36. **Grover, J. and Roughley, P.J.** Expression of cell-surface proteoglycan mRNA by human articular chondrocytes. *Biochem. J.* **309** (1995) pp. 963–968

37. **Prockop, D.J. & Kivirikko, K.I.** Collagens: molecular biology, diseases, and potentials for therapy. *Annu. Rev. Biochem.* **64** (1995) pp. 403-434

38. **van der Rest M & Garrone, R** Collagen family of proteins. *FASEB J.* **5** (1991) pp. 2814-2823

39. **Bi, W., Deng, J.M., Zhang, Z., Behringer, R.R., and de Crombrugghe, B.** Sox9 is required for cartilage formation. *Nat. Genet.* **22** (1999) pp. 85–89

40. **Soullier, S., Jay, P., Poulat, F., Vanacker, J.M., Berta, P., Laudet, V.** Diversification pattern of the HMG and SOX family members during evolution. *J. Mol. Evol.* **48** (1999) pp.517–27

41. **Zhou, G., Lefebvre, V., Zhang, Z., Eberspaecher, H., de Crombrugghe, B.** Three high mobility group-like sequences within a 48-base pair enhancer of the Col2a1 gene are required for cartilage-specific expression in vivo. *J. Biol. Chem.* **273** (1998) pp.14989–97

42. **Erlebacher, A., Filvaroff, E.H., Gitelman, S.E., Derynck, R.** Toward a molecular understanding of skeletal development. *Cell* **80** (1995) pp.371–78

43. **Kadler, K.E.** Learning how mutations in type I collagen genes cause connective tissue disease. *Int. J. Exp. Pathol.* **4** (1993) pp. 319-23

44. **Kocher, M.S., Shapiro, F.** Osteogenesis imperfecta. *J. Am. Acad. Orthop. Surg.* **6** (1998) pp.225–36

45. **Cole, W.G.** The Nicholas Andry Award-1996. The molecular pathology of osteogenesis imperfecta. *Clin. Orthop.* **343** (1997) pp. 235–48

46. **Mundlos, S., Olsen, B.R.** Heritable diseases of the skeleton. Part II: Molecular insights into skeletal development-matrix components and their homeostasis. *FASEB J.* **11** (1997) pp. 227–33

47. **Spranger, J., Winterpacht, A., Zabel, B.** The type II collagenopathies: a spectrum of chondrodysplasias. *Eur. J. Pediatr.* **153** (1994) pp. 56–65

48. **Jacenko, O., LuValle, P.A., Olsen, B.R.** Spondylometaphyseal dysplasia in mice carrying a dominant negative mutation in a matrix protein specific for cartilage-to-bone transition. *Nature* **365** (1993) pp.56–61

49. **Warman, M.L., Abbott, M.H., Apte, S.S., Hefferon, T., McIntosh, I., et al.** A type X collagen mutation causes Schmid metaphyseal chondrodysplasia. *Nat. Genet.* **5** (1993) pp. 79–82

50. **Chan, D., Weng, Y.M., Hocking, A.M., Golub, S., McQuillan, D.J., Bateman, J.F.** Site-directed mutagenesis of human type X collagen. Expression of alpha1(X) NC1, NC2, and helical mutations in vitro and in transfected cells. *J. Biol. Chem.* **271** (1996) pp.13566–72

51. **Mäkitie, O., Susic, M., Ward, L., Barclay, C., Glorieux, F., Cole, W.** Schmid type of metaphyseal chondrodysplasia and *COL10A1* mutations - findings in 10 patients. *Am. J. Med. Genet. A.* **137** (2005) pp. 241-8

52. **Braverman, N., Lin, P., Moebius, F., Obie, C., Moser,A.,Glossmann, H., Wilcox, W., Rimoin, D., Smith, M., Kratz, L., Kelley, R., & Valle, D.** Mutations in the gene encoding 3β-hydroxysteroid-Δ ^{8},Δ^{7}-isomerase cause X-linked dominant Conradi-Hünermann syndrome. *Nat. Genet.* **22** (1999) pp. 291 - 294

53. **Schlombs, K., Wagner, T. and Scheel, J.** Site-1 protease is required for cartilage development in zebrafish. *Proc. Natl. Acad. Sci. U. S. A.* **24** (2003) pp.14024-9

54. **Zhou, A., Webb, G., Zhu, X., and Steiner, D. F.** Proteolytic Processing in the Secretory Pathway. *J. Biol. Chem.* **274** (1999) pp. 20745-20748

55. **Seidah, N. G., Mowla, S. J., Hamelin, J., Mamarbachi, A. M., Touré, B. B., Benjannet, S., Basak, A., Munzer, J. S., Zhong, M., Marcinkiewicz, J., Barale, J.-C., Lazure, C., Murphy, R. A., Chrétien, M., and Marcinkiewicz, M.** Mammalian subtilisin/kexin isozyme SKI-1: A widely expressed proprotein convertase with a unique cleavage specificity and cellular localization. *Proc. Natl. Acad. Sci. U. S. A.* **96** (1999) pp.1321-1326

56. **Brown, M. and Goldstein, J.** The SREBP Pathway: Regulation of Cholesterol Metabolism by Proteolysis of a Membrane-Bound Transcription Factor. *Cell* **89** (1997) pp.331-340

57. **Sakai, J., Rawson, R. B., Espenshade, P. J., Cheng, D., Seegmiller, A. C., Goldstein, J. L., and Brown, M. S.** Molecular identification of the sterol-regulated luminal protease that cleaves SREBPs and controls lipid composition of animal cells. *Mol. Cell* **2**(1998) pp.505-514

58. **Duncan, E. A., Brown, M. S., Goldstein, J. L., and Sakai, J.** Cleavage Site for Sterol-regulated Protease Localized to a Leu-Ser Bond in the Lumenal Loop of Sterol Regulatory Element-binding Protein-2. *J. Biol. Chem.* **272** (1997) pp.12778-12785

59. **Kaufman, R. J.** Orchestrating the unfolded protein response in health and disease. *J. Clin. Investig.* **110**(2002) pp.1389-1398

60. **Yoshida, H., Haze, K., Yanagi, H., Yura, T., and Mori, K.** Identification of the cis-Acting Endoplasmic Reticulum Stress Response Element Responsible for Transcriptional Induction of Mammalian Glucose-regulated Proteins. *J. Biol. Chem.* **273** (1998) pp.33741–33749

61. **Li, W. W., Sistonen, L., Morimoto, R. I., and Lee, A. S.** Stress induction of the mammalian GRP78/BiP protein gene: in vivo genomic footprinting and identification of p70CORE from human nuclear extract as a DNA-binding component specific to the stress regulatory element. *Mol. Cell. Biol.* **14** (1994) pp.5533–5546

62. **Haze, K., Yoshida, H., Yanagi, H., Yura, T., and Mori, K.** Mammalian Transcription Factor ATF6 Is Synthesized as a Transmembrane Protein and Activated by Proteolysis in Response to Endoplasmic Reticulum Stress. *Mol. Biol. Cell* **10** (1999) pp. 3787–3799

63. **Yoshida, H., Okada, T., Haze, K., Yanagi, H., Yura, T., Negishi, M., and Mori, K.** ATF6 Activated by Proteolysis Binds in the Presence of NF-Y (CBF) Directly to the cis-Acting Element Responsible for the Mammalian Unfolded Protein Response. *Mol. Cell. Biol.* **20** (2000) pp. 6755–6767

64. **Raggo, C., Rapin, N., Stirling, J., Gobeil, P., Smith-Windsor, E., O'Hare, P., and Misra, V.** Luman, the Cellular Counterpart of Herpes Simplex Virus VP16, Is Processed by Regulated Intramembrane Proteolysis. *Mol. Cell. Biol.* **22** (2002) pp. 5639-5649

65. **Lenz, O., ter Meulen, J., Klenk, H. D., Seidah, N. G., and Garten, W.** The Lassa virus glycoprotein precursor GP-C is proteolytically processed by subtilase SKI-1/S1P. *Proc. Natl. Acad. Sci. U. S. A.* **98** (2001) pp.12701-12705

66. **Kunz, S., Edelmann, K. H., de la Torre, J. C., Gorney, R., and Oldstone, M. B.** Mechanisms for lymphocytic choriomeningitis virus glycoprotein cleavage, transport, and incorporation into virions. *Virology* **314** (2003) pp.168-178

67. **Vincent, M. J., Sanchez, A. J., Erickson, B. R., Basak, A., Chretien, M., Seidah, N. G., and Nichol, S. T.** Crimean-Congo Hemorrhagic Fever Virus Glycoprotein Proteolytic Processing by Subtilase SKI-1. *J. Virol.* **77** (2003) pp. 8640-8649

68. **Yang, J., Goldstein, J. L., Hammer, R. E., Moon, Y. A., Brown, M. S., and Horton, J. D.** Decreased lipid synthesis in livers of mice with disrupted Site-1 protease gene. *Proc. Natl. Acad. Sci. U. S. A.* **98** (2001) pp.13607-13612

69. **Okada, T., Haze, K., Nadanaka, S., Yoshida, H., Seidah, N. G., Hirano, Y., Sato, R., Negishi, M., and Mori, K.** A Serine Protease Inhibitor Prevents Endoplasmic Reticulum Stress-induced Cleavage but Not Transport of the Membrane-bound Transcription Factor ATF6. *J. Biol. Chem.* **278** (2003) pp. 31024-31032

70. **Pullikotil, P., Vincennt, M., Nichol, S.T., and Seidah,** S. Development of Protein-based Inhibitors of the Proprotein of Convertase SKI-1/S1P. *J. Biol. Chem.* **279** (2004) pp. 17338-17347

71. **Habuchi, H., Conrad, H.E., Glaser, J.H.** Coordinate regulation of collagen and alkaline phosphatase levels in chick embryo chondrocytes. *J. Biol. Chem.* **260** (1985) pp.13029-13034

72. **Gerstenfeld, L.C., Landis, W.J.** Gene expression and extracellular matrix ultrastructure of a mineralizing chondrocyte cell culture system. *J. Cell Biol.* **104** (1991) pp. 1435-1441

73. **Atsumi,T., Miwa,Y., Kimata, K., Ikawa, Y.** A chondrogenic cell line derived from a differentiating culture of AT805 teratocarcinoma cells. *Cell Diff. Dev.* **30** (1990) pp.109-116

74. **Sullivan, T.A., Uschmann, B., Hough, R., and Leboy, P.S.** Ascorbate modulation of chondrocyte gene expression is independent of its role in collagen secretion. *J. Biol. Chem.* **269** (1994) pp. 22500-22506

75. **Altaf, F.M., Kazim, N., Yoo, Hering, T.M., J.U. Yoo and Johnstone, B.** Ascorbate-enhanced chondrogenesis of ATDC5 cells. *51st Annual Meeting of the Orthopaedic Research Society* (2005) Poster No: 1113

76. **Shukunami, C., Shigeno, C., Atsumi, T., Ishizeki, K., Suzuki, F., Hiraki, Y.** Chondrogenic differentiation of clonal mouse embryonic cell line ATDC5 in vitro: Differentiation-dependent gene expression of parathyroid hormone (PTH)/PTH-related peptide receptor. *J. Cell Biol.* **133** (1996) pp. 457468

77. **Hale J.E., Wuthier, R.E.** The mechanism of matrix vesicle formation. Studies on the composition of chondrocyte microvilli and on the effects of microfilament-perturbing agents on cellular vesiculation. *J. Biol. Chem.* **262** (1987) pp.1916-1925

78. **Shukunami, C., Ishizeki, K., Atsumi, T., Otha, Y., Suzuki, F. and Hiraki, Y.** Cellular hypertrophy and calcification of embryonal carcinoma-derived chondrogenic cell line ATDC5 in vitro. *J. Bone Miner. Res.* **12** (1997) pp. 1174-1188

79. **Shukunami, C., Akiyama, H., Nakamura, T. and Hiraki, Y.** Requirement of autocrine signaling by bone morphogenetic protein-4 for chondrogenic differentiation of ATDC5 cells. *FEBS Lett.* **469** (2000) pp. 8387-8397

80. **de Crombrugghe, B., Lefebvre, V., Behringer, R.R., Bi, W., Murakami, S. and Huang, W.** Transcriptional mechanisms of chondrocyte differentiation. *Matrix Biol.* **19** (2000) pp. 389394-389406

81. **Loveridge, N. and Farquharson, C.** Studies on growth plate chondrocytes in situ: Cell proliferation and differentiation. *Acta. Paediatr. Suppl.* **82** (1993) pp. 4249-4260

82. **Siegfried, G., Khatib, A-M., Benjannet, S., Chrétien, M., and Seidah, N.** The proteolytic processing of pro-platelet-derived growth factor-A at $RRKR^{86}$ by members of the proprotein convertase family is functionally correlated to platelet-derived growth factor-A-induced functions and tumorigenicity. *Cancer Res.* **63** (2003) pp. 1458-1463

83. **Matsuda, M., Korn, BS., Hammer, RE, Moon, YA., Komuro, R., Horton, J, Goldstein, J., Brown, M. and Shimomura, I.** SREBP cleavage-activating protein (SCAP) is required for increased lipid synthesis in liver induced by cholesterol deprivation and insulin elevation. *Genes Dev.* **10** (2001) pp. 1206-16

84. **Beaudet, A. L., Scriver, C. R., Sly, W. S. & Valle, D.** The Metabolic and Molecular Bases of Inherited Disease. *McGraw-Hill, New York* (2001) pp. 3-45

85. **Patra, D.; Davies, S. R.; Xing, X., Sandell, L. J.** Severe chnodrodysplasia in Site-1 protease knockout mice. *51st Annual Meeting of the Orthopaedic Research Society* (2006) Poster No: 1331.

86. **Herman, Gail.** Disorders of cholesterol biosynthesis: prototypic metabolic malformation syndromes. *Hum. Mol. Genet.* **12** (2003) pp. 75–88

87. **Stirling, Julie and O' Hare, Peter.** CREB4, a transmembrane bZip transcription factor and potential new substrate for regulation and cleavage by S1P. *Mol. Biol. Cell* **17** (2006) pp. 413-426

88. **Zhang, K., Shen, X., Wu, J., Sakaki, K., Saunders, T., Rutkowski, T., Back, S. and Kaufman, R.** Endoplasmic reticulum stress activates cleavage of CREBH to induce a systemic inflammatory response. *Cell* **124** (2006) pp. 587-599

89. **Kondo, S., Murakami, T., Tatsumi, K., Ogata, M., Kanemoto, S., Otori, K., Iseki, K., Wanaka, A. and Imaizumi, K.** OASIS, a CREB/ATF-family member, modulates UPR signalling in astrocytes. *Nat. Cell Biol.* **7** (2005) pp. 186-194

90. **Nikaido, T., Yokoya, S., Mori, T., Hagino, S., Iseki, K., Zhang, Y.,Takeuchi, M., Takaki, H, Kikuchi, S., and Wanaka, A.** Expression of the novel transcription factor OASIS, which belongs to the CREB/ATF family, in mouse embryo with special reference to bone development. *Histochem. Cell Biol.* **116** (2001) pp. 141-148